

On the total geostrophic circulation of the South Atlantic Ocean: Flow patterns, tracers, and transports

JOSEPH L. REID

*Marine Life Research Group, Scripps Institution of Oceanography,
La Jolla, California 92093, U.S.A.*

Abstract — The South Atlantic Ocean receives waters from the North Atlantic, the Weddell Sea, and from the Circumpolar Current through the Drake Passage. The circumpolar and North Atlantic waters are of widely different characteristics (temperature, salinity, oxygen and nutrients) but of overlapping density ranges, and as they enter the South Atlantic are caught up in the circulation imposed by the winds and thermohaline processes. Interleaving of these different characteristics takes place in various ranges of depth and density, and more than a dozen vertical extrema are created in the tracer fields. These are spread by lateral flow in recognizable layers.

These patterns as seen on vertical sections and on isopycnals can be taken to indicate the sense of flow in various areas and depths, and I have used them, with the density field, to add the barotropic component to the baroclinic flow defined by the density field. This gives the total geostrophic flow at all depths in a manner that appears to be consonant with the tracer patterns, and that satisfies continuity of mass.

The resulting flow field has the traditional western boundary current from the Weddell Sea to the equator, beneath a poleward flow north of 50°S. In the upper waters the flow pattern shows a cyclonic gyre in the Weddell Sea, a northward flow from the Antarctic along the western boundary from 55°S to 40°S, an anticyclonic gyre between 15°S and 40°S, and an eastward flow near 10°S.

Below the upper layer the axis of the anticyclonic gyre shifts southward, to 35°S at 1500 m, and at greater depths the gyre is confined to the Brazil Basin, west of the Mid-Atlantic Ridge and north of the Rio Grande Rise.

Below the crest of the Mid-Atlantic Ridge in the Brazil Basin waters from the south flow northward along the Ridge, and part of them crosses the Ridge at or near the equator and returns southward in the eastern basin, joined by waters from the North Atlantic. The northward abyssal flow in the Brazil Basin is not confined to the western boundary but extends some distance across the basin, diverted only slightly at 3500 m by the small deep remnant of the overlying anticyclonic gyre.

From 3000 to 4000 decibars the flow within the Weddell Sea and the Argentine Basin form a single cyclonic gyre and the flow within the Cape Basin is cyclonic below 3000 m.

CONTENTS

1. Introduction	150
2. Limitations	153
3. The Data Presentation	155
4. The Flow Near the Surface	156
5. The Principal Sources	167
6. The Layers and Their Extrema	169
7. The Intermediate Water	187
8. Circumpolar Water and Water from the North Atlantic	191
9. The Upper Circumpolar Water	192
10. Water from the North Atlantic	198
11. The Lower Layer of Circumpolar Water	219
12. The Weddell Sea Upper Layers	223
13. The Deeper Waters of the Weddell Sea	226
14. The Falkland-Brazil Confluence and Interleaving	232
15. The Agulhas Extension	234
16. Current Measurements	234
17. The Total Geostrophic Transport	235
18. Conclusion	236
19. Acknowledgements	238
20. References	238

I. INTRODUCTION

The purpose of this study is to use the observed characteristics and the geostrophic shear to estimate a pattern of general circulation of the South Atlantic Ocean at all depths that satisfies continuity in water transport. The area studied is shown in Fig. 1, with the pertinent topographic features labeled and depths less than 3500 m shaded.

The two major assumptions used herein are that the flow is geostrophic and that both flow and mixing take place approximately along isopycnal surfaces. Characteristics acquired at the outcrops either in the South Atlantic or farther upstream are modified by both lateral and vertical diffusion along the flow. Some tracers show extrema in concentration along isopycnals as well as along vertical sections, and their patterns can be used to estimate the sense of flow.

In the following discussion the terms baroclinic and barotropic will have the meaning as in FOFONOFF (1962). That is, by baroclinic component I mean the geostrophic flow relative to the deeper water (in this case, the bottom), and by barotropic component I mean the component of geostrophic flow that is uniform with depth and equal to the geostrophic flow at the bottom. The baroclinic component of the geostrophic flow is given by the density field, and the barotropic component is estimated herein by examination of the tracers. The density field is fairly well defined over most of the South Atlantic Ocean by the present data set. While the flow is known to vary with time, the large-scale baroclinic flow below the upper layer appears to be steady enough to allow data sets from different periods to be combined and the general circulation to be examined usefully.

The characteristics used as tracers have various sources and lie in various depth and density ranges, and are spread throughout the ocean by both flow and mixing. Their patterns are examined along vertical sections and along isopycnal surfaces. In some density-ranges the patterns are sharply defined and show features that appear to be the result of advection. For example, along the western boundary the characteristics indicate that the deepest waters derive from the south and the mid-depth waters from the north, and appear to extend meridionally as narrow features that suggest

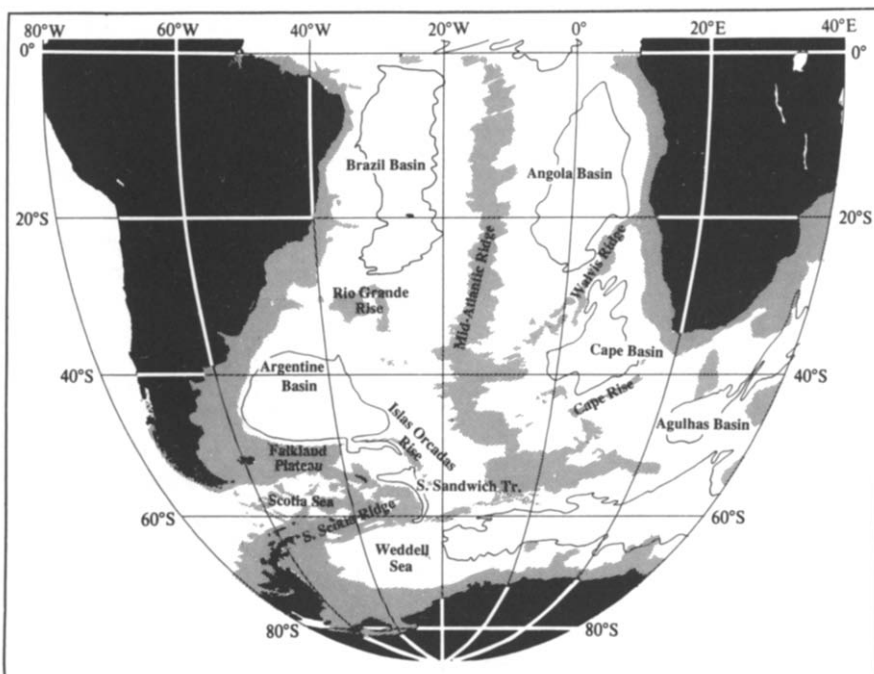


Fig. 1. Principal topographic features referred to in the text, shown on a Molleweide projection. Depths less than 3500 m are shaded and the 5500-m depth contour is shown.

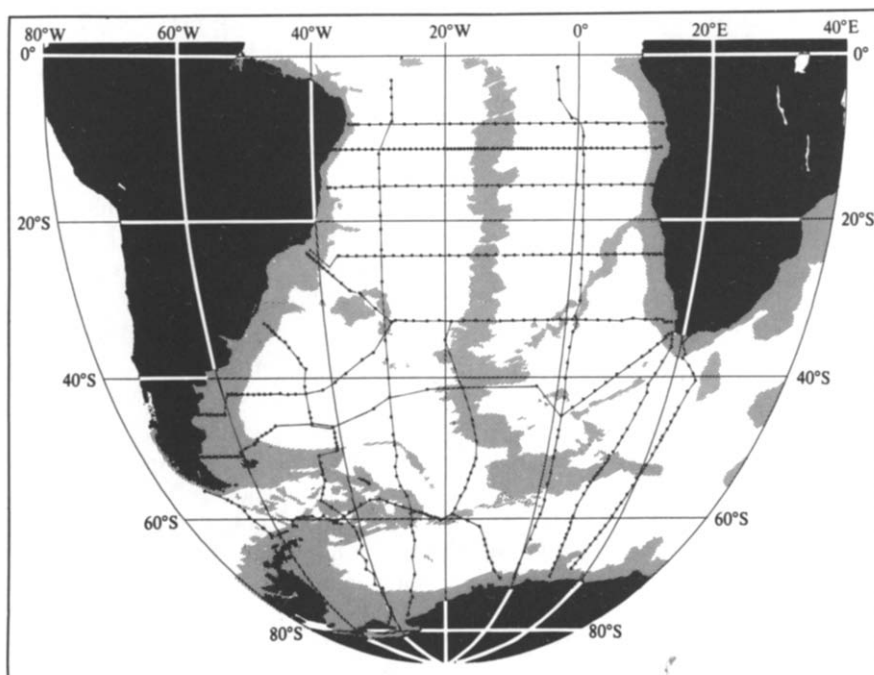


Fig. 2. Positions of stations used in the calculation of the geostrophic flow. Lines connecting stations indicate the paths along which the geostrophically-balanced slopes of the isobars were integrated to provide the adjusted geopotential (steric) height (ϕ_A) of the isobars with respect to a level surface. Depths less than 3500 m are shaded.

advection rather than horizontal diffusion alone. These and other patterns, both shallower and deeper, can in some places indicate flow components in opposite senses at different depths and thus, with the known baroclinic component, constrain the value of the barotropic component to a narrow range of velocity.

The work was carried out in two stages. First, on selected lines of stations (Fig. 2), components of geostrophic motion were calculated relative to the deepest common depth of each consecutive pair of stations. Where the sense of this baroclinic flow, relative to the bottom, appeared initially to be consonant with the tracer patterns, no barotropic component was added initially. Where it did not appear to be consonant with the sense indicated by the tracers, a barotropic component (uniform from top to bottom) was added, just large enough to achieve the sense assumed for that pair of stations. The adjusted flows for the station pairs along these lines of stations define adjusted pressure gradients, and these were integrated horizontally to obtain the steric height adjusted to include the assumed barotropic component. For each line the integration begins at the station pair nearest the coast and the value of steric height, at the first station of the pair, relative to the bottom, was taken initially as the constant of integration for each line. The greatest common depth of the initial pair varied from line to line, though it was usually in shallow water. Where the first two lines intersected the adjusted steric heights (ϕ_A) at the common station were, of course, different, and a new constant of integration was added to one of the lines to remove the offset. Each of the other lines was treated the same way. Of course, as more lines were added to complete the grid (Fig. 2), some of the initially adjusted steric heights did not match at the intersections in the interior. Some increases or decreases in the constants of integration for some lines, and in the barotropic components between various station pairs, were required to make them fit. This was somewhat tedious, but not difficult to do.

A second stage was necessary because no constraint of continuity was used in the first stage, and the resulting transports had not been made to balance. The transport into the South Atlantic Ocean through the Drake Passage was taken to be $130 \times 10^6 \text{ m}^3 \text{ s}^{-1}$ (WHITWORTH, NOWLIN, and WORLEY, 1982), and a net transport of $2 \times 10^6 \text{ m}^3 \text{ s}^{-1}$ from the Pacific through the Arctic and southward through the Atlantic was assumed. A further adjustment to match these constraints required very little change in the barotropic components and resulting flow patterns.

The array of stations used for the maps of adjusted steric height (Fig. 2) was chosen to include, where possible, those expeditions in which a single ship occupied a long line roughly normal to a major flow. Some combinations of expeditions were needed, especially to include the high latitudes. In all, 556 stations (Fig. 2) were used to calculate the adjusted steric height. The expeditions from which they are chosen are listed in Table 1. A much larger set of expeditions could be used to prepare the maps of tracers, and the total was 1693 stations.

For the barotropic components I have chosen the minimum value that would provide the sense of flow suggested by the tracers and would satisfy continuity of volume transport. These are shown for depths below 3000 m as the component of bottom velocity normal to the integration paths (Fig. 3).

It is not surprising that at 3000 m and below the higher speeds are found along the western boundary, particularly along the Falkland Plateau, and that the highest is found near 59°S, 25°W, against the Scotia Ridge. Another high value is found within an Agulhas eddy just south of the tip of Africa. Except for the specified net transports through the Drake Passage, southward between the continents, and south of Africa, the only constraint applied herein was quite simple, that the large-scale flow should be qualitatively coherent with the tracer patterns. No constraint on heat transport was applied and no Ekman transport accommodated.

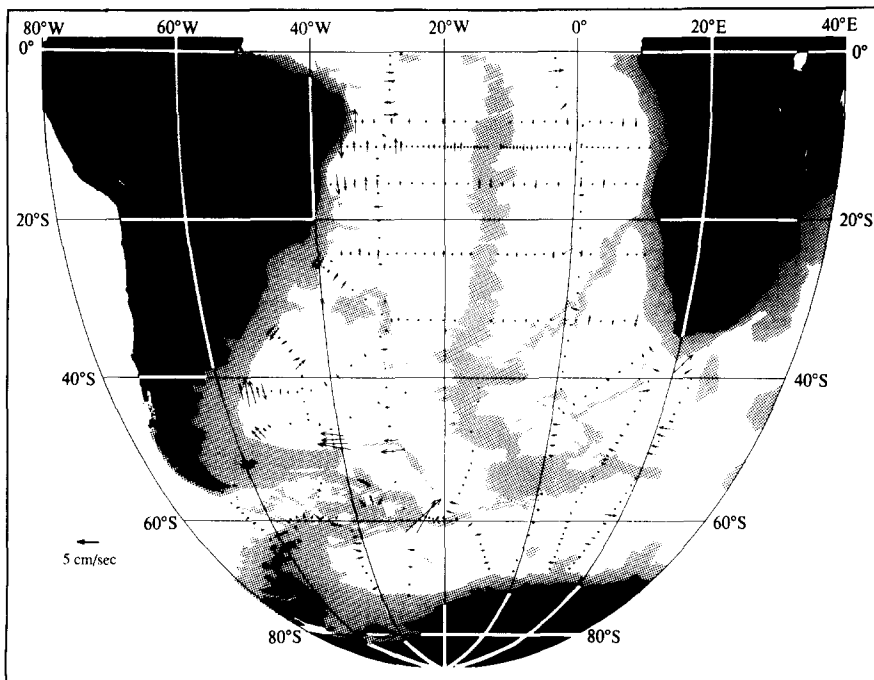


Fig. 3. Barotropic component of flow (bottom speed) estimated for each consecutive station pair along the integration paths shown in Fig. 2. Only those below 3000 m are shown, and depths less than 3500 m are shaded. All vectors are (of course) normal to the integration paths.

2. LIMITATIONS

The method used here is of course qualitative. Aside from this limitation, there are several others that may be less obvious. Not all stations reached as close to the bottom as I would have liked. Station spacing across ridges and near the continental slopes was not always adequate. There were very few deep stations in the equatorial zone, and some were not of high quality. The 32°S line lost some salinities in the eastern part of the Cape Basin. These were filled in from T/S relations from the nearest good stations, but these were not very close. Many of the oxygen and nutrient data were not of modern quality.

While a coherent picture of a large-scale general circulation is presented here, there can be some question as to what it is meant to represent. The data were not synoptic nor are they the averages of measurements taken over a long period. The greatest differences in data were encountered in the upper few hundred meters and appear to result from seasonal variations. For example, the IGY section along 24°S (FUGLISTER, 1960), made in October 1958, was repeated by McCARTNEY and WARREN (personal communication) from 4 February through 3 March 1983, and has much higher temperatures and steric heights in the upper 400 m. It was necessary to use the IGY data for the steric height to avoid the large seasonal differences from the other lines. The later data were used for the tracer patterns, as they included more tracers. Such differences occurred at various intersections of the lines shown in Fig. 2 and resulted in a few extrema in the adjusted steric height from the sea surface to about 500 decibars. At greater depths this did not occur, but several deep eddies were found, particularly on the line along 32°S.

TABLE 1. EXPEDITIONS FROM WHICH STATIONS WERE CHOSEN
TO CALCULATE THE ADJUSTED STERIC HEIGHT.

Expedition/Ship	Dates	NODC #	Source
AFRICANA II		910007	S. AFRICA
AJAX Leg 1	7 Oct. - 6 Nov. 1983	318628	SIO, TAMU (1985)
AJAX Leg 2	11 Jan. - 19 Feb. 1984	318629	SIO, TAMU (1985)
ATLANTIS Cr. 247	Jan. - Jun. 1959	310837	WHOI (1960)
ATLANTIS II	Mar. - Apr. 1971	312296	WHOI
ATLANTIS II Cr. 107	10 Dec. 1979 - 10 Jan. 1980	LDGO (1982)	Near-surface
PESQUERIA XI	3 Mar. - 23 Apr. 1969	080060	ARGENTINA (1971)
CATO VI	7 Nov. - 16 Dec. 1972	313060	SIO (1979)
CONRAD 17	5 Jan. - 11 Apr. 1974	LDGO (1980)	Intermediate
CONRAD 18	2 Feb. - 12 Mar. 1975	LDGO (1976)	water
CRAWFORD Cr. 10	5 Feb. - 27 May 1957	310827	WHOI (1957)
CRAWFORD Cr. 22	2 Oct. - 29 Nov. 1958	310583	WHOI (1960)
DISCOVERY	1932	310831	DISC. COMM. (1942)
ELTANIN Cr. 7	9 Feb. - 14 Mar. 1963	749038	LDGO (1965)
ELTANIN Cr. 8	7 Apr. - 12 Jun. 1963	310707	LDGO (1965)
ELTANIN Cr. 12	15 Mar. - 20 Apr. 1964	310707	LDGO (1965)
ELTANIN Cr. 22	21 Jan. - 14 Mar. 1966	311207	LDGO (1967)
IWSOE 68	Feb. - Mar. 1968	310837	USCG
IWSOE 69	Feb. - Mar. 1969	310805	USCG
IWSOE 73	Jan. - Feb. 1973	318197	USCG
IWSOE 75	Feb. 1975	318215	USCG
IWSOE 76	Feb. 1976	318216	USCG
HUDSON 70	Nov. 1969 - Feb. 1970	180833	BEDFORD
INDOMED	9 Nov. - 22 Dec. 1978	313061	SIO (1979)
ISLAS ORCADAS	Oct. - Dec. 1976	081011	LDGO (1981)
ISLAS ORCADAS	Jan. - Feb. 1977	081012	LDGO (1981)
ISLAS ORCADAS	Apr. - May 1978	081013	LDGO (1981)
J.D. GILCHRIST	9 Aug. - 29 Aug. 1960	910043	U. CAPETOWN (1961)
METEOR	6 June 1925 - 5 May 1927	060004	DEUTSCHE ATLANT. EXPED... (1932)
OCEANUS Cr. 133	Feb. - Apr. 1983	311221	WHOI
PIQUERO Leg 3	13 Jan. - 16 Feb. 1969	910052	SIO (1974)
SARDINOPS			S. AFRICA
TTO TAS	1 Dec. - 18 Feb. 1983		SIO (1986)

TABLE 2. SPECIFICATIONS OF THE ISOPYCNAL SURFACES.

The potential density is expressed as σ_0 from 0-500 db, as σ_1 from 500-1500 db, as σ_2 from 1500-2500 db, as σ_3 from 2500-3500 db, and as σ_4 from 3500 db to the bottom. It is given in units of σ , which is $\rho - 1000$, where ρ is in kg m^{-3} . This table lists the different numbers used for each isopycnal as it extends to the different pressure ranges. The numbers in bold-face type are those used in the text and figures to identify each isopycnal.

3	26.75 in σ_0
4	27.30 in σ_0
5	31.938 in σ_1
6	27.55 in σ_0 south of 60°S, 27.563 north of 60°S
7	32.20 in σ_1 , 36.731 in σ_2
8	Water
9	27.648 in σ_0
10	32.296 in σ_1
11	32.322, 30°S-20°S; 32.335, 20°S-10°S; 32.342, 10°S-10°N
12	36.84 in σ_2
13	27.755 in σ_0 , 32.425 in σ_1 , 36.98 in σ_2 , 41.40 in σ_3
14	27.777 in σ_0 , 32.458 in σ_1 , 37.02 in σ_2 , 41.48 in σ_3
15	Lower circum polar water
16	27.794 in σ_0 , 32.482 in σ_1 , 37.051 in σ_2 , 41.515 in σ_3 , 45.860 in σ_4
17	27.812 in σ_0
18	32.523 in σ_1 , 37.110 in σ_2 , 41.592 in σ_3 , 45.970 in σ_4
19	27.821 in σ_0 80°S-70°S, 27.841 north of 70°S
20	32.549 in σ_1 , 37.151 in σ_2 , 41.647 in σ_3 , 46.04 in σ_4
21	Deep Weddell Sea

With the assumption that the large-scale pattern of subsurface flow does not vary widely over short periods, I hope that the flow pictured here approximates the large-scale flow pattern that has obtained with only minor variations over some long period, perhaps the 60 years spanning the data used in the calculations of total geostrophic flow. The general circulation proposed here is of course not a unique solution for the tracer patterns: various of the opposing flows could be strengthened or weakened somewhat while still maintaining the balance of net transport and qualitative coherence with the tracer patterns. I believe, however, that the large-scale flow derived here is close enough to reality to provide a useful background for other studies.

3. THE DATA PRESENTATION

The characteristics of the waters of the South Atlantic are illustrated at the sea surface, on vertical sections, and on isopycnal surfaces. It must be kept in mind that the isopycnal surfaces mapped are not truly isentropic or ideal neutral surfaces. They are approximations, but the range of the temperature and salinity fields in the South Atlantic Ocean is such that if chosen carefully they can be useful representations of such idealized surfaces.

They are defined by different values at different pressures. As pointed out by REID and LYNN (1971), a deep parcel near the equator, defined by the density it would have at 4000 decibars, may rise to shallower depths and lower pressures both north and south of the equator. As it rises (in the Atlantic, for example) it will extend into warm and saline waters in the north, and into colder, fresher waters in the south; its potential density where it crosses 3000 decibars may be different at the northern and southern crossings. Following such isopycnals of potential density from one pressure range to a lower pressure range in different areas requires different labels. The isopycnal slopes in the anticyclonic gyres are much weaker in the zonal than meridional directions, and the east-west differences are less important, and have been neglected herein. Table 2 lists for each isopycnal mapped the σ -values in all the pressure-ranges, including the values for its northern and southern extensions when they are different. Each isopycnal map is labeled with a single density-number, usually corresponding to the pressure-range of its greatest σ -value, and these values are bold-face in the table.

The International Equation of State for Seawater, 1980, as given by FOFONOFF (1985), is used herein for the South Atlantic Ocean. The differences from the earlier Knudsen-Ekman version used for the South Pacific Study (REID, 1986) are not significant to these results. The major difference is that the calculated density will be lower in the new than the old equation. That is, a value of 46.046 (near 4000 decibars) in the old equation corresponds to about 46.00 in the new equation.

The horizontal flow of the waters of the South Atlantic proposed here is illustrated in a set of maps of adjusted steric height (ϕ_A) along various isobaric surfaces from the sea surface to 4500 decibars. This study of steric height can use only stations that extend to or near the bottom. As there are few such stations and lines taken near the equator, and the flow there is so highly variable as to require a nearly synoptic coverage, the area north of about 8°S is not well defined herein.

The maps of characteristics are mostly along isopycnal surfaces but the maps of flow are along isobaric surfaces. The flow at the different depths to which an isopycnal extends must be examined from maps of flow along different isobars.

4. THE FLOW NEAR THE SURFACE

In discussing a circulating medium there may be no obvious or best place to start or best sequence to follow. I have chosen to discuss the various layers in order of density, starting from the top, rather than in order of source. This requires referring to the sources more than once, and involves some repetition.

Several investigators have displayed the baroclinic flow in the South Atlantic usually assuming zero flow along some isobaric surface, though recognizing that this is an approximation. In only a few cases were some direct measurements of flow available. This helped to show some of the smaller-scale features but were not enough in time or space to define the flow over any large area.

The larger-scale studies of the upper waters have shown some consonance between the tracer patterns and the upper shear field (WUST, 1935; and DEFANT, 1941a and b; CLOWES, 1950; KIRWAN, 1963; TAFT, 1963; BUSCAGLIA, 1971; REID, NOWLIN, and PATZERT, 1977; MERLE, 1978; DEACON, 1979; BURKCV, 1980; GORDON, and MOLINELLI, 1982; and TSUCHIYA, 1986). FU (1981) has used the inverse technique to study the subtropical anticyclonic gyre, and RINTOUL (1988) has applied it to the area south of 32°S. Many of the earlier studies were based upon the data taken by the Meteor in 1925–27 and other data available to WUST and DEFANT when they prepared their atlas (1936), and from the IGY data in 1957–58 (FUGLISTER, 1960). Some of these are used herein (Table 1).

There is an extensive literature on the equatorial circulation, including the Equalant Atlases (KOLESNIKOV, 1973a and 1973b), studies of the geostrophic flow by ENIKEYEV and KOSHLYAKOV (1973), studies of the subthermocline countercurrents by COCHRANE, KELLY, and OLLING (1979), direct measurement by BUBNOV and YEGORIKHIN (1977), MERLE's (1978) atlas, variations of sea-surface topography by KATZ (1981), and variations of topography and characteristics by MERLE and ARNAULT (1985), surface flow and upper-layer flow and tracers by TSUCHIYA (1985 and 1986), and geostrophic currents and ship drift by ARNAULT (1987), and by surface drifters, current meters, and ship drifts by RICHARDSON and REVERDIN (1987).

MOROSHKIN, BUBNOV and BULATOV (1970) found an eastward flow of the upper waters (relative to 1000 decibars) in the zone from 5°S to 10°S east of 5°W, turning southward at the coast as a strong narrow feature they refer to as the Angola Current. In the area of the Benguela Current HART and CURRIE (1960) have studied the upper layer and VISSER (1969) examined the depth, salinity, and oxygen along three isopycnals at depths between 30 and 900 m and interpreted the flow just beneath the surface to be southward near the coast between 18°S and 25°–30°S and northward south of 30°S.

In SHANNON's (1985) study of the Benguela ecosystem he included a review of the circulation that included a northward surface flow along the coast to about 20°S, where it met a southward coastal current, and a subsurface southward flow in the depth range 200 m to at least 300 m, to about 27°S. Later SHANNON and HUNTER (1988) described the southward flow beneath the Benguela Current.

The waters off Brazil and Argentina have been studied by EMILSSON (1961), MASCARENAS, MIRANDA, and ROCK (1971), SIGNORINI (1978), ZYRYANOV and SEVEROV (1979), LUSQUINOS and SCHROTT (1983), MIRANDA (1985), and OLSON, PODESTA, EVANS and BROWN (1988). RODEN (1989) has examined the frontal features and baroclinic flow off Argentina, and GORDON and GREENGROVE (1986) have discussed the Brazil–Falkland convergence.

DIETRICH (1935), using mostly *Discovery* and *Meteor* data, but with some temperature data from as early as 1873, made composite maps of the area of the Agulhas extension showing temperature and salinity from 50 m down to 2000 m and steric height 0/1000 decibars. He found a strong penetration of Agulhas Current Water as far west as 15°E, where it turned back to the south and east, leaving a large eddy at 38°S, 20°E. This is much like the pattern found in more recent data.

BANG (1970) used the surface temperature measured by a three-ship intensive survey off the south coast of Africa to demonstrate the Agulhas loop into the Atlantic and the high variability of the intense flow. GORDON, LUTJEHARMS, and GRUNDLINGH (1987) have discussed the flow in the upper 1500 m of the Agulhas extension from data collected late in 1983, and found two large warm-core rings west of the main extension at that time. Their data did not extend deep enough to be used herein, but show the main flow much as in Fig. 4 and in BANG's (1970) study. The two lines of data used here in that area are from different periods. They have been contoured as one large feature but of course may be separate rings. LUTJEHARMS (1988) has discussed the movement of these rings from both satellite data and subsurface data.

These investigators have addressed the surface flow of the South Atlantic Ocean in various ways, but principally by examining the geostrophic shear between some shallow isobar and a deeper reference isobar, such as that shown by Figs. 4 and 5 and the surface and near-surface characteristics (Figs. 6a–6f).

These show the major large-scale features of the surface flow — the Weddell Sea gyre, the circumpolar flow, the anticyclonic gyre centered near 25°S in mid-ocean, and partly broken in the west at the Rio Grande Rise near 30°S, an eastward geostrophic shear between about 5°S and 10°S in the east, the boundary currents in the east and west, and, at 40°S, 20°E, a coarse realization of the Agulhas extension. All of these were seen in DEFANT's (1941a) study of the relative flow and his Absolute Topography (DEFANT, 1941b) is much the same. With later data they are shown in more detail by TSUCHIYA (1985).

The velocity difference between the sea surface and 1000 decibars is shown in Fig. 4. Because the greatest shear over much of the ocean is found in the upper layers, such patterns can be useful for the near-surface flow. At greater depths the shear is weaker and the sense of flow may change, and maps prepared for flow along deeper isobars may not be useful, and indeed in many areas and depths may indicate the wrong sense of flow.

Combining a barotropic component (Fig. 3) with the baroclinic (which has been calculated relative to the greatest common depth of adjacent stations) yields an adjusted field of geostrophic flow (Fig. 7). This pattern is roughly similar to that of Fig. 4, except that it contains fewer data. However, it can extend into areas shallower than 1000 m, and include the shallow northward flow over the Argentine shelf south of 40°S.

The tracer patterns in the upper waters are illustrated along an isopycnal defined by 26.75 in σ_0 . Its depth (Fig. 8a) reflects the shear shown in Figs. 4 and 5 north of its outcrop near 50°S. South of the outcrop the surface patterns are shown. The salinity (Fig. 8b) is highest in the anticyclonic gyre, in the zone north of 15°S, and at the southern tip of Africa. These high values are separated by an extension of lower-salinity from the south along the eastern and northern limbs of the gyre.

Oxygen (Fig. 8c) decreases northward from the high concentrations in the colder waters at the surface in the south and is lowest along 10°–15°S in the east. Phosphate (Fig. 8d) is high in the circumpolar flow, low within the anticyclonic gyre, and highest in the area of the oxygen minimum at 10°–15°S in the east, and silica (Fig. 8e) has a somewhat similar pattern. These extrema extend downward through a substantial depth range (WATTENBERG, 1938 and 1957; MERLE, 1978; REID, 1981; TSUCHIYA, 1986). The minimum value of oxygen is less than 0.5×10^3 near 200–400 m and values less than 1×10^3 are found to about 500 m, and the lateral minimum extends to at least 2000 m. The phosphate maximum is a little deeper, about 500–600 m at $2.8 \mu\text{M kg}^{-1}$.

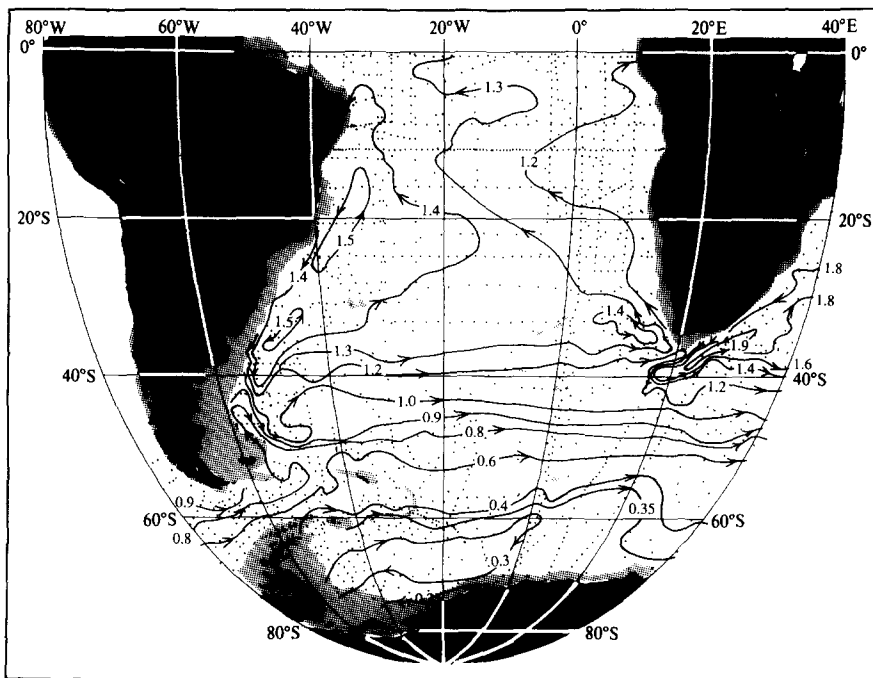


Fig. 4. Geopotential anomaly of the 0 db surface with respect to the 1000 db surface ($10 \text{ m}^2 \text{ s}^{-2}$ or 10 J kg^{-1}). Depths less than 1000 m are shaded.

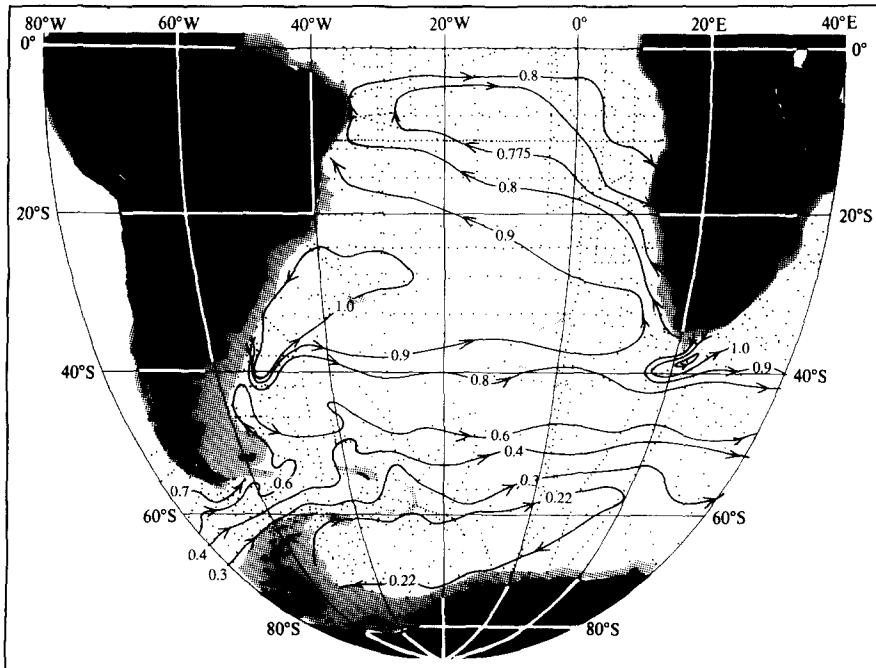


Fig. 5. Geopotential anomaly of the 200 db surface with respect to the 1000 db surface ($10 \text{ m}^2 \text{ s}^{-2}$ or 10 J kg^{-1}). Depths less than 1000 m are shaded.

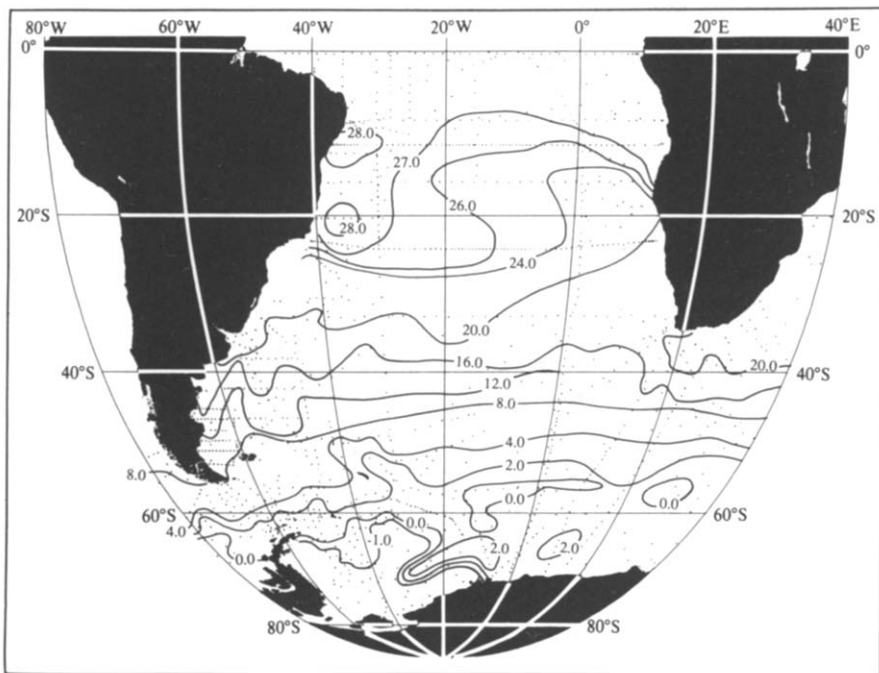


Fig. 6a. Temperature ($^{\circ}\text{C}$) at the sea surface.

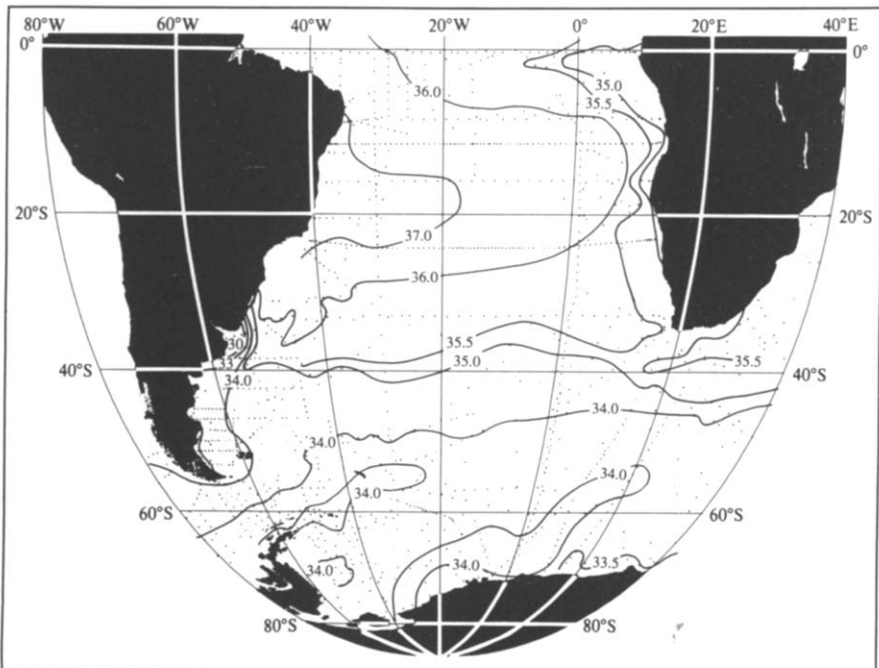
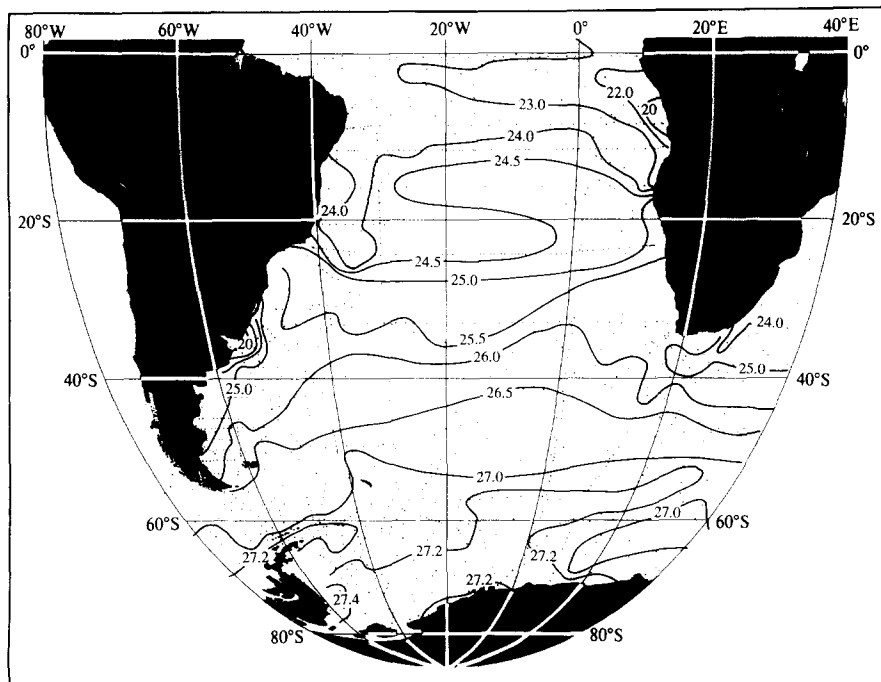
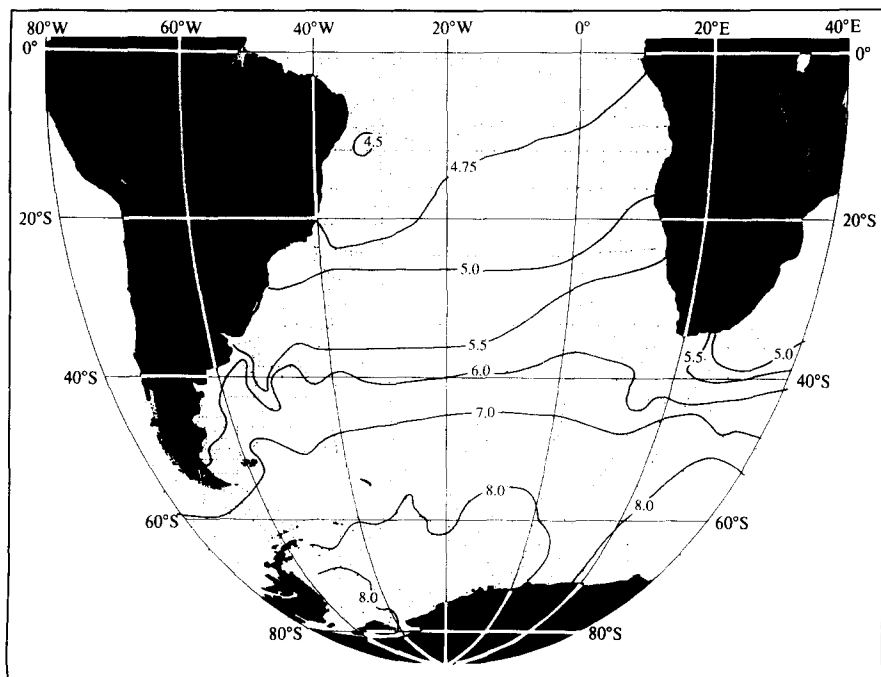


Fig. 6b. Salinity at the sea surface.

Fig. 6c. Potential density (σ_θ) at the sea surface.Fig. 6d. Oxygen ($\times 10^3$) at the sea surface.

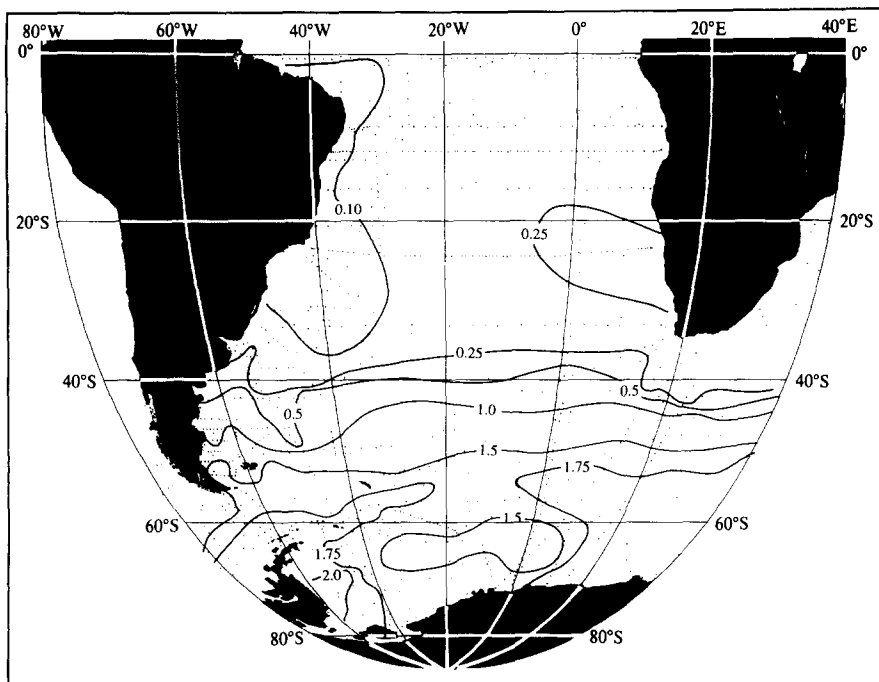


Fig. 6e. Phosphate (m mol m^{-3}) at the sea surface.

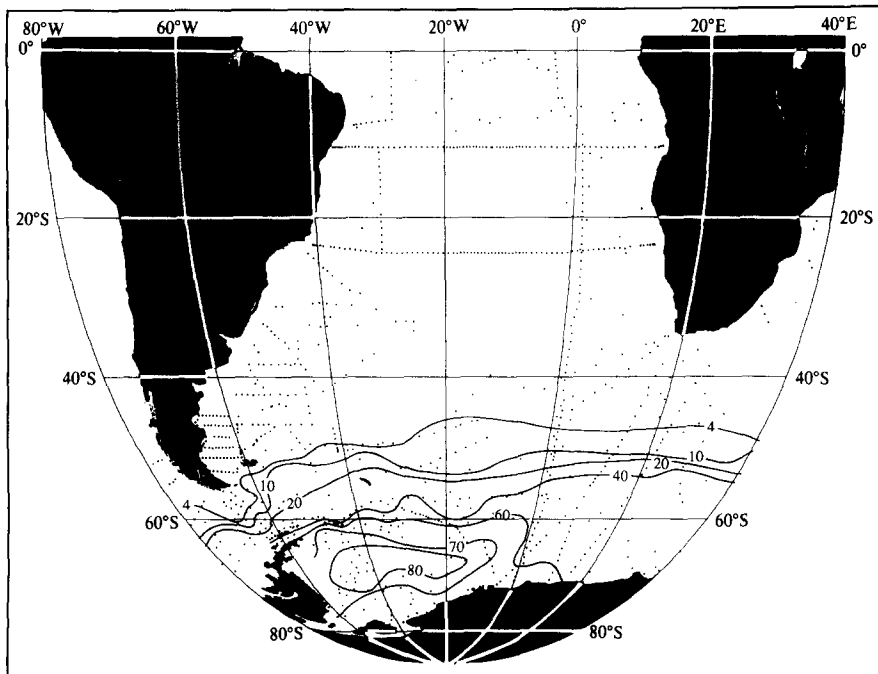


Fig. 6f. Silica (m mol m^{-3}) at the sea surface.

These extreme values appear to result from the baroclinic field, which shows a cyclonic pattern near 10°–15°S in the east (DEFANT, 1941a and 1941b; REID, NOWLIN, and PATZERT, 1977; MERLE and ARNAULT, 1985; TSUCHIYA, 1986; GORDON and BOSLEY, in press), and from the Ekman divergence (HELLERMAN and ROSENSTEIN, 1983) and upwelling. The associated shoaling of the shallower isopycnals as shown by MERLE (1978) and TSUCHIYA (1986) provide nutrients to the euphotic zone there. Zooplankton volumes are high in the high-phosphate zone (HENTSCHEL and WATTENBERG, 1930). Beneath the euphotic layer oxygen is consumed and nutrients are regenerated. The fallout of materials from the euphotic zone into the upwelling waters within the cyclonic flow accumulates high nutrient concentrations, and the extrema in oxygen and nutrients in this zone can be detected to more than 1000 m.

The patterns of flow and tracers near the surface (Figs. 8, 7, 9 and 10) are consonant with TSUCHIYA's (1986) maps. His acceleration potential differs only slightly from the adjusted steric height at 500 decibars (Fig. 10). The westward flow at 3°–5°S in TSUCHIYA's (1986) acceleration potential cannot be examined from the deeper but sparser data used for Fig. 10, and the trough in acceleration potential (less than $10.5 \text{ m}^2 \text{ s}^{-2}$) near 5°–10°S is broader and somewhat farther south in Fig. 10.

The patterns of flow and tracers in this shallow layer are much like those in the upper layer of the Pacific (REID, 1973) and the North Atlantic (TSUCHIYA, 1986), as they are dominated by roughly the same wind patterns, surface divergence, and exchange of heat and water with the atmosphere.

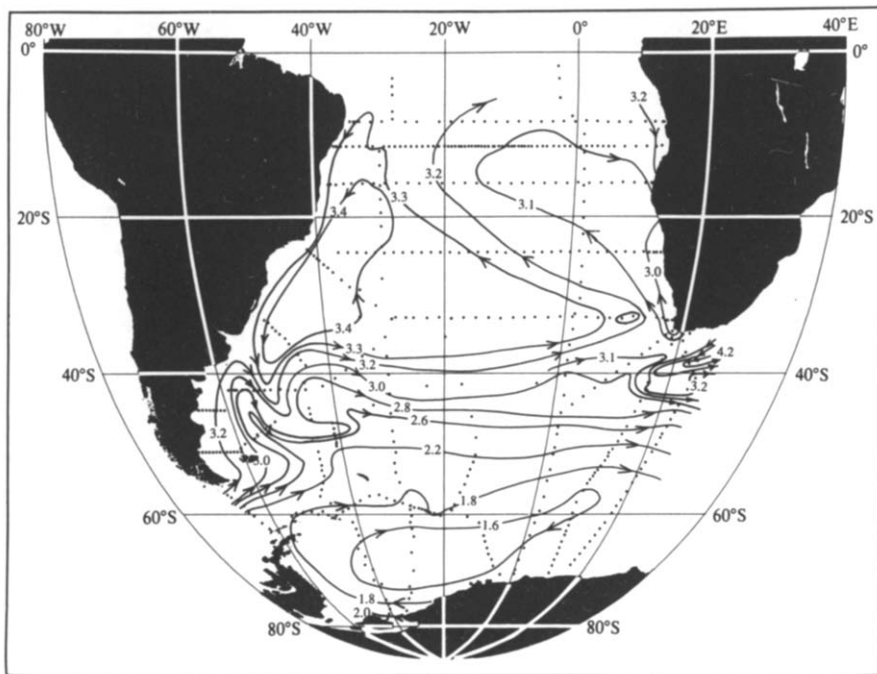


Fig. 7. Adjusted steric height ϕ_A at 0 db ($10 \text{ m}^2 \text{ s}^{-2}$ or 10 J kg^{-1}).

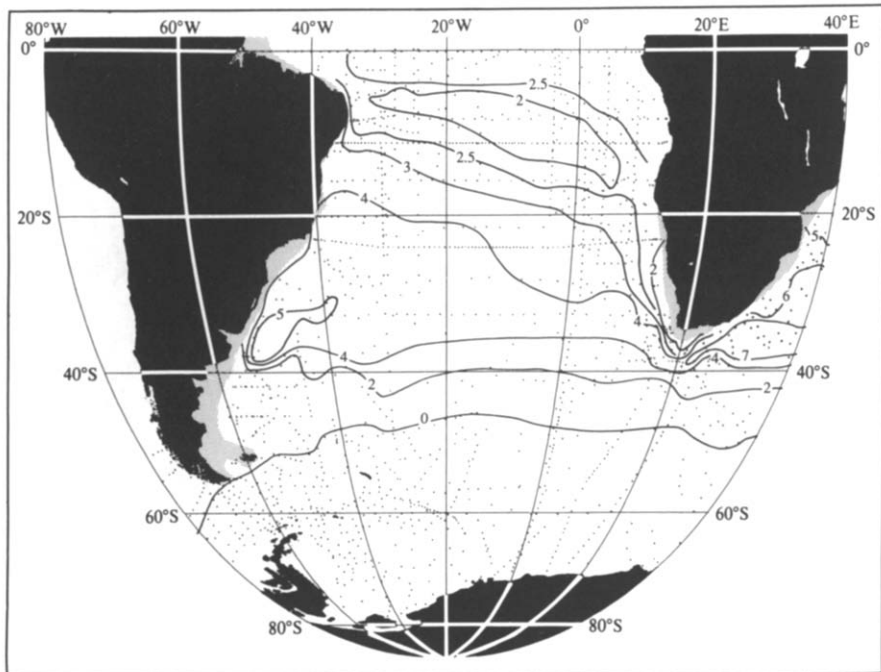


Fig. 8a. Depth (hm) of the isopycnal defined by 26.75 in σ_0 .

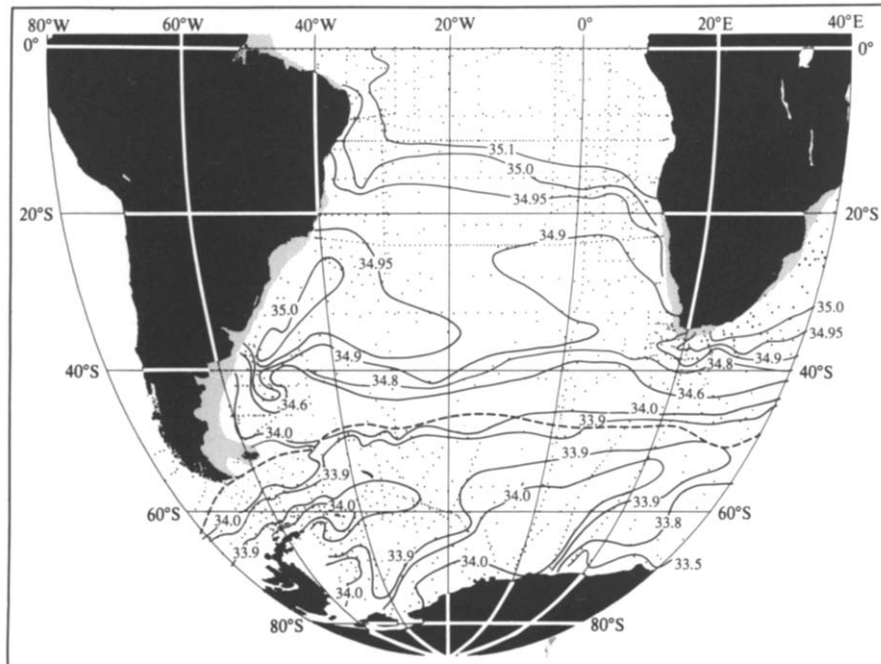


Fig. 8b. Salinity on the isopycnal defined by 26.75 in σ_0 .

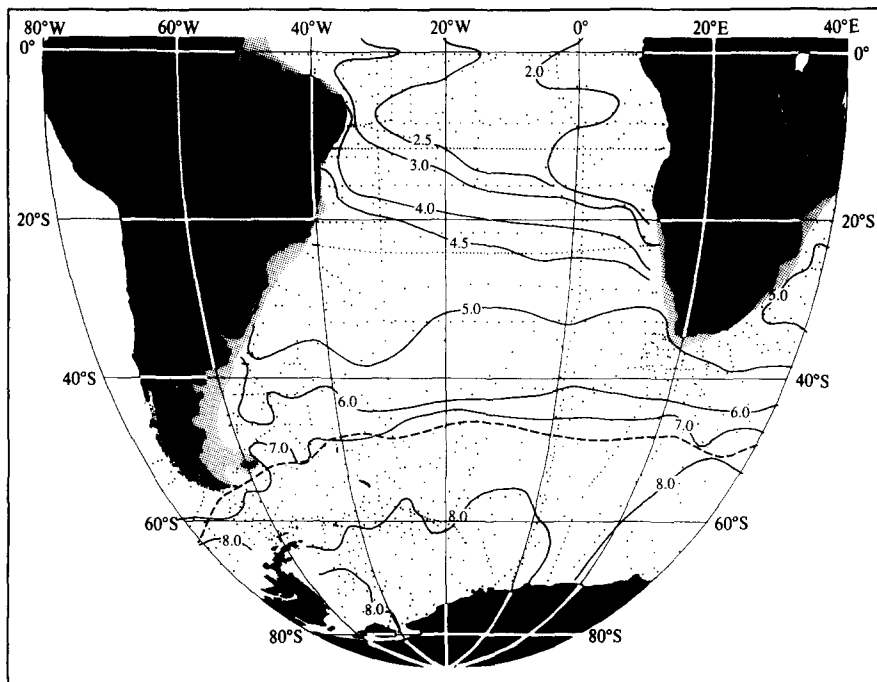


Fig. 8c. Oxygen ($\times 10^3$) on the isopycnal defined by 26.75 in σ_0 .

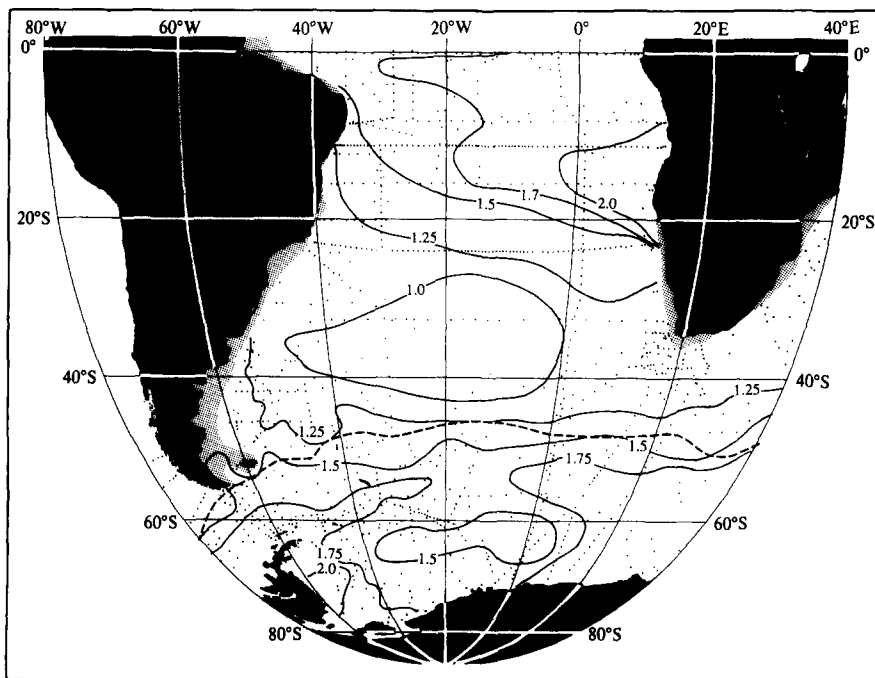


Fig. 8d. Phosphate ($m\text{ mol m}^{-3}$) on the isopycnal defined by 26.75 in σ_0 .

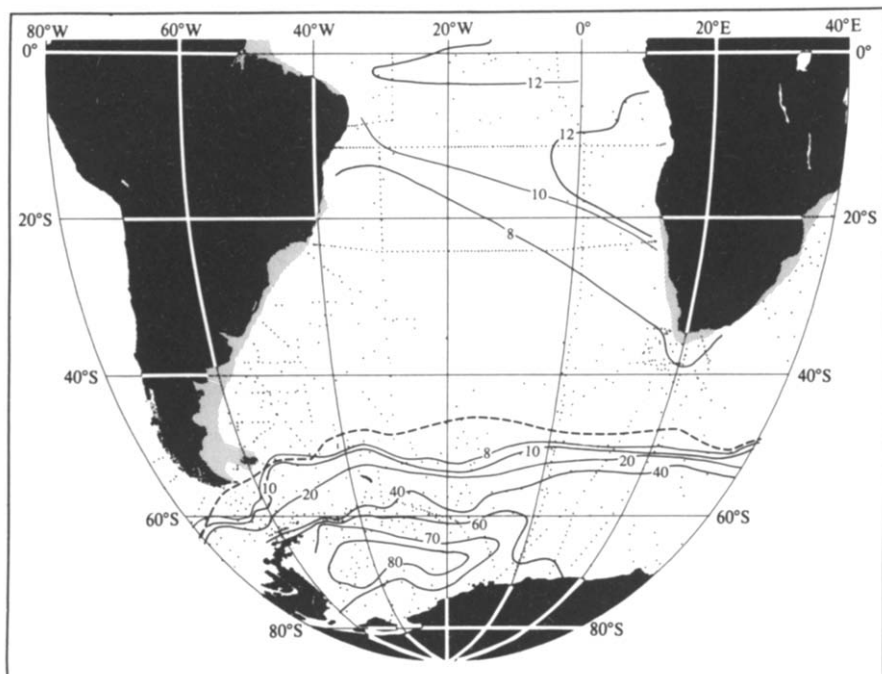


Fig. 8e. Silica (m mol m^{-3}) on the isopycnal defined by 26.75 in σ_0 .

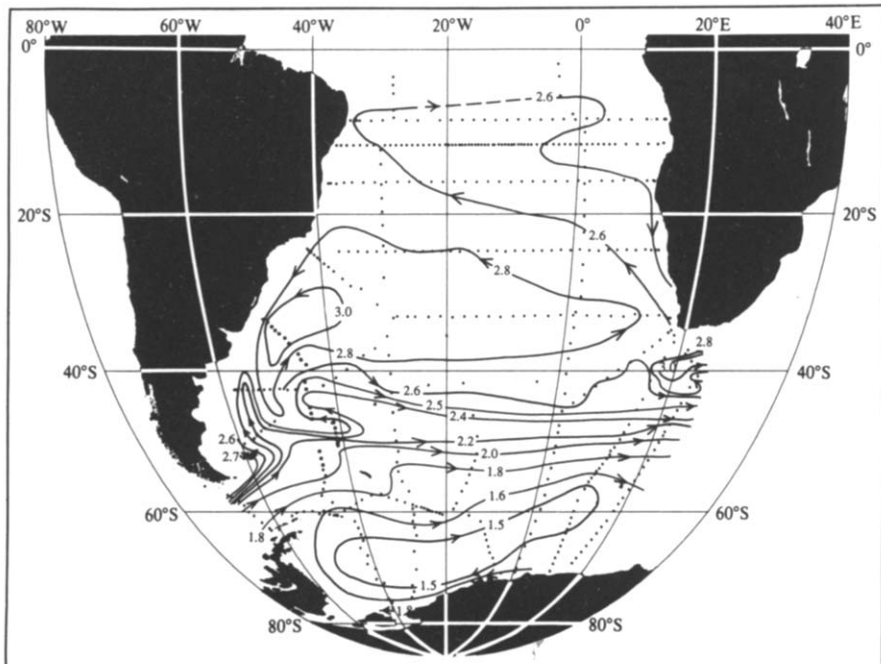


Fig. 9. Adjusted steric height ϕ_A at 250 db ($10 \text{ m}^2 \text{ s}^{-2}$ or 10 J kg^{-1}).

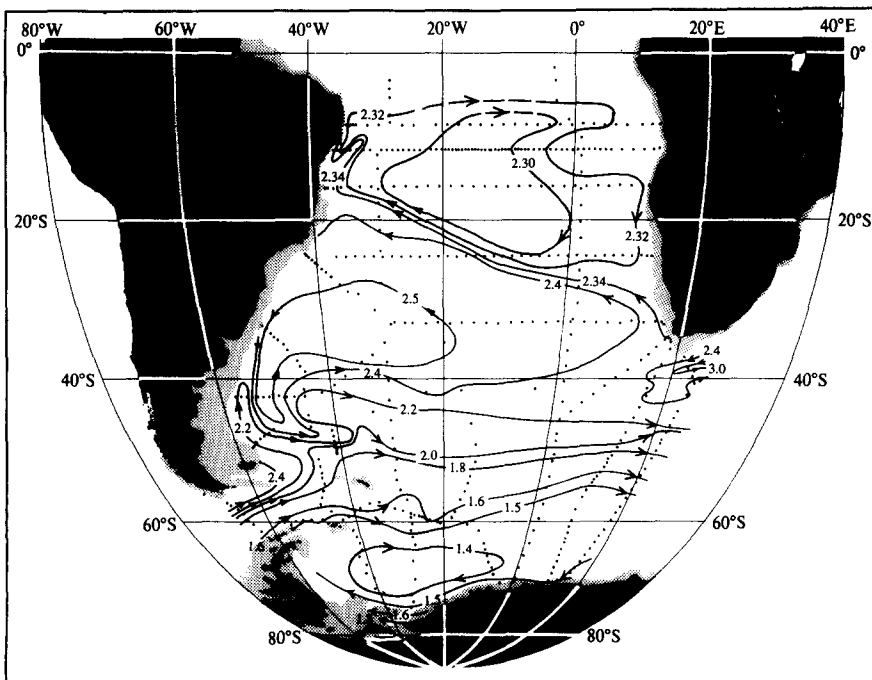


Fig. 10. Adjusted steric height ϕ_A at 500 db ($10 \text{ m}^2 \text{ s}^{-2}$ or 10 J kg^{-1}). Depths less than 500 m are shaded.

5. THE PRINCIPAL SOURCES

The South Atlantic Ocean receives waters from the North Atlantic, the Pacific, the Weddell Sea, and a small part from the Indian Ocean through the westward extension of the Agulhas Current. These waters have different density-ranges and characteristics and they circulate along different paths and at different depths, and interleave. The shallower layers appear to circulate much like the other oceans, but at greater depths the Mid-Atlantic Ridge, the Rio Grande Rise, and the Walvis Ridge divide the South Atlantic into the Argentine, Brazil, Angola, and Cape basins.

The North Atlantic provides, beneath the surface waters, a warm thick layer of high salinity and oxygen and very low nutrients. These extrema extend southward into the circumpolar water as far as 50° – 55°S , where the North Atlantic layers turn eastward as part of the Antarctic Circumpolar Current. The layer of high salinity does not terminate in the South Atlantic, but continues with the Antarctic Circumpolar Current all around Antarctica. It spreads northward to the equator in the Indian and Pacific oceans. Along its path its salinity and oxygen are decreased and its nutrients increased, but it is still a recognizable layer of maximum salinity as it returns to the Atlantic through the Drake Passage as circumpolar water. The circumpolar water is therefore a product of the North Atlantic, depleted in its extreme characteristics along its path around Antarctica, and renewed as it flows northward with the Falkland Current and encounters the newer waters from the North Atlantic.

The waters from the south include, beneath the surface waters, the thick layer of this circumpolar water that has entered with the Antarctic Circumpolar Current, and a bottom layer of water

from the Weddell Sea. The circumpolar waters have entered from the Pacific through the Drake Passage, and are colder and less saline than those from the north, are high in nutrient concentration, and have a wide range of oxygen. Their density range includes that of the waters entering from the North Atlantic, which are higher in temperature, salinity, and oxygen, and lower in nutrients.

Some part of the higher-density circumpolar water turns cyclonically around the Weddell Sea gyre and provides the near-surface waters of the Weddell Sea. They are warmer and more saline than the surface waters. They extend to the shelf break of the Weddell Sea and mix there with the denser shelf waters of near-freezing temperature and relatively high salinity to form a deeper layer with densities greater than that of the maximum density of the Drake Passage (about 46.06–46.07 in σ_4). These waters fill the deep Weddell Sea, where they flow cyclonically and turn eastward south of the South Scotia Ridge. They extend both northward around the Scotia Ridge into the Argentine Basin and eastward south of the Mid-Atlantic Ridge.

The contribution from the Indian Ocean is through the extension of the Agulhas Current westward south of Africa to about 15°E. It turns southward and eastward, but appears to form rings that may separate and move westward, and contribute warm and saline upper water from the Indian Ocean to the Atlantic (OLSON and EVANS, 1986). This manner of contribution would not be revealed directly by the method used herein. The westward extension of the Agulhas waters to about 15°E is clear, but they do not show a distinct signal of northward flow, but instead return toward the Indian Ocean.

6. THE LAYERS AND THEIR EXTREMA

The various layers within the South Atlantic Ocean are illustrated on vertical sections (Figs. 11–15). From the pycnocline downward they are: the layer of high oxygen and low salinity that WUST (1935) called the Intermediate Water, the thick layer of cold, low-oxygen and high-nutrient circumpolar water from the Drake Passage whose deepest part extends to the bottom north of the equator, the saline and oxygen-rich, nutrient-poor layer that WUST (1935) called the North Atlantic Deep Water, which spreads into the circumpolar water and splits it into an upper and a lower part, and the cold, low-salinity and high-oxygen Weddell Sea water, which extends northward along the bottom to about 10°S.

Various vertical maxima and minima in characteristics are found in all of the source-waters as they enter the South Atlantic. The flow paths are three-dimensional and vary with depth, as will be seen, and the source-waters interleave as they flow, creating still more vertical extrema in the tracers. In all, temperature, salinity, oxygen and nutrients provide more than a dozen vertical extrema in the South Atlantic. Carbon dioxide, ^{14}C , ^3He , and freon provide still more.

These extrema are seen on the vertical sections (Figs. 11–15). Along 30°W (Fig. 12) the maxima in temperature, salinity, and oxygen, and the minima in phosphate and silica, all from the North Atlantic, are seen in the northern part of the section. They do not lie at a common depth or density, however. The temperature maximum is shallowest, then the silica minimum, salinity maximum, and finally the maximum oxygen and minimum phosphate, which are at about the same depth.

The extreme characteristics of the circumpolar water are seen between 50° and 60°S and extend toward the north beneath a shallow oxygen maximum and salinity minimum of the Intermediate Water, and contribute a phosphate maximum and oxygen minimum, a temperature minimum and a silica maximum.

Much the same features are seen on the western section, from the Weddell Sea to Brazil near 42°–50°W (Fig. 11). North of 39°S the section turns northwestward toward the coast, and the strong maxima in temperature, salinity, and oxygen, and the minimum in silica from the North Atlantic are seen near the western boundary.

On the section at the Greenwich Meridian (Fig. 13) the characteristics from the north are much the same as at 30°W near the equator. But the principal southward flow is in the west, and along the Greenwich Meridian the northern characteristics weaken to the south more, and the temperature, salinity, and oxygen are all lower at mid-depth than in the west. The deeper part of the Angola Basin is cut off from the denser southern waters by the Walvis Ridge, and is filled by waters entering from the west through the Romanche Fracture Zone which are warmer, more saline, higher in oxygen, and lower in nutrients than the deeper parts of the Brazil Basin.

The section along about 20°E (Fig. 14) shows the circumpolar features in the south, and the salinity and oxygen maxima in the north. The deeper waters are slightly less dense, warmer, and lower in oxygen than along the Greenwich Meridian.

The section near 32°S (Fig. 15) cuts across the meridional flow and shows the temperature maximum and minimum and the salinity maximum, which is strongest near the western boundary. The oxygen in the west between 2000 and 3000 m shows a minimum inside the great oxygen maximum, which decreases to a minimum near 4500 m, and a thin layer of higher oxygen at the bottom, corresponding to the cold abyssal water from the south.

Some of these extrema have been taken as cores of flow, but this is not quite correct. At any point such cores may relate the characteristics to their sources, but the successive downstream positions do not necessarily represent three-dimensional flow paths, as exchange with surrounding waters may shift the extrema to successively different depths and densities downstream. They may

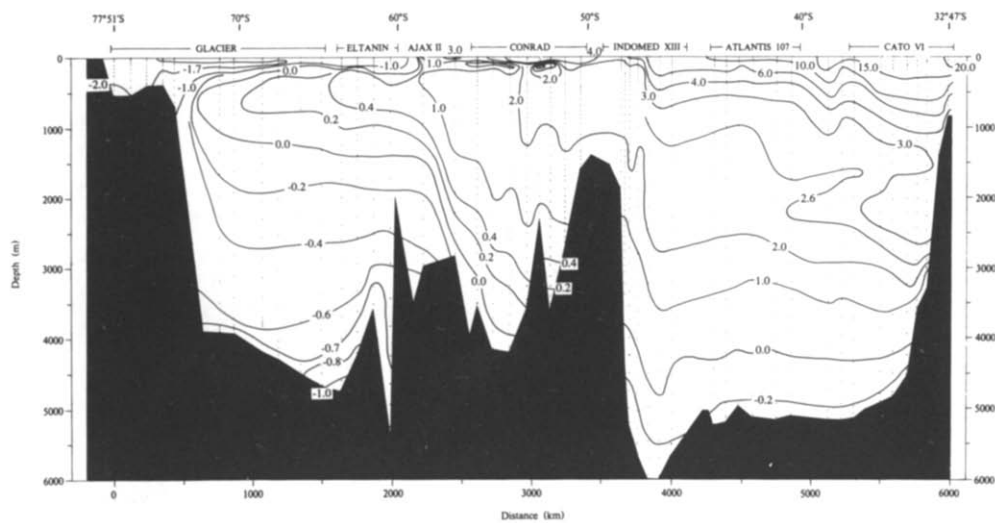


Fig. 11a. Potential temperature ($^{\circ}$ C) on the section from Antarctica to Brazil, along 40°W in the Weddell Sea and northwestward to the coast at 32°S.

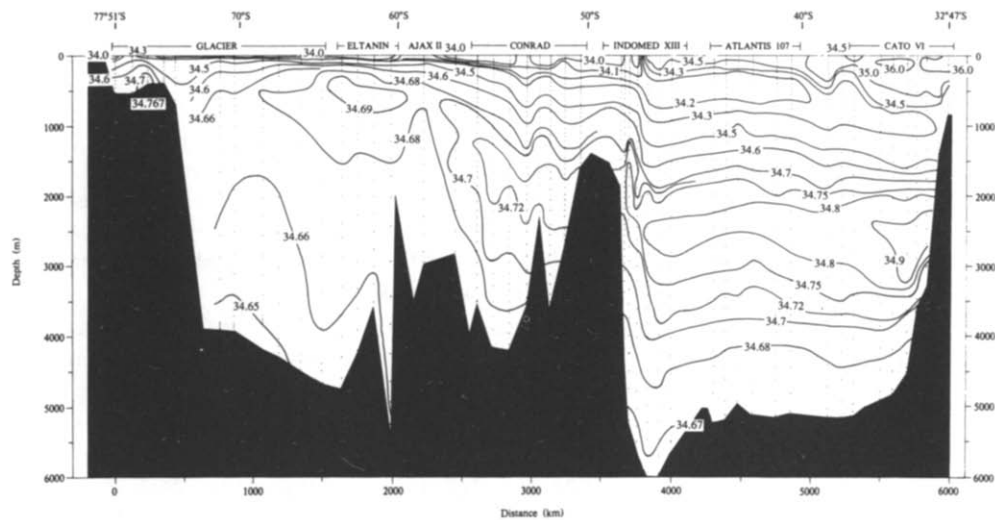


Fig. 11b. Salinity on the section from Antarctica to Brazil, along 40°W in the Weddell Sea and northwestward to the coast at 32°S.

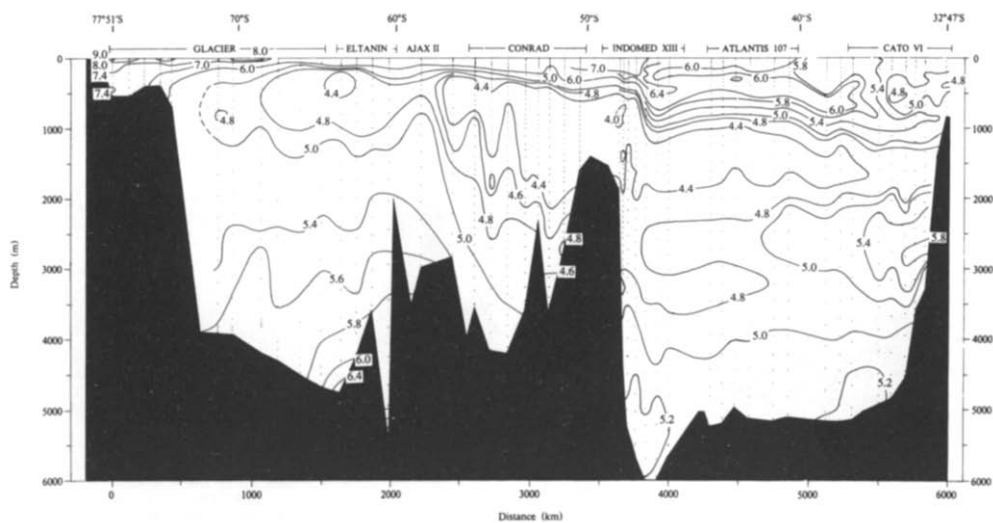


Fig. 11c. Oxygen ($\times 10^3$) on the section from Antarctica to Brazil, along 40°W in the Weddell Sea and northwestward to the coast at 32°S .

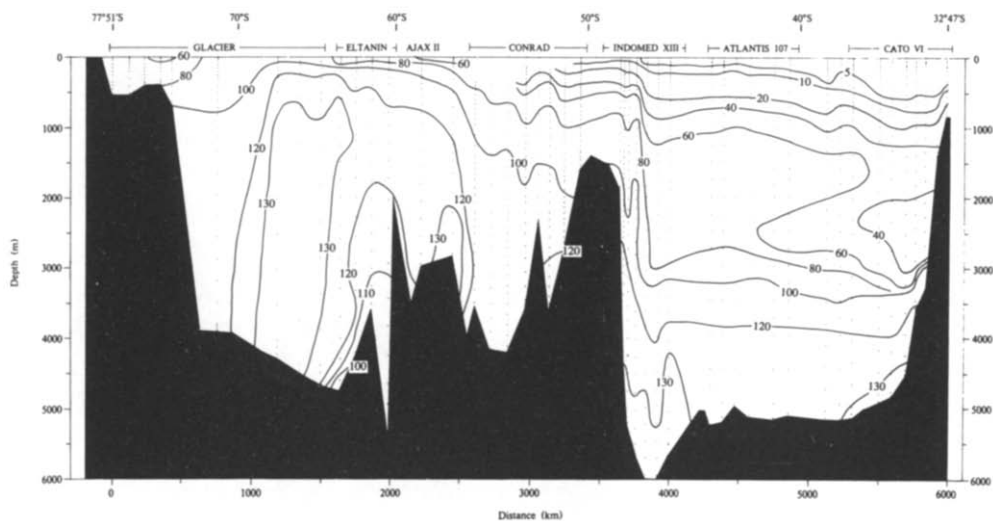


Fig. 11d. Silica (m mol m^{-3}) on the section from Antarctica to Brazil, along 40°W in the Weddell Sea and northwestward to the coast at 32°S .

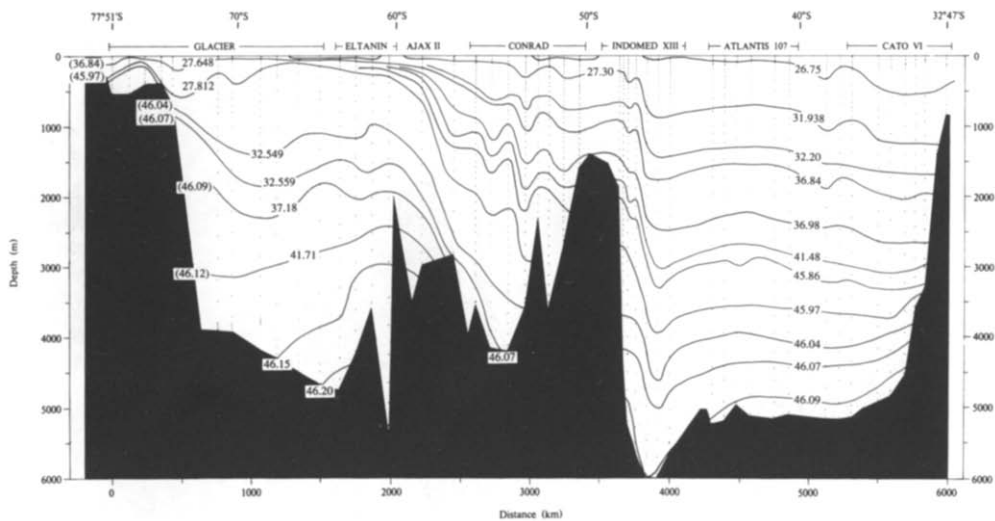


Fig. 11e. Potential density (σ_0 - σ_4) on the section from Antarctica to Brazil, along 40°W in the Weddell Sea and northwestward to the coast at 32°S.

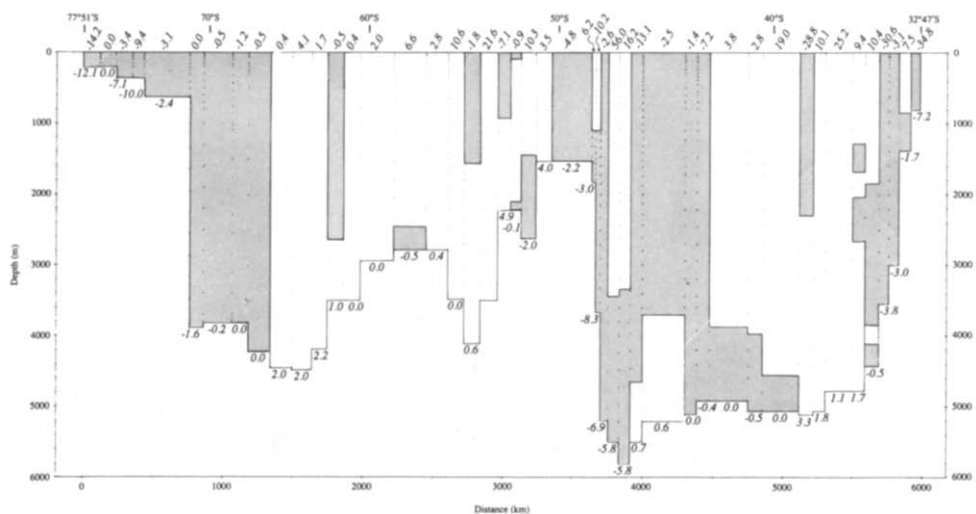


Fig. 11f. Total geostrophic speed in cm s^{-1} across the section from Antarctica to Brazil, along 40°W in the Weddell Sea and northwestward to the coast at 32°S . Numbers along the bottom give the bottom velocity (barotropic component). Hatching indicates westward flow. Slanting numbers at the top give the total geostrophic velocity at the surface.

represent only the least-altered remnants of the source-waters rather than continuous paths of flow. Further, such extrema may be mixed away or may disappear by passing over or under layers of more extreme concentrations. Extrema in the conservative characteristics can define their origins beyond doubt, but in the non-conservative characteristics the extrema can wax or wane downstream, independent of mixing, and may leave their sources uncertain. In oxygen and nutrients extrema can be produced subsurface by local processes, as in the case of the oxygen-minimum nutrient-maximum layers near 10°S in the east.

In the north, where the mid-depth waters are warmest and most saline, they occupy a broad density range. As they spread southward between layers of circumpolar water, vertical exchange takes place with the overlying colder and less saline waters and the extrema from the north (maxima in temperature, salinity, and oxygen, and minima in phosphate and silica) are found at successively higher densities farther south. Concurrently, the extrema in the overlying layer of circumpolar water (minima in temperature and oxygen, maxima in phosphate and silica) are found at lower densities toward the north.

Because of the vertical exchange that takes place along the flow, there is no single isopleth of depth, density, or tracer that can mark the boundary between two layers over any distance. Some generalizations can be made. The densest water entering through the Drake Passage can be taken as the maximum density of the circumpolar water in the South Atlantic: water densities greater than this must include a component from the denser waters formed within the Weddell Sea. And waters less dense than this in the abyssal Atlantic may contain a component of Weddell Sea water.

A maximum in Vaisala frequency near 3000–3500 m in the South Atlantic has been noted by SCHUBERT (1935) and taken as the boundary between the waters from the north and south. It lies just below the bend in the θ/S curve that has been detected over much of the North and South Atlantic. Both features lie at lower densities farther south.

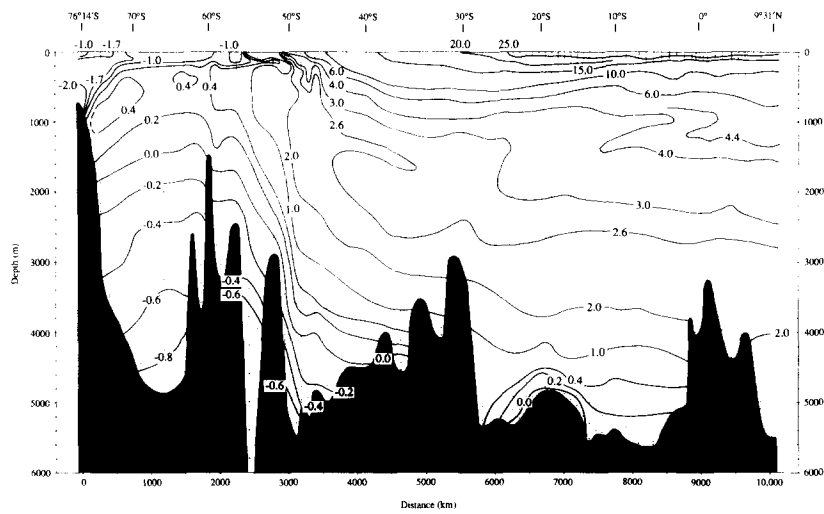


Fig. 12a. Potential temperature ($^{\circ}$ C) on the section near 30°W from Antarctica to 10°N.

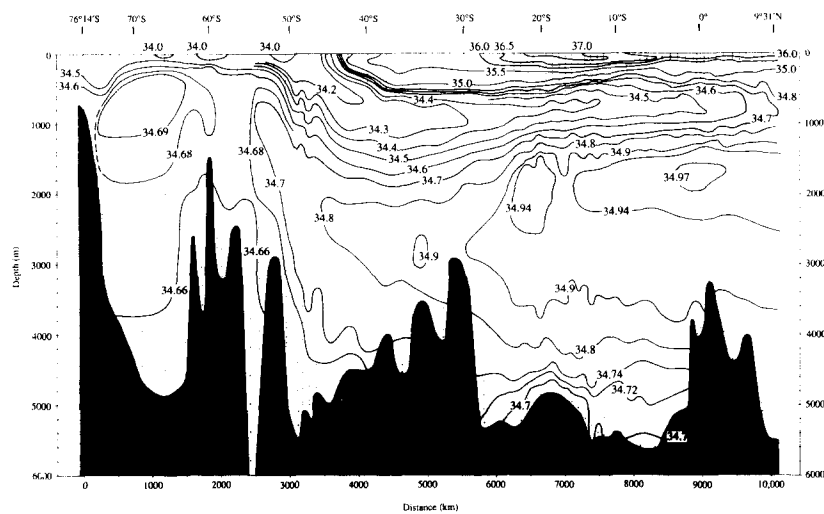


Fig. 12b. Salinity on the section near 30°W from Antarctica to 10°N.

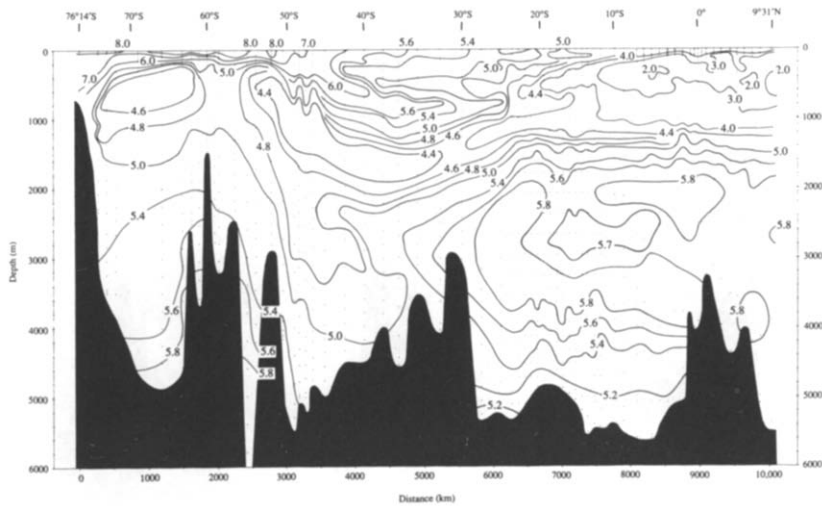


Fig. 12c. Oxygen ($\times 10^3$) on the section near 30°W from Antarctica to 10°N.

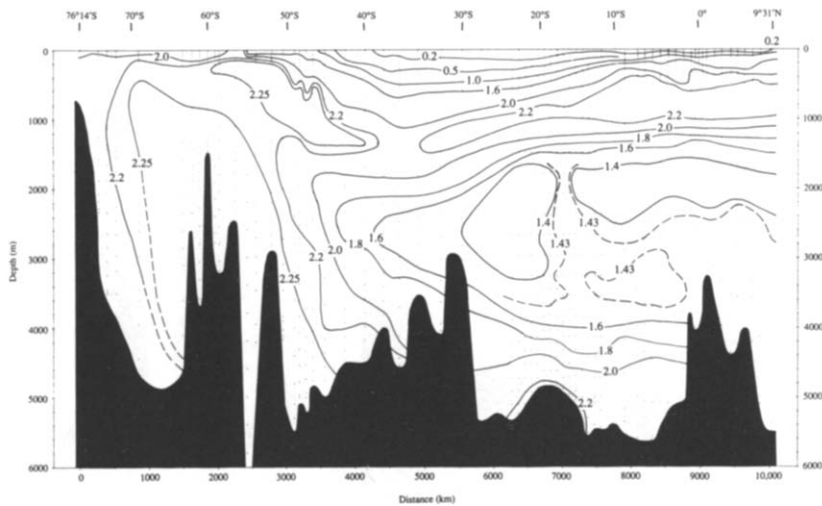


Fig. 12d. Phosphate (m mol m^{-3}) on the section near 30°W from Antarctica to 10°N.

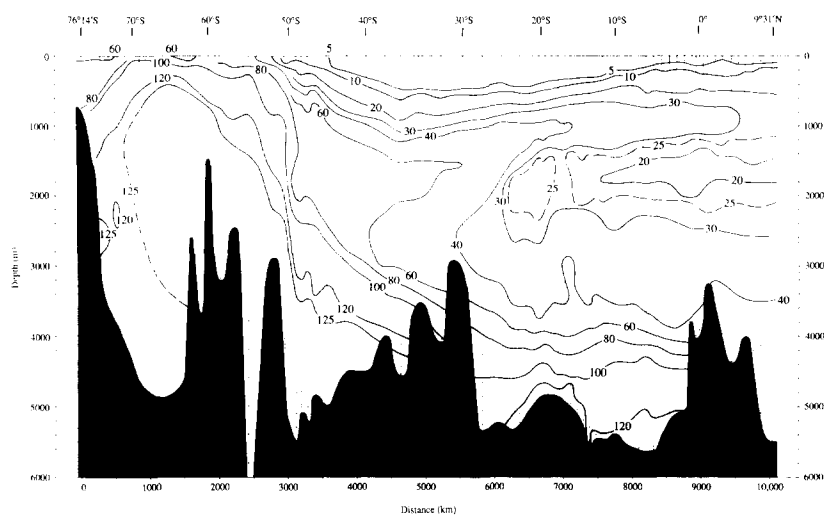


Fig. 12e. Silica (m mol m^{-3}) on the section near 30°W from Antarctica to 10°N .

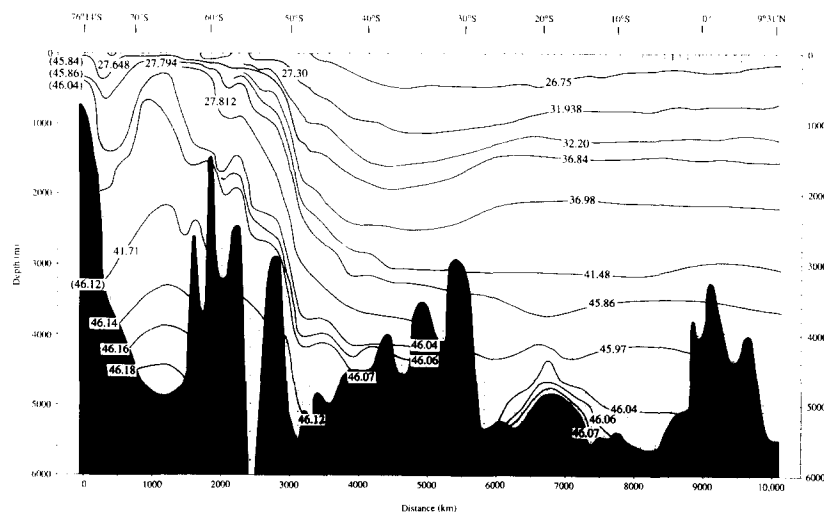


Fig. 12f. Potential density ($\sigma_0 - \sigma_4$) on the section near 30°W from Antarctica to 10°N .

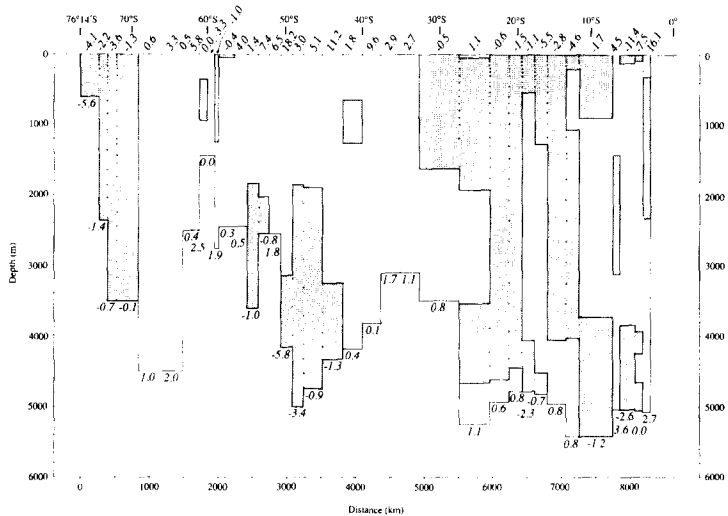


Fig. 12g. Total geostrophic speed in cm s^{-1} across the section near 30°W from Antarctica to 10°N . Numbers along the bottom give the bottom velocity (barotropic component). Hatching indicates westward flow. Slanting numbers at the top give the total geostrophic velocity at the surface.

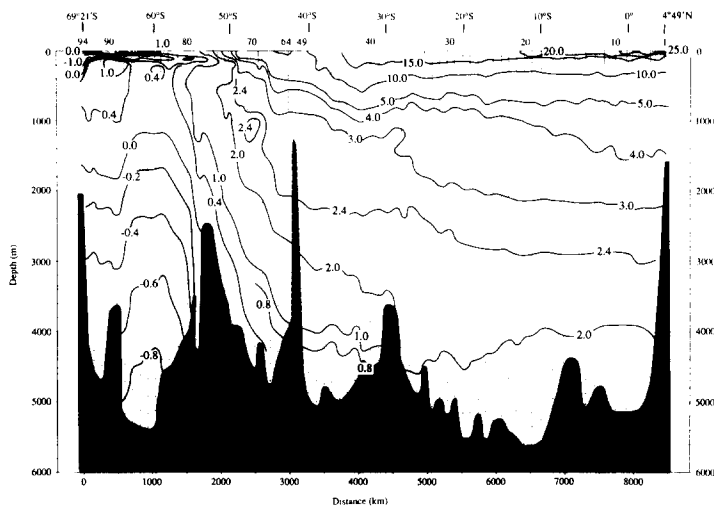


Fig. 13a. Potential temperature ($^{\circ}$ C) on the section near the Greenwich Meridian from Antarctica to 5 $^{\circ}$ N. The hatched feature rising to about 1300 m near 42 $^{\circ}$ S is not a ridge, but one of the *Discovery Seamounts*.

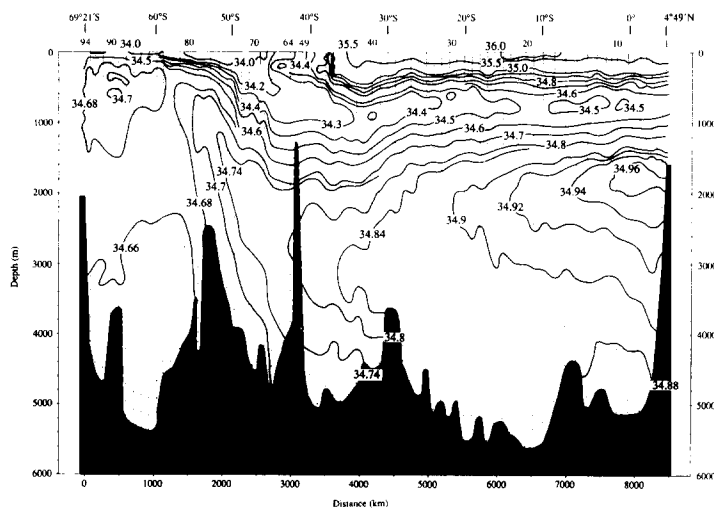


Fig. 13b. Salinity on the section near the Greenwich Meridian from Antarctica to 5 $^{\circ}$ N.

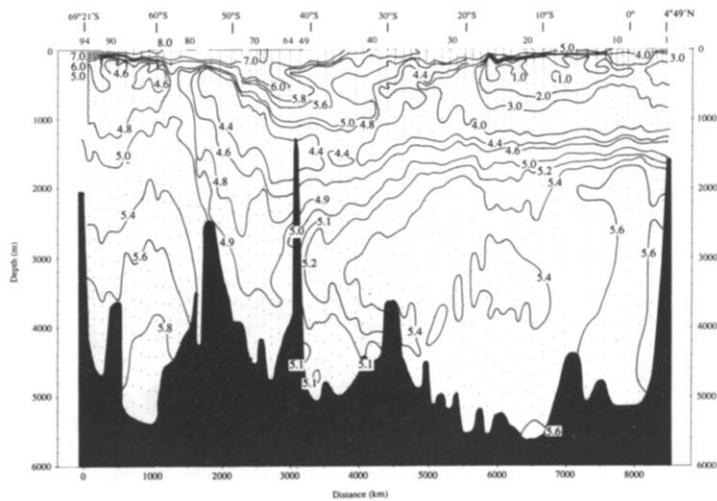


Fig. 13c. Oxygen ($\times 10^3$) on the section near the Greenwich Meridian from Antarctica to 5°N .

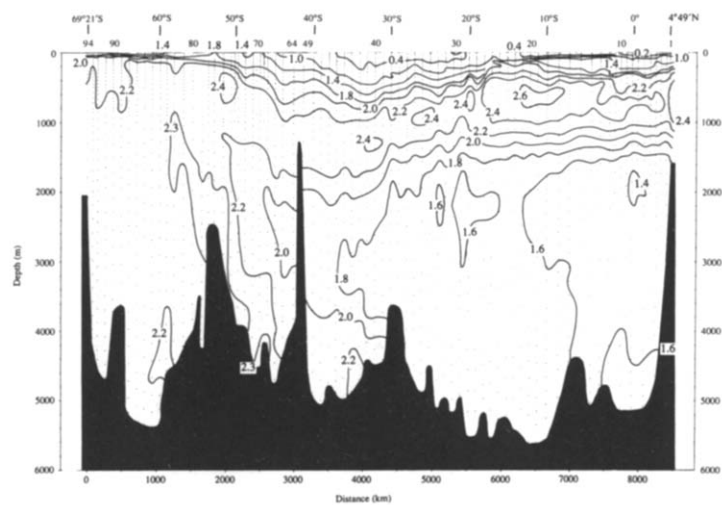


Fig. 13d. Phosphate (m mol m^{-3}) on the section near the Greenwich Meridian from Antarctica to 5°N .

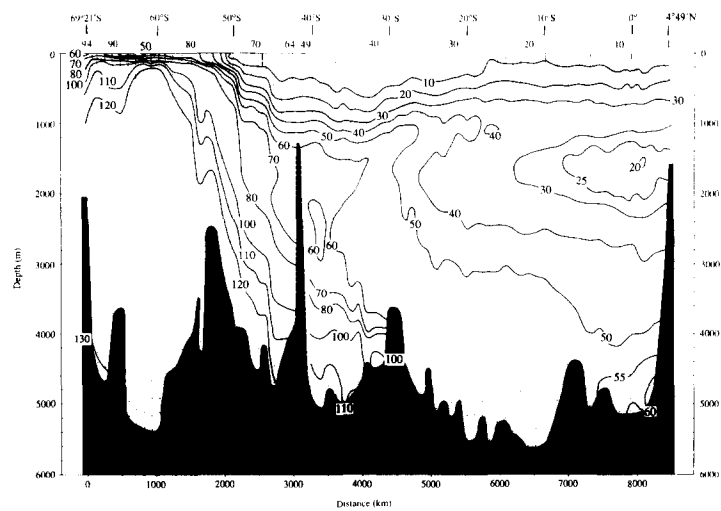


Fig. 13e. Silica (m mol m^{-3}) on the section near the Greenwich Meridian from Antarctica to 5°N .

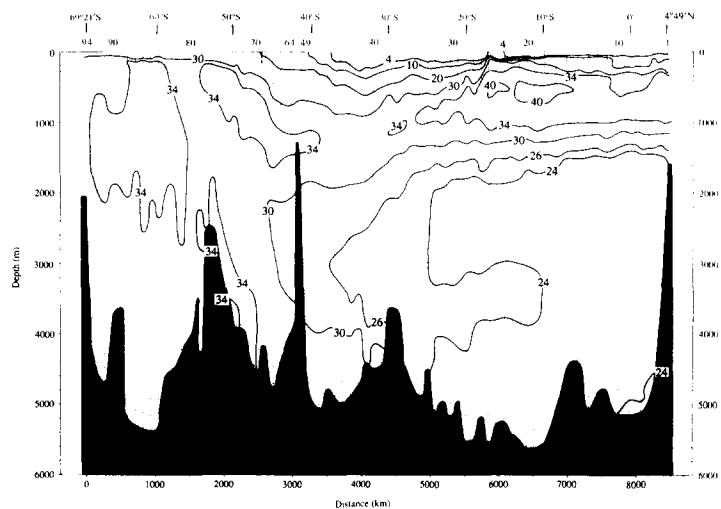


Fig. 13f. Nitrate (m mol m^{-3}) on the section near the Greenwich Meridian from Antarctica to 5°N .

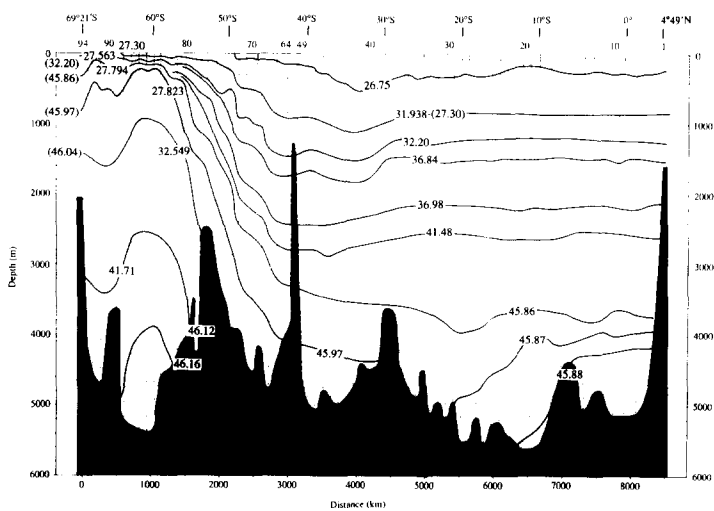


Fig. 13g. Potential density ($\sigma_0 - \sigma_4$) on the section near the Greenwich Meridian from Antarctica to 5°N .

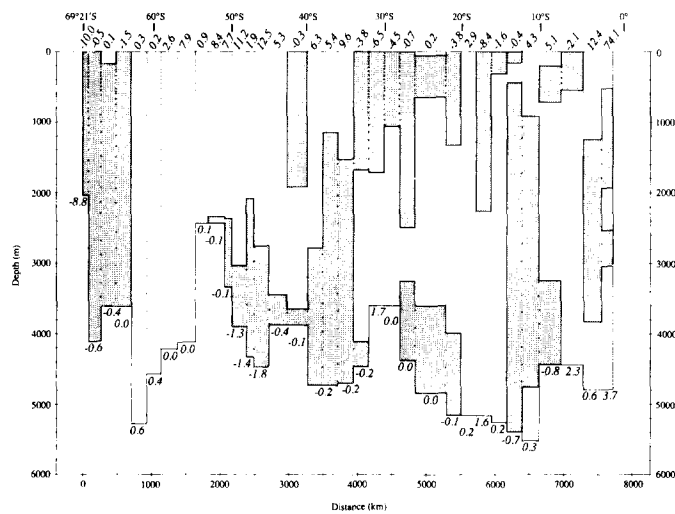


Fig. 13h. Total geostrophic speed in cm s^{-1} across the section near the Greenwich Meridian from Antarctica to 5°N . Numbers along the bottom give the bottom velocity (barotropic component). Hatching indicates westward flow. Slanting numbers at the top give the total geostrophic velocity at the surface.

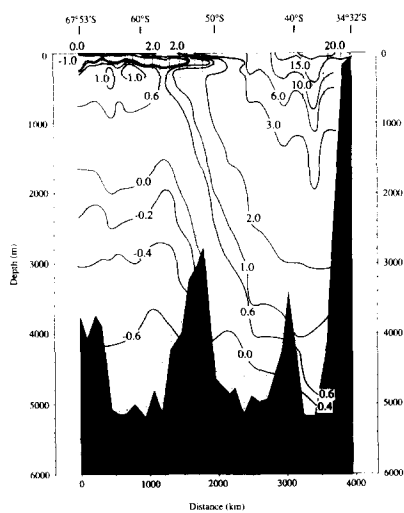


Fig. 14a. Potential temperature ($^{\circ}$ C) on the section near 20 $^{\circ}$ E from Antarctica to Africa.

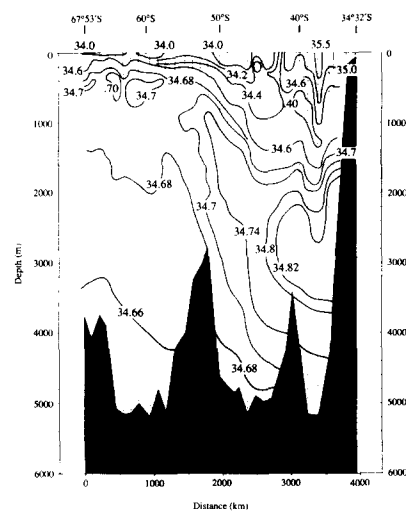


Fig. 14b. Salinity on the section near 20 $^{\circ}$ E from Antarctica to Africa.

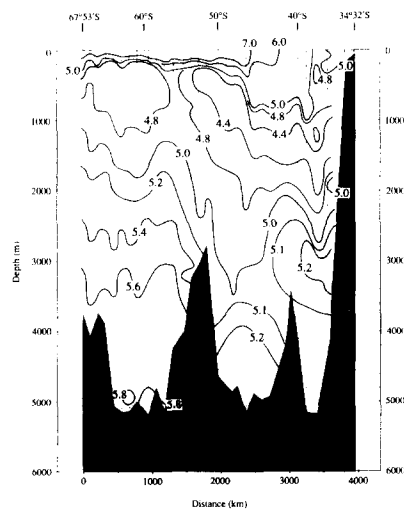


Fig. 14c. Oxygen ($\times 10^3$) on the section near 20 $^{\circ}$ E from Antarctica to Africa.

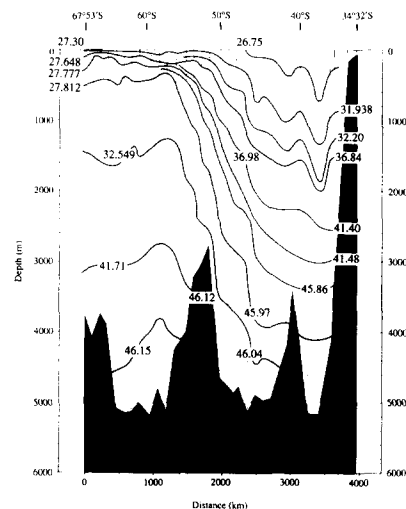


Fig. 14d. Potential density ($\sigma_0 - \sigma_4$) on the section near 20 $^{\circ}$ E from Antarctica to Africa.

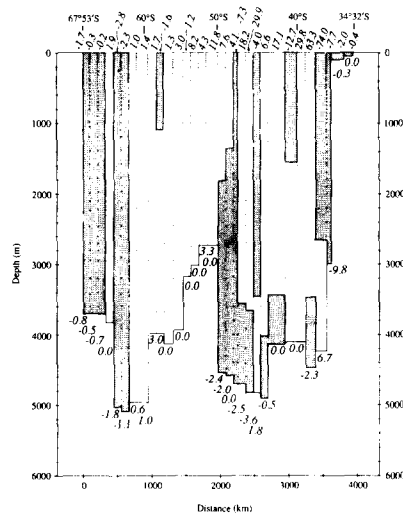


Fig. 14e. Total geostrophic speed in cm s^{-1} across the section near 20°E from Antarctica to Africa. Numbers along the bottom give the bottom velocity (barotropic component). Hatching indicates westward flow. Slanting numbers at the top give the total geostrophic velocity at the surface.

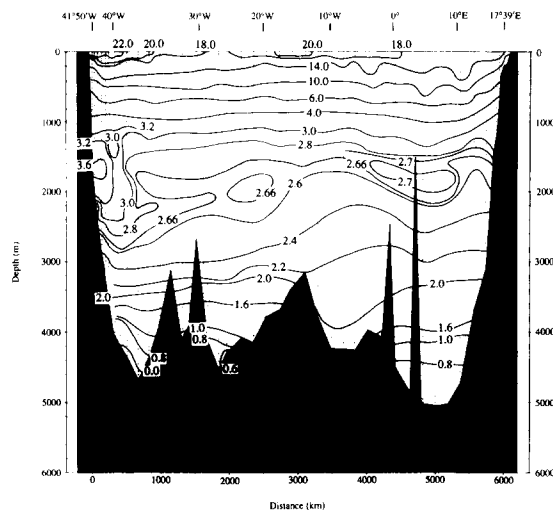


Fig. 15a. Potential temperature ($^{\circ}$ C) on the section along 32°S east of 30°W and northwestward to the coast.

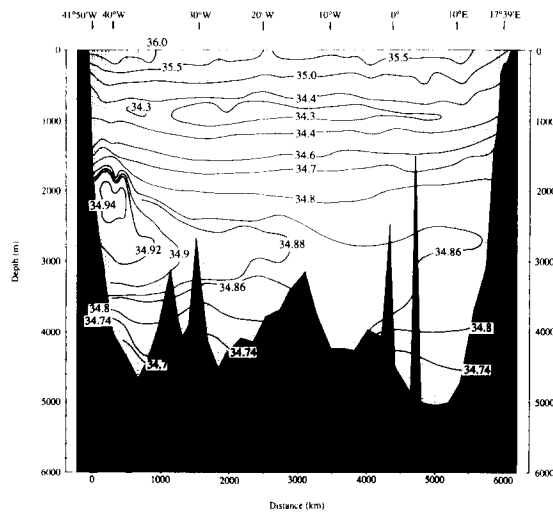


Fig. 15b. Salinity on the section along 32°S east of 30°W and northwestward to the coast.

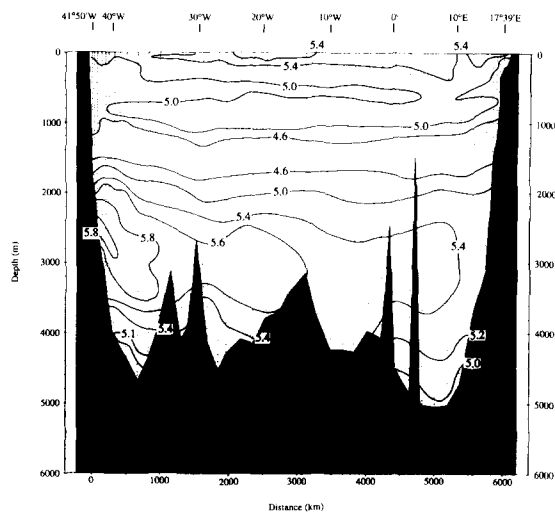


Fig. 15c. Oxygen ($\times 10^3$) on the section along 32°S east of 30°W and northwestward to the coast.

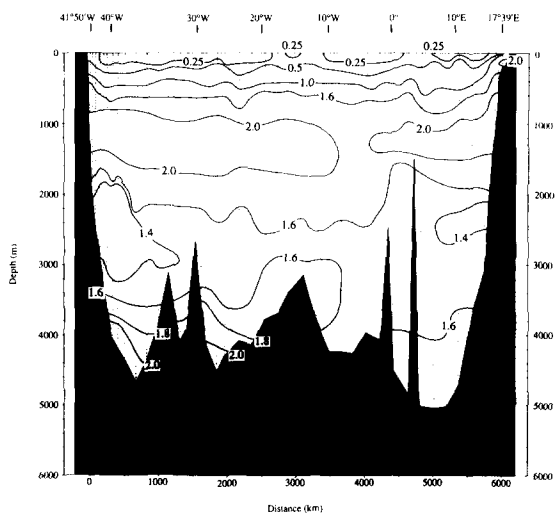


Fig. 15d. Phosphate (m mol m^{-3}) on the section along 32°S east of 30°W and northwestward to the coast.

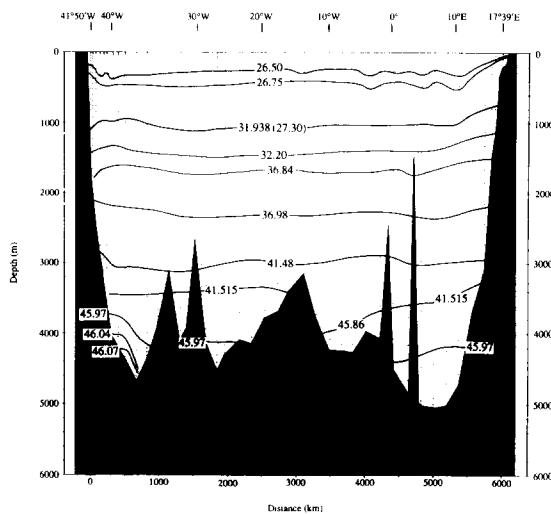


Fig. 15e. Potential density ($\sigma_0 - \sigma_4$) on the section along 32°S east of 30°W and northwestward to the coast.

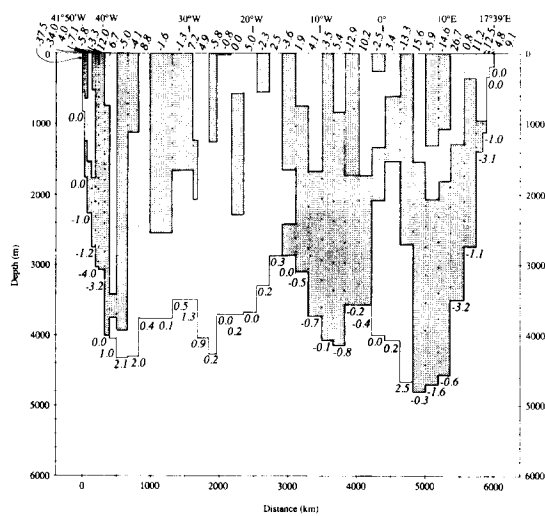


Fig. 15f. Total geostrophic speed in cm^{-1} across the section along 32°S east of 30°W and northwestward to the coast. Numbers along the bottom give the bottom velocity (barotropic component). Hatching indicates southward flow. Slanting numbers at the top give the total geostrophic velocity at the surface.

7. THE INTERMEDIATE WATER

The shallowest distinct layer includes a subsurface oxygen maximum and just below it a salinity minimum, which WUST (1935) called Intermediate Water. As they exist all around the Southern Ocean these might be included with the circumpolar layer, but as they derive directly from the surface layer, they have been treated separately here.

They are recognized as subsurface extrema north of about 50°S. The density at the oxygen maximum increases from about 27.12 in σ_0 near 45°S to about 27.23 at 15°S in the west (Fig. 12). The oxygen maximum disappears as it meets the strong oxygen minimum of the equatorial zone, near 15°S in the west and 25°S in the east. The salinity minimum lies a little deeper, near 27.20 in σ_0 at 45°S, and 27.30 and 31.938 in σ_1 near the equator. A value of 31.938 in σ_1 was chosen to represent the Intermediate Water. It lies deepest, slightly below 1000 m, near 30°–35°S and rises to about 800 m where it extends across the equator and outcrops south of 60°S (Fig. 16). North of 20°S the isopycnal does not vary much in depth, indicating very little shear in this depth range, but not necessarily a weaker flow: as will be seen, the circulation from 500 db down through 1500 db is fairly uniform north of 20°S.

The water along the salinity minimum just north of the outcrop has the high oxygen and lower phosphate characteristic of its surface origin, but the Weddell Sea silica is so high, even in the surface water, that it shows as the maximum value on the map (Figs. 16c, d, e). As it is even higher than in the Drake Passage water, it is seen as a lateral maximum extending around the anticyclonic gyre.

As the isopycnal deepens farther north (Fig. 16a), respiration decreases the oxygen and increases the phosphate along the flow. The extreme values are found in the east along about 10°–15°S. They appear to result from fallout and regeneration of materials from the euphotic layer within the zone of cyclonic flow and upwelling, as on the shallower isopycnal.

On this isopycnal the salinity pattern (Fig. 16b) does not show the enclosed high value that was seen at shallower depths near the western boundary between 20°S and 40°S (Fig. 8). Though the large-scale flow pattern is much the same (Fig. 17), this isopycnal lies deeper within the anticyclonic cell that is centered near 35°S, 40°W, and the great accumulation of highly-saline waters found near 26.75 in σ_0 there does not result in a lateral maximum on this isopycnal (Fig. 16b). The highest salinity on this isopycnal has entered from the North Atlantic, extending southward near the eastern boundary and eastward along the equator.

WUST (1935) had proposed that the principal northward flow of the Intermediate Water is along the western boundary, in a continuous flow from the Falkland Current to the equator, where part of it continues into the North Atlantic and part turns eastward just south of the equator. Other investigators (TAFT, 1963; BUSCAGLIA, 1971) have proposed that the northward flow of the Intermediate Water does not take place everywhere along the western boundary, but only south of about 40°S in the Falkland Current and north of about 25°S; between those two latitudes it flows around the great anticyclonic gyre eastward, northward, and westward to the boundary again, and then northward to the equator. For the immediately overlying water (as in Fig. 8) this would appear to be true, but the salinity pattern of Fig. 16b does not resolve the question at this depth.

With Pegasus measurements, EVANS and SIGNORINI (1985) have found some northward flow of Intermediate Water near 23°S. This is about where at that depth the westward-flowing limb of the anticyclonic gyre approaches the coast, with part continuing southward around the gyre and part continuing northward (Fig. 17). The presence of a narrow northward flow from 35°S to 25°S in the far west at the depth of the salinity minimum is not demonstrated by the present data set, nor is it entirely precluded. Perhaps direct measurements near 30°S would be required to resolve the matter.

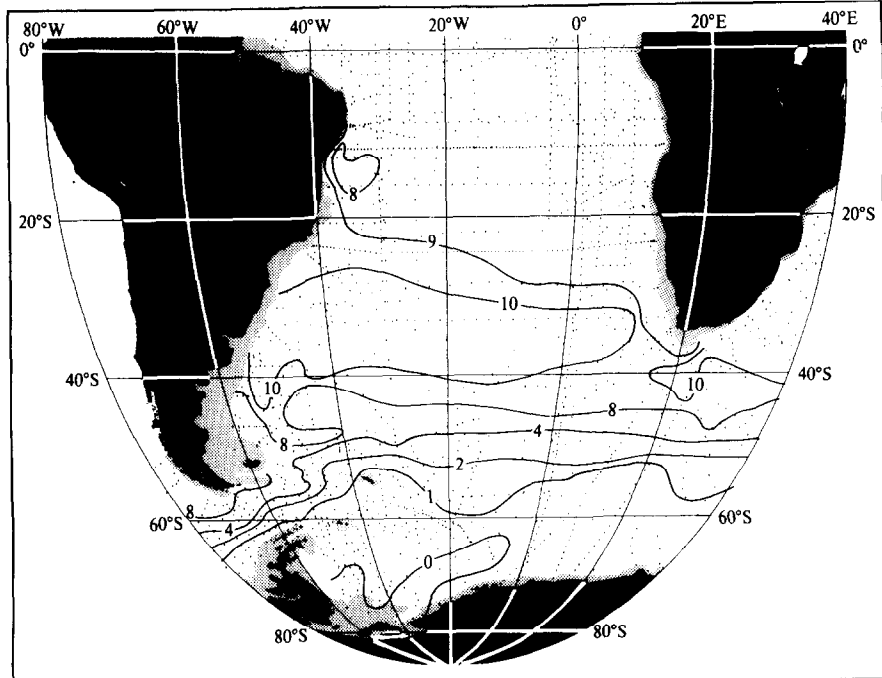


Fig. 16a. Depth (hm) of the isopycnal defined by 31.938 in σ_1 (27.30 in σ_0). On this and all the other isopycnal maps the shaded parts represent areas where all the water is less dense than the isopycnal value.

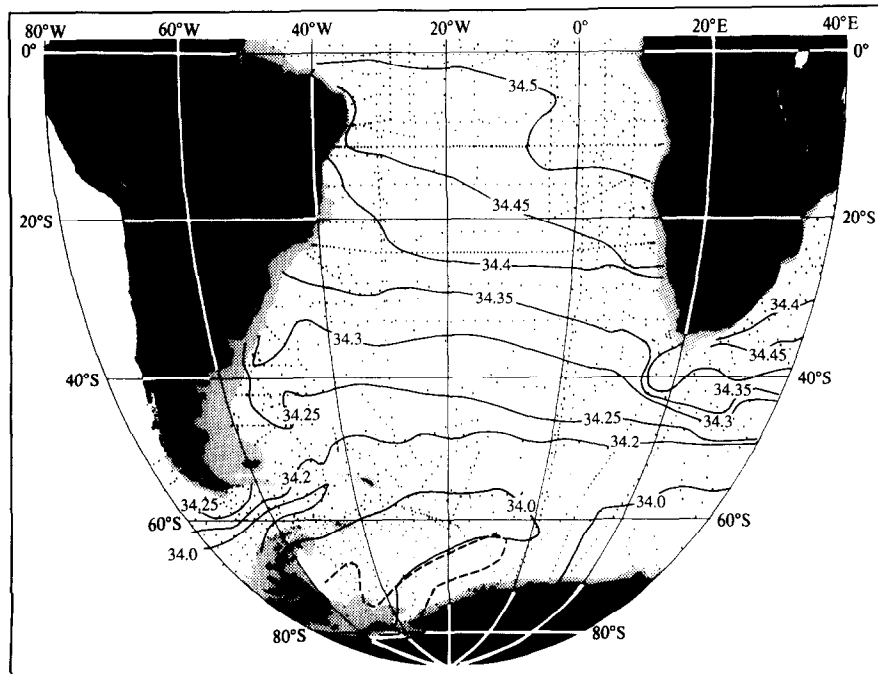


Fig. 16b. Salinity on the isopycnal defined by 31.938 in σ_1 (27.30 in σ_0).

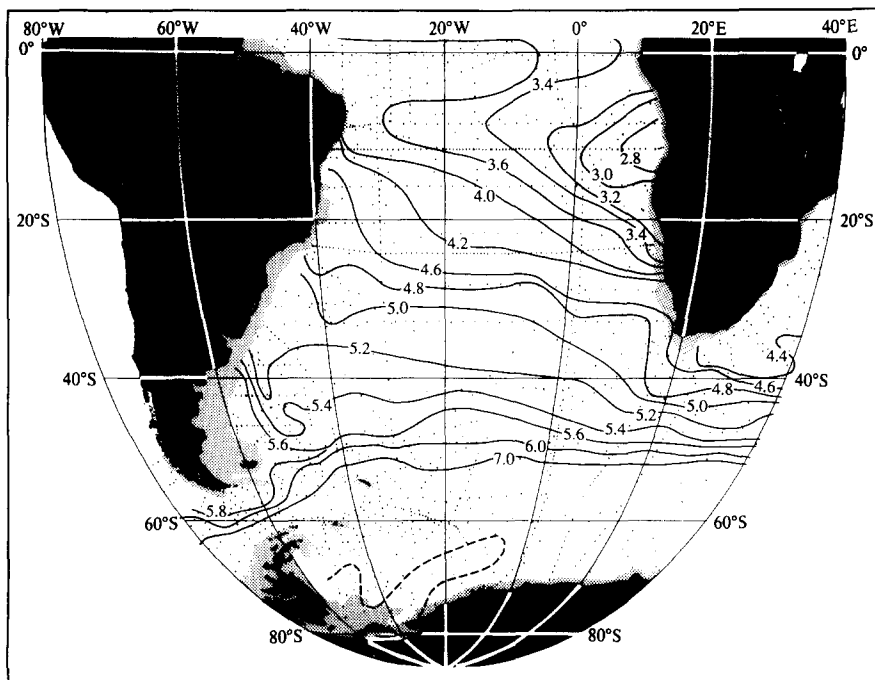


Fig. 16c. Oxygen ($\times 10^3$) on the isopycnal defined by 31.938 in σ_1 (27.30 in σ_0).

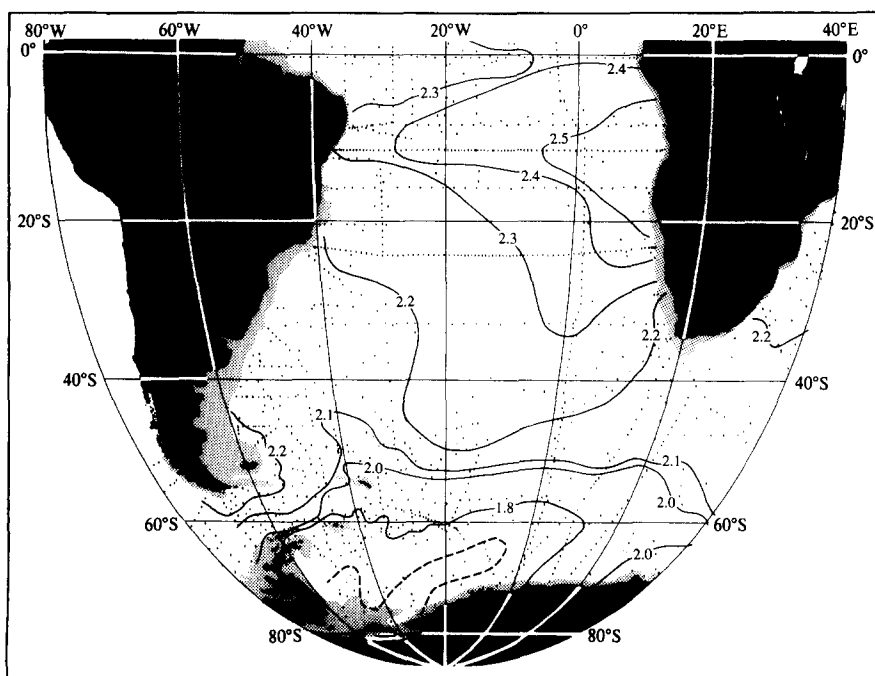


Fig. 16d. Phosphate (m mol m^{-3}) on the isopycnal defined by 31.938 in σ_1 (27.30 in σ_0).

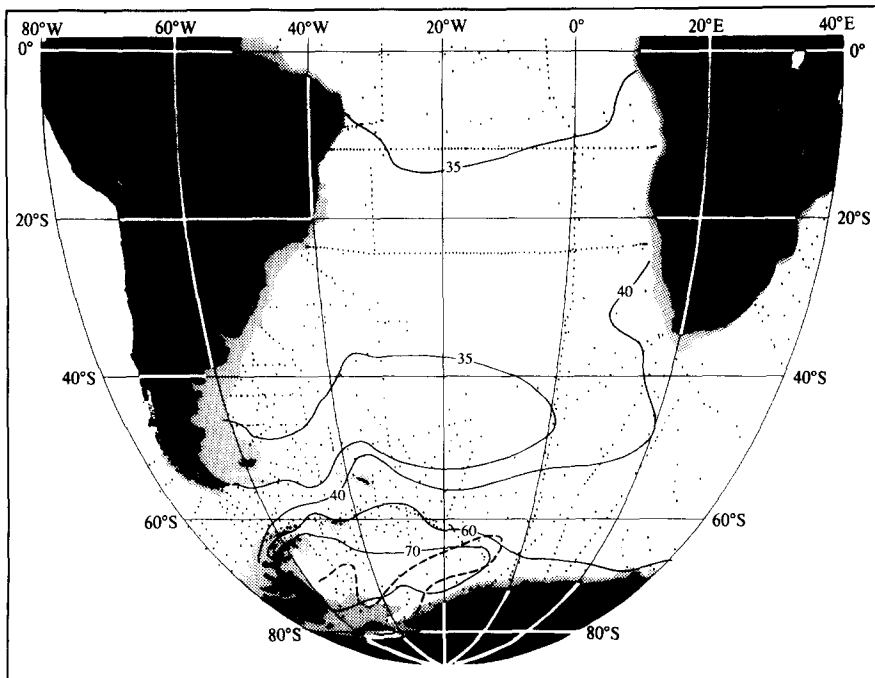


Fig. 16e. Silica (m mol m^{-3}) on the isopycnal defined by 31.938 in σ_1 (27.30 in σ_0).

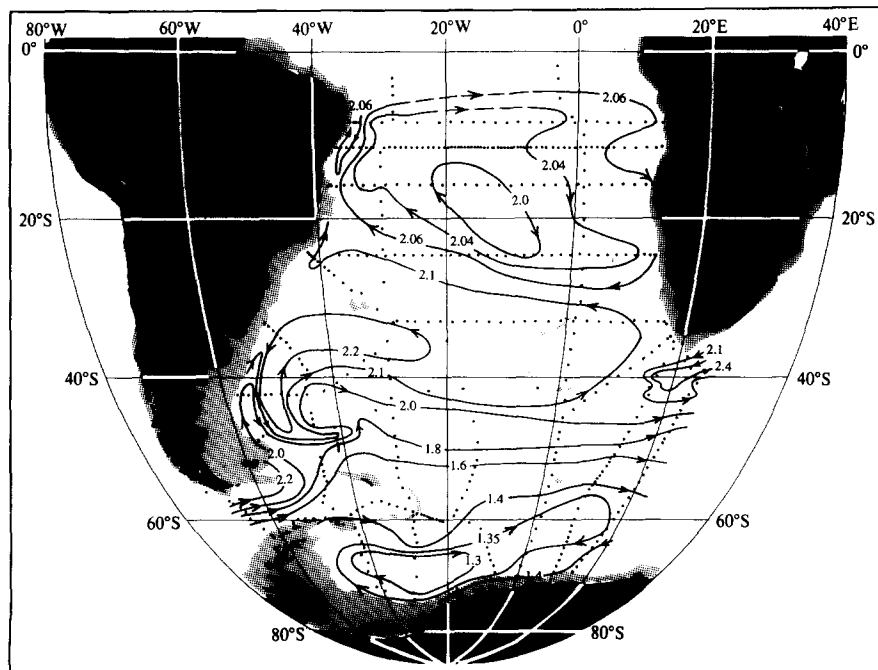


Fig. 17. Adjusted steric height ϕ_A at 800 db ($10 \text{ m}^2 \text{ s}^{-2}$ or 10 J kg^{-1}). Depths less than 1000 m are shaded.

8. CIRCUMPOLAR WATER AND WATER FROM THE NORTH ATLANTIC

The upper waters of the Antarctic Circumpolar Current just north of the axis of the Weddell Sea gyre have come directly from the Drake Passage (CLOWES, 1933 and 1938), where the density ranges from about 27.40 in σ_0 at the sea surface in winter to about 46.06–46.07 in σ_4 at the bottom. These are circumpolar waters and their characteristics and extrema (temperature and oxygen minima, nutrient maxima) are found all across the South Atlantic in this density range, above the dense waters deriving from the Weddell Sea. Their characteristics within the Drake Passage have been described and discussed by SIEVERS and NOWLIN (1984), and WHITWORTH and NOWLIN (1987) have discussed the transformation that takes place between the Drake Passage and the Greenwich Meridian.

The denser layer of maximum salinity in the circumpolar water continues eastward from the Drake Passage across the South Atlantic, and near 20°E–30°E, part of it also turns cyclonically around the Weddell Sea gyre. It provides the layer of high temperature, salinity, and nutrients and low oxygen seen south of the gyre axis (Fig. 12). The ridging of the isopycnals south of about 60°S reflects the axis of the baroclinic gyre and the surface divergence, and vertical exchange in this constricted depth-range maintains the separation of the warm and saline layers to the north and south of the axis.

North of about 55°S the circumpolar water encounters the layer of warm, saline, oxygen-rich and nutrient-poor water from the North Atlantic. The density range of this northern water is narrower than that of the circumpolar water, from about 32.28 in σ_1 to 45.86 in σ_4 . It lies within the circumpolar density range and in the western South Atlantic penetrates it from the north, dividing it into an upper and a lower layer as far as about 55°S (REID, NOWLIN, and PATZERT, 1977), where the northern water turns eastward with the Circumpolar Current. Also, another layer, from the mid-density range of the circumpolar water, extends northward near the Mid-Atlantic Ridge, mixing with the northern waters along the path. The mixed water turns westward near 20°S, penetrating some distance into the North Atlantic water at mid-depth, near 2000–3000 m (Figs. 12b–e).

As the northern and southern waters have different characteristics their interleaving provides several extrema. Neither layer is from a point-source and each source has several extrema, at different depths and densities. Where they interleave in the South Atlantic and undergo some mixing, it is not possible to define the upper and lower transitions from circumpolar to northern water by unique depth- or density-boundaries that apply for the whole South Atlantic.

As the northern waters penetrate southward into the circumpolar layer their density-range is thinned by vertical exchange with the overlying and underlying waters, which have opposite extrema. Likewise the density range of the two layers of circumpolar waters is thinned as they extend northward.

Approximate limits can be chosen to apply near 10°S, dividing the upper layer of circumpolar water from the North Atlantic water at about 32.28 in σ_1 , and the lower layer at about 45.85 in σ_4 . The deeper limit lies in the top of the layer of high stability that SCHUBERT (1935) identified from the Meteor data, and that has been taken as a shift from the warmer and more saline northern water to the deeper southern water. The high values in Vaisala frequency begin just below the break in the θ/S curve that is observed from about 40°N to 30°S. Below the break the curve lies more nearly parallel to the isopycnals appropriate to the local pressure. The change in slope is so sharp the isopycnals calculated assuming zero hydrostatic pressure would cross the θ/S curve twice near the break, showing a maximum in σ_0 (LYNN and REID, 1968): isopycnals calculated for the appropriate pressures (σ_3 and σ_4) do not cross twice. Near 10°S the maximum frequency appears to be at about 45.88 in σ_4 . WRIGHT (1970) pointed out the break that is found in the θ/S curve

near 2°C over much of the western Atlantic and used it in a calculation of the deep northward transport. BROECKER, TAKAHASHI, and LI (1976) and BROECKER, TAKAHASHI, and STUIVER (1980) discussed it in a study of the sources and exchange of waters along the feature and pointed out that its temperature and salinity decrease southward.

9. THE UPPER CIRCUMPOLAR WATER

The circumpolar water is lower in temperature, salinity and oxygen and higher in nutrients than the North Atlantic waters. In the part of the circumpolar water that turns northward into the western Atlantic along 30°W the layer above the water from the north shows four separate extrema, beginning near 45°S with a phosphate maximum (at about 32.13 in σ_1), an oxygen minimum (at about 32.28 in σ_1), a temperature minimum near 32.15 and a silica maximum near 32.25 in σ_1 .

The near-coincidence of the temperature minimum with the oxygen minimum and silica maximum suggests that it derives from a source different from the surface-layer source of the overlying Intermediate Water, which is higher in oxygen (indeed, a vertical maximum south of 20°S) and lower in silica south of 30°S. The water at the temperature minimum requires a southern source, but the two non-conservative characteristics, oxygen and silica, which are not directly related through regeneration, require a sub-surface origin, which by comparison with the Drake Passage characteristics (SIEVERS and NOWLIN, 1984), must be the circumpolar water.

The phosphate and silica maxima on the vertical sections extend across the equator, decreasing northward in concentration and terminating in the upper pycnocline near 50°N (TSUCHIYA, 1989). The oxygen minimum also extends to the north but near 10°S it passes beneath the even lower equatorial concentration and loses its identity (BAINBRIDGE, 1980).

The temperature minimum extends to about 10°N in the west (WUST, 1935). It lies deepest at about 1500 m near 40°S (near 32.15 in σ_1) and rises to about 1000 m (near 32.03 in σ_1) near the equator. It lies close to the oxygen minimum from about 40°S to 5°S, where the oxygen maximum of the Intermediate Water ends and the circumpolar layer of low oxygen merges with the shallower oxygen minimum.

WUST (1935) has taken this temperature minimum to be the bottom of the Intermediate Water. However, as it derives from the subsurface waters of the Drake Passage, and is low in oxygen, it is taken here to be part of the circumpolar water. He illustrated the temperature profile in various places in his comparisons of Meteor and other stations in an examination of secular variations. As the temperature minimum lies deeper than the salinity minimum, in the depth range with wider bottle spacing, it was not defined well enough in some areas, to serve as a core in his data. He did recognize it as lying at about the same depth as an oxygen minimum, which was thicker and defined better.

The patterns of tracers for this layer are illustrated on the isopycnal surface where $\sigma_1 = 32.20$ (Fig. 18) and the flow pattern on Figs. 7, 9, 10, 17, 19 and 20.

Its salinity pattern (Fig. 18b) is much like that of the Intermediate Water, though the values are higher by about 0.25, but the oxygen and nutrients show opposite extrema in the waters flowing through the Drake Passage (Figs. 18c–e).

On the shallower isopycnal (Fig. 16) the waters are derived from the surface layer, and are high in oxygen and low in phosphate (Figs. 16c–e); downstream into the South Atlantic oxygen decreases and phosphate increases. But the circumpolar waters entering from the Drake Passage are low in oxygen and high in phosphate (Figs. 18c, d). These waters flow eastward along about 45°S and turn northward and westward near the Greenwich Meridian (Fig. 20). As the oxygen in

this layer is a vertical minimum, its concentration increases to its highest values within the gyre near 30°S (Fig. 12), beneath the oxygen maximum of the Intermediate Water. The lowest oxygen values are found under the area of the oxygen minimum in the upper waters near 10°S in the east. The phosphate in this layer is a vertical maximum, and its concentration decreases northward (Fig. 18d) along the path of flow, except where it lies beneath the area of the phosphate maximum in the upper waters near 10°S along the eastern boundary.

Silica (Fig. 18e) is also a maximum in this layer and diminishes downstream to the north. In the South Atlantic it is lowest in the western equatorial zone (MANN, COOTE, and GARNER, 1973). Unlike oxygen and phosphate, it is not affected substantially by fallout from the overlying waters in the northeast. The oxygen minimum and nutrient maximum of the overlying waters in that area does not bear upon the silica pattern.

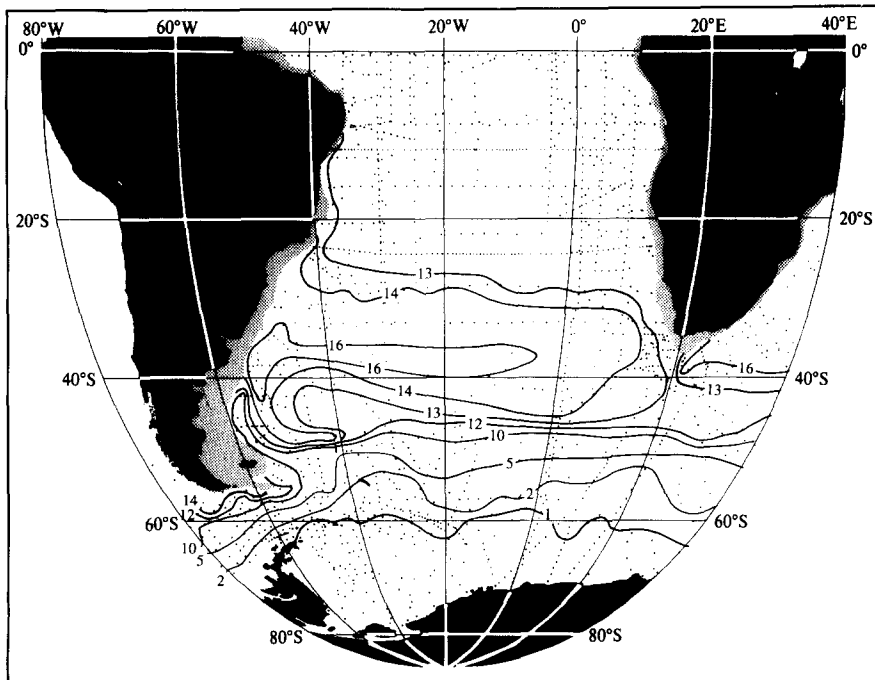


Fig. 18a. Depth (hm) of the isopycnal defined by 32.20 in σ_1 below 500 m.

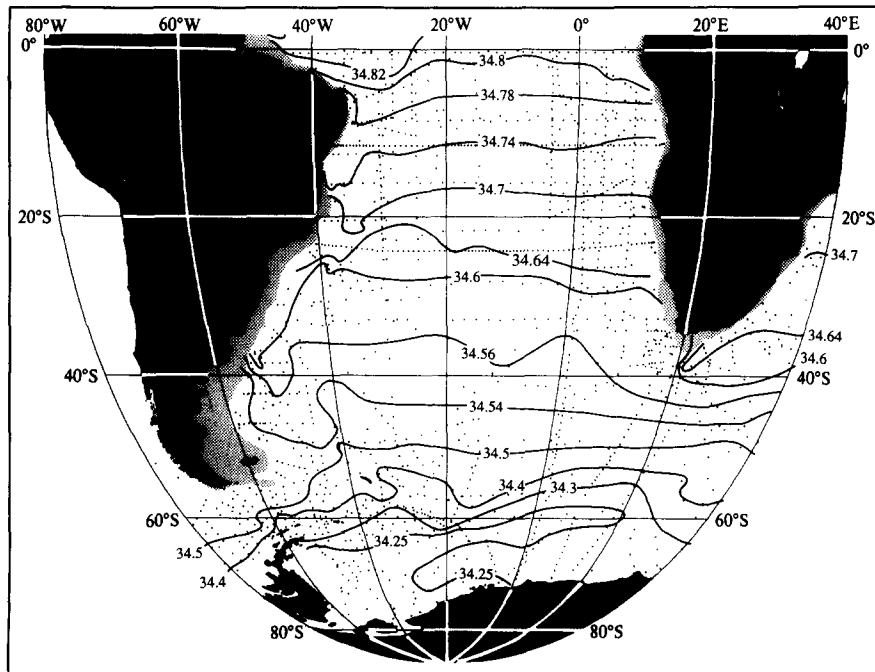


Fig. 18b. Salinity on the isopycnal defined by 32.20 in σ_2 below 500 m.

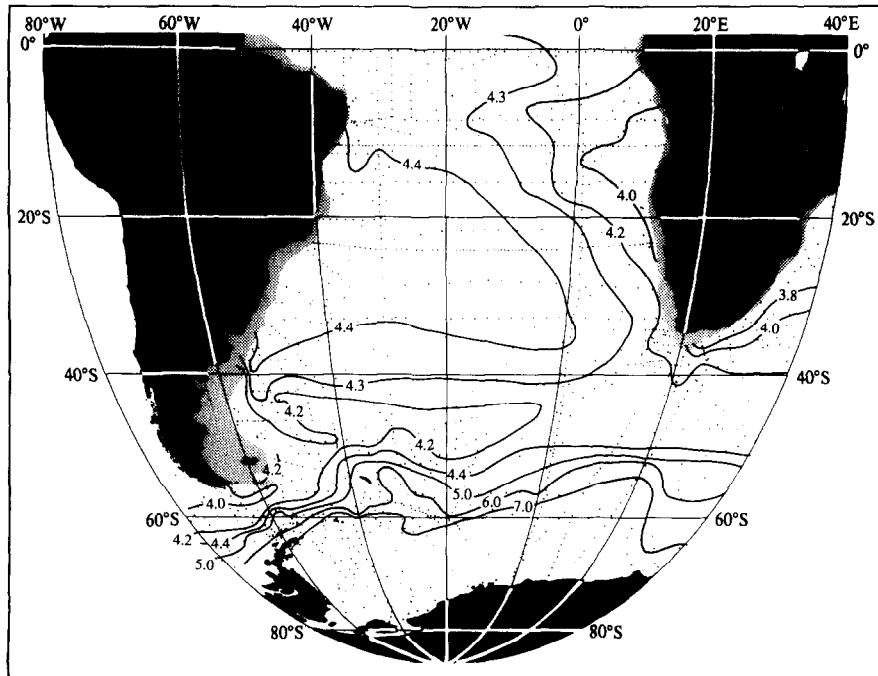


Fig. 18c. Oxygen ($\times 10^3$) on the isopycnal defined by 32.20 in σ_2 below 500 m.

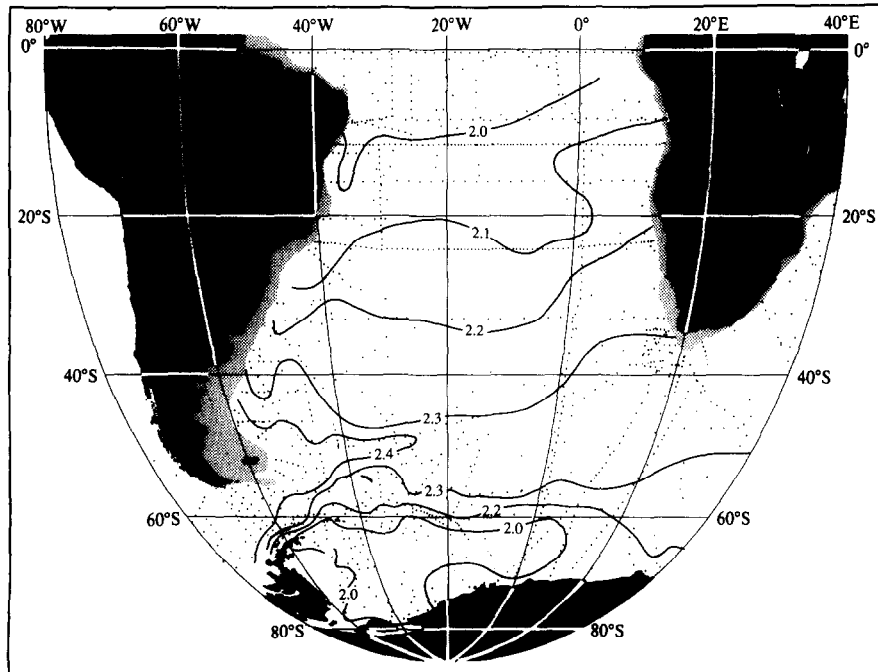


Fig. 18d. Phosphate ($m\text{ mol m}^{-3}$) on the isopycnal defined by 32.20 in σ_2 below 500 m.

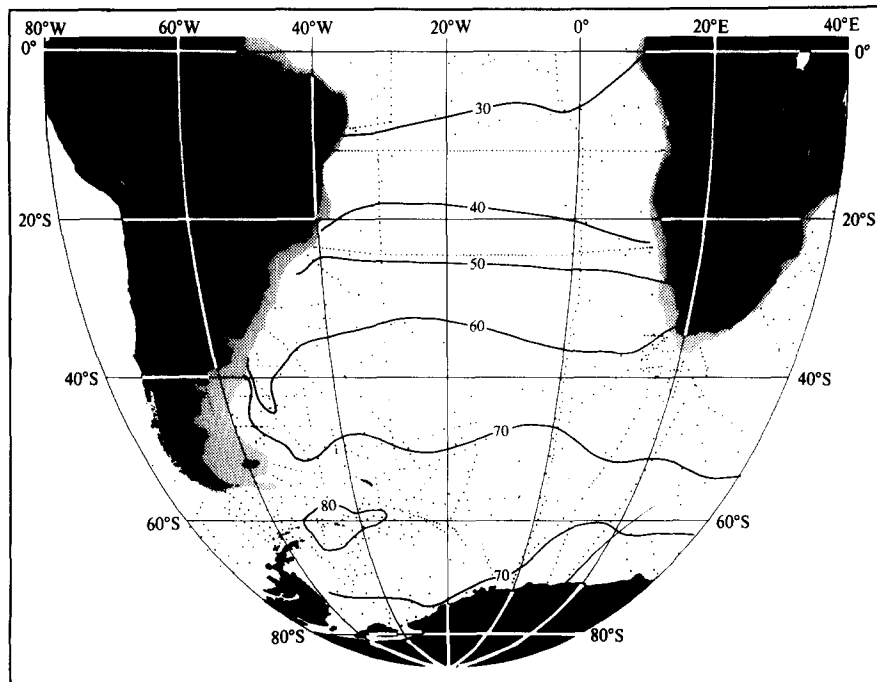


Fig. 18e. Silica (m mol m^{-3}) on the isopycnal defined by 32.20 in σ_2 below 500 m.

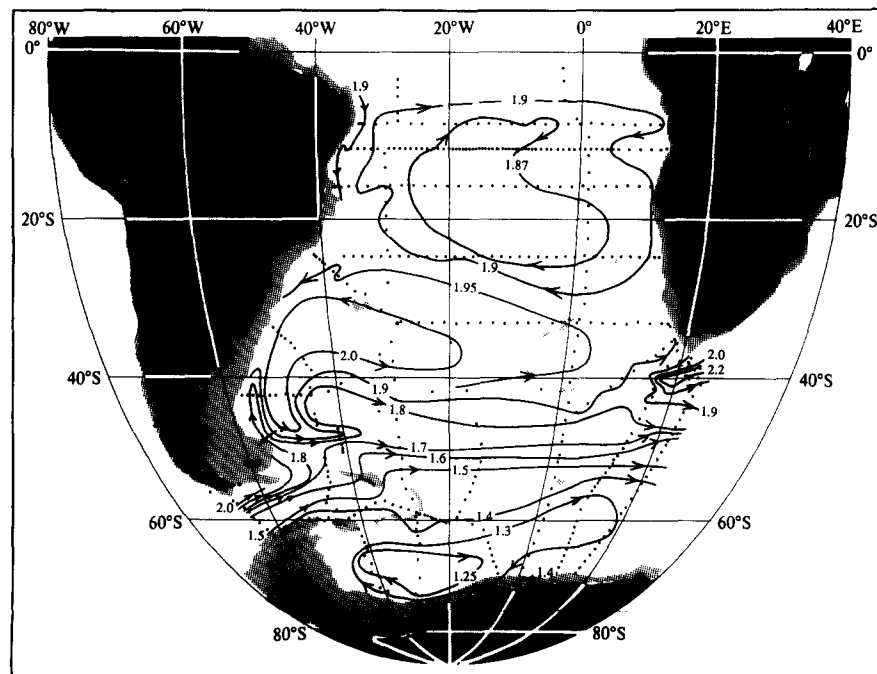


Fig. 19. Adjusted steric height ϕ_A at 1000 db ($10 \text{ m}^2 \text{ s}^{-2}$ or 10 J kg^{-1}). Depths less than 1000 m are shaded.

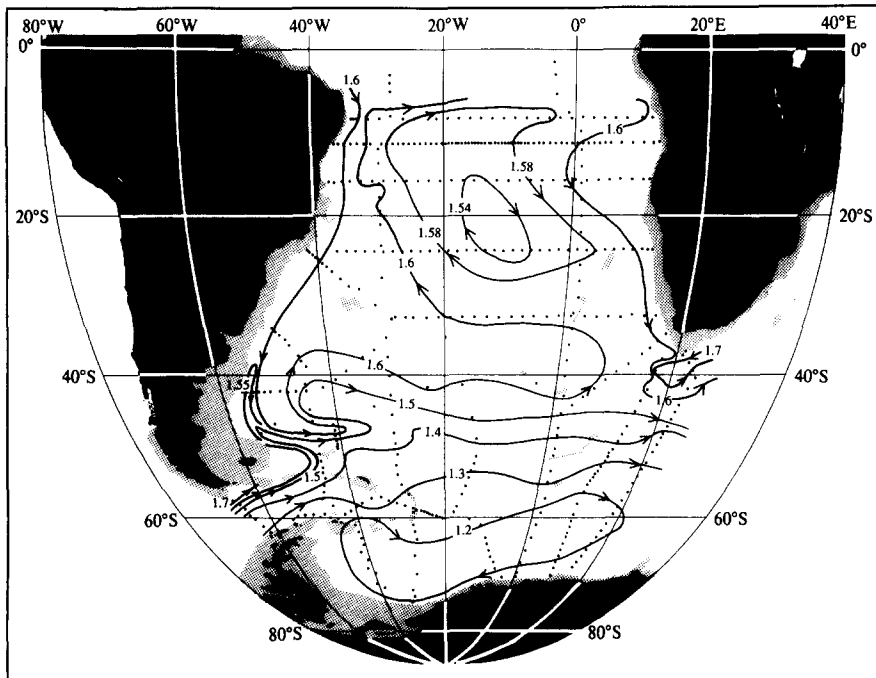


Fig. 20. Adjusted steric height ϕ_A at 1500 db ($10 \text{ m}^2 \text{ s}^{-2}$ or 10 J kg^{-1}). Depths less than 1500 m are shaded.

10. WATER FROM THE NORTH ATLANTIC

A thick layer of warm, highly-saline, oxygen-rich and nutrient-poor water extends southward across the equator. This is what WUST (1935) called the North Atlantic Deep Water. WARREN (1981) has discussed the meridional circulation of the layer of warm deep water from the North Atlantic and the deep and bottom layer from the circumpolar water and the Weddell Sea. He dealt principally with the intensified flow along the western boundary in the Argentine and Brazil basins, and pointed out the shift of the colder, deeper, northward-flowing layer to the eastern part of the basin between the equator and 20°N. He reviewed the history of their investigations and discussed them in terms of the more recent dynamical concepts.

The layer of warm, saline, and oxygen-rich water from the North Atlantic is very thick, extending from about 1000 m to below 3500 m at the equator, but most of its extrema are near the top of the layer. Along 30°W (Fig. 12) maximum temperature near the equator is at about 1100 m (32.20 in σ_1 , 36.73 in σ_2), the minimum silica and maximum salinity at about 1700–1800 m (32.35 in σ_1 , 36.89 in σ_2), the minimum phosphate near 1800 m (32.40 in σ_1 , 36.94 in σ_2), and the oxygen maximum at about 2000 m (near 36.98 in σ_2). WEISS, BULLISTER, GAMMON, and WARNER (1985) have shown that a vertical extremum in freon near the equator at about 1700 m and 36.89 in σ_2 has extended from the Labrador Sea southward along the western boundary, crossing the equator in the west, and also extending some distance eastward along the equator.

The layer of maximum temperature found beneath the temperature minimum of the circumpolar water is the shallowest of the extrema extending southward from the North Atlantic. Just south of the equator, where it lies at about 1100–1200 m in the west, the maximum temperature is found near 32.20 in σ_1 , beneath the temperature minimum that lies near 900 m at about 32.03 in σ_1 . Water at the temperature maximum at 5°S (32.20 in σ_1) is only slightly denser than that of the temperature minimum where it enters at 45°S (32.15 in σ_1). But as the colder layer passes over the warmer layer, the vertical exchange between them erodes the minimum from below and the maximum from above: the minimum temperature is found at successively lower densities as the layer extends northward, and the maximum temperature is found at higher densities farther south.

The isopycnal 32.20 in σ_1 (Fig. 18) closely represents both extrema as they first appear near 45°S and the equator, and illustrates the lateral exchange that takes place as they flow. The vertical exchange is seen on the section (Fig. 12a). The continuation of the temperature minimum into the North Atlantic would be illustrated on a shallower isopycnal, and the continuation of the temperature maximum to 45°S and eastward with the Circumpolar Current would be illustrated on a deeper isopycnal. Because of this vertical exchange the isopycnal 32.20 in σ_1 appears to represent the top of the North Atlantic water near the equator and the top of the circumpolar water near 45°S.

Just as all of the circumpolar extrema are shifted to lower densities as they are carried equatorward above their opposites from the north, the extrema from the North Atlantic are found at slightly higher densities as they are carried poleward. Of these extrema from the north, the layer of high temperature is shallowest and undergoes the greatest exchange with the overlying water during the southward flow. The temperature and density at the extremum near the equator are about 4.5°C and 32.20 in σ_1 ; near 45°S they are about 2.6°C and 32.35.

Both the silica minimum and the salinity maximum have their extrema at the equator near 32.35 in σ_1 , 36.89 in σ_2 , but near 45°S they may have diverged slightly: the salinity maximum is at about 37.02 in σ_2 and the silica minimum appears to be about 36.98 in σ_2 , but the silica profile is not well defined there in this data set. Although the layer of low phosphate has its minimum at about 36.94 in σ_2 at the equator, substantially deeper than the silica minimum and salinity maximum, at 45°S the phosphate minimum lies at about 36.97 in σ_2 , very near the other two extrema.

Because of these shifts, no extremum lies at a single density over the entire range from 5°S to 40°S. The layers are thick enough, however, to allow the general pattern of the tracer to be

represented on an isopycnal that intersects the tracer-extremum. The isopycnal will lie close to the extremum where it exists, and can also follow the flow beyond the area where the tracer appears as an extremum, as in the case of the shallower oxygen minimum from the south, which passes beneath an even lower oxygen concentration near the equator.

The previous isopycnal 32.20 in σ_1 (Fig. 18) has reflected the northern characteristics near the equator, but their extrema are found near higher densities, near 32.32 in σ_1 , 36.84 in σ_2 , as they extend across 45°S and the flow turns eastward with the Antarctic Circumpolar Current. This isopycnal, 36.84 in σ_2 , lies only about 200 m deeper (Fig. 21). The salinity is higher everywhere, and there is an extension of high salinity (temperature) and oxygen and low nutrients eastward along the equator. On the shallower isopycnal oxygen was highest within the anticyclonic gyre, with low oxygen values entering from both the south and the equatorial zone. Here (Fig. 21c) the waters from the north are high in oxygen, the circumpolar waters are low, with the highest values where the isopycnal lies shallower in the Weddell Sea. The phosphate pattern (Fig. 21d) is almost the mirror image of the oxygen. It is lower than in the shallower water (Fig. 18d) except in the Weddell Sea.

The circulation near 1500 db (Fig. 20) has somewhat the same large-scale pattern as the near-surface waters (Fig. 7). The major differences are a generally weaker flow and the southward flow along the eastern boundary. The great anticyclonic gyre, with its east-west axis near 30°–35°S in mid-ocean, is much the same.

At greater depths, however, the anticyclonic gyre retreats west of the Mid-Atlantic Ridge. South of the Rio Grande Rise it becomes quite narrow, with its northward branch well west of 40°W. North of the Rise it extends eastward to the Mid-Atlantic Ridge (Figs. 22, 23 and 24). This shift results in an eastward flow near 25°S of part of the North Atlantic water from the western boundary current, producing the eastward bulges of high salinity and oxygen WUST (1935) mapped for his Upper and Middle North Atlantic Deep Water. He did not recognize the anticyclonic gyre, and indicated that the eastward spreading continued across the Atlantic and south of Africa.

The baroclinic flow along 2000 db relative to 3500 db (Fig. 25) is much like that at 1000 db relative to 2000 db (Fig. 26), and appears to retain the anticyclonic gyre in the east. This might be two separate gyres, as the 3500 db surface is not continuous across the Ridge, and it appears as two on the map at 3000 db relative to 3500 db (Fig. 27) and in DEFANT's (1941a and 1941b) study of the relative and absolute topography. But this is only the baroclinic flow relative to 3500 db. Below the sill depth of the Ridge the flow in the Cape Basin is cyclonic (Figs. 28, 29, and 30) and stronger than at 2000 db, and the baroclinic flow at 2000 db and 3000 db (Figs. 25 and 27) is reversed from the total geostrophic flow.

The deep cyclonic flow within the Cape Basin (REID, 1987) was required as the Mid-Atlantic Ridge bars a deep extension of the anticyclonic flow, and the abyssal characteristics indicate a source from the south as WUST (1933) showed for the temperature and salinity and MANTYLA and REID (1983) showed for density, oxygen, and silica. RINTOUL (1988) also found the flow to be cyclonic there in his treatment of the southern South Atlantic circulation by the inverse method. In their study of the abyssal flow off South Africa, TUCHOLKE and EMBLEY (1984) had also found a cyclonic flow in the Cape Basin from the sediment patterns (Fig. 31).

The extrema from the north are found at successively higher densities as they extend southward but the patterns of characteristics are much the same for the next few hundred meters below 36.84 in σ_2 . They are shown on the isopycnal 36.98 in σ_2 (Fig. 32), which lies about 600 m deeper than the 36.84 isopycnal in the area north of 45°S, and at 37.02 in σ_2 , 41.48 in σ_3 (Fig. 33), which is still deeper. The salinity and oxygen are higher and the phosphate lower on the two deeper isopycnals (Figs. 32 and 33) than on the shallower isopycnal (36.84; Fig. 21), especially so in the western boundary current. These represent the most extreme characteristics of the North Atlantic water south of the equator.

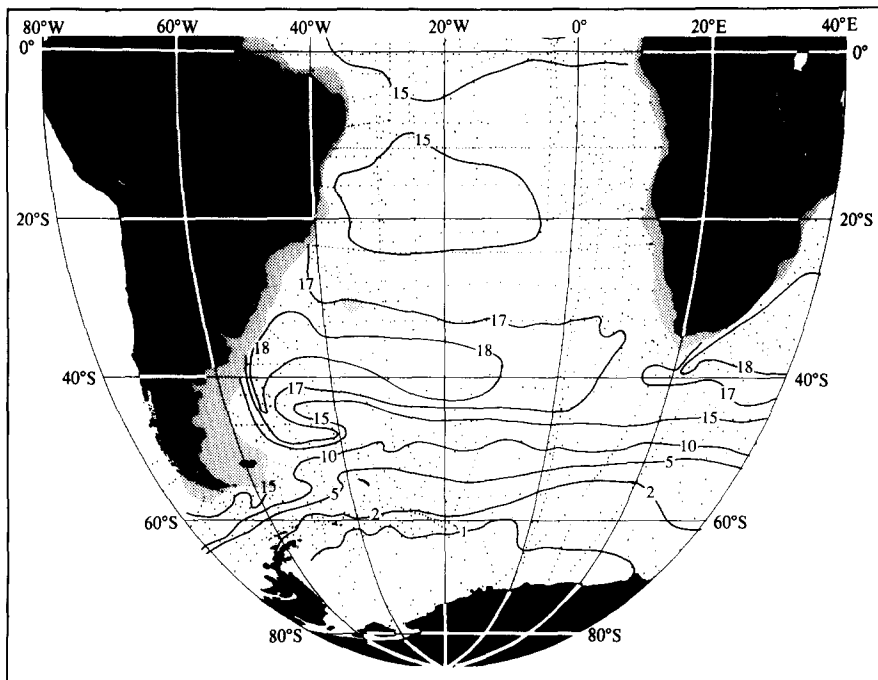


Fig. 21a. Depth (hm) of the isopycnal defined by 36.84 in σ_2 below 1500 m.

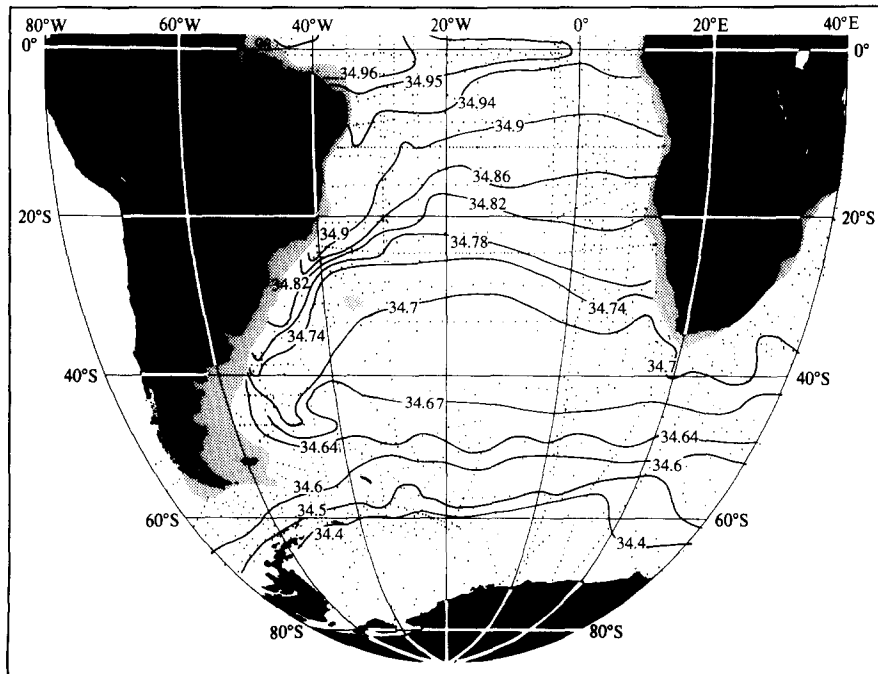


Fig. 21b. Salinity on the isopycnal defined by 36.84 in σ_2 below 1500 m.

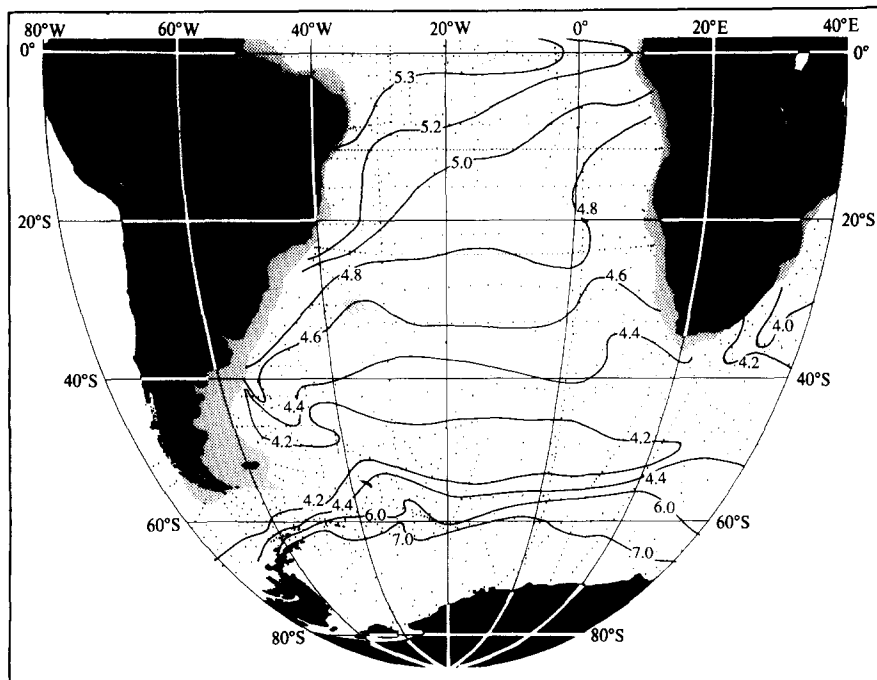


Fig. 21c. Oxygen ($\times 10^3$) on the isopycnal defined by 36.84 in σ_2 below 1500 m.

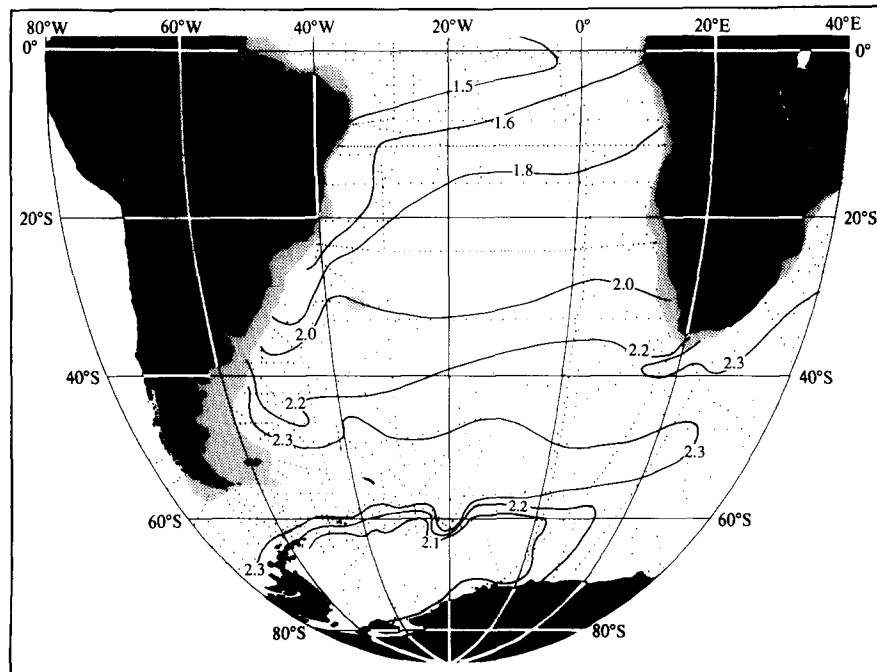


Fig. 21d. Phosphate (m mol m^{-3}) on the isopycnal defined by 36.84 in σ_2 below 1500 m.

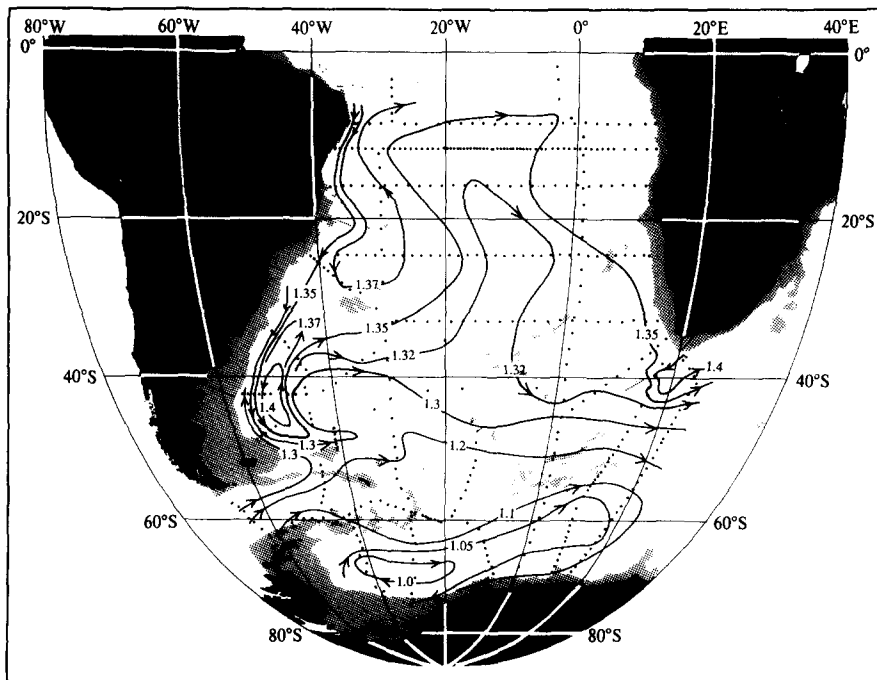


Fig. 22. Adjusted steric height ϕ_A at 2000 db ($10 \text{ m}^2 \text{ s}^{-2}$ or 10 J kg^{-1}). Depths less than 2000 m are shaded.

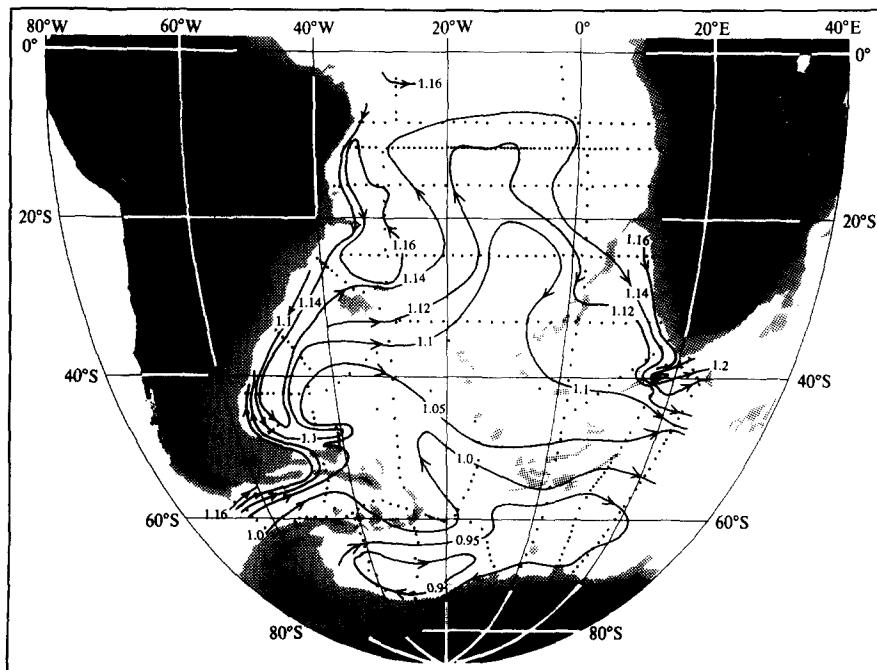


Fig. 23. Adjusted steric height ϕ_A at 2500 db ($10 \text{ m}^2 \text{ s}^{-2}$ or 10 J kg^{-1}). Depths less than 2500 m are shaded.

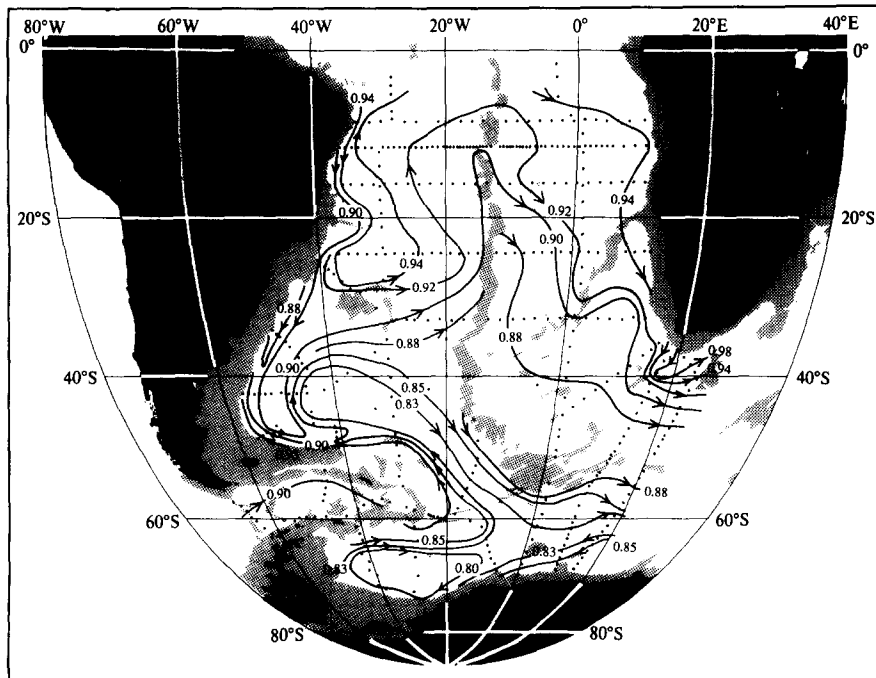


Fig. 24. Adjusted steric height ϕ_A at 3000 db ($10 \text{ m}^2 \text{ s}^{-2}$ or 10 J kg^{-1}). Depths less than 3000 m are shaded.

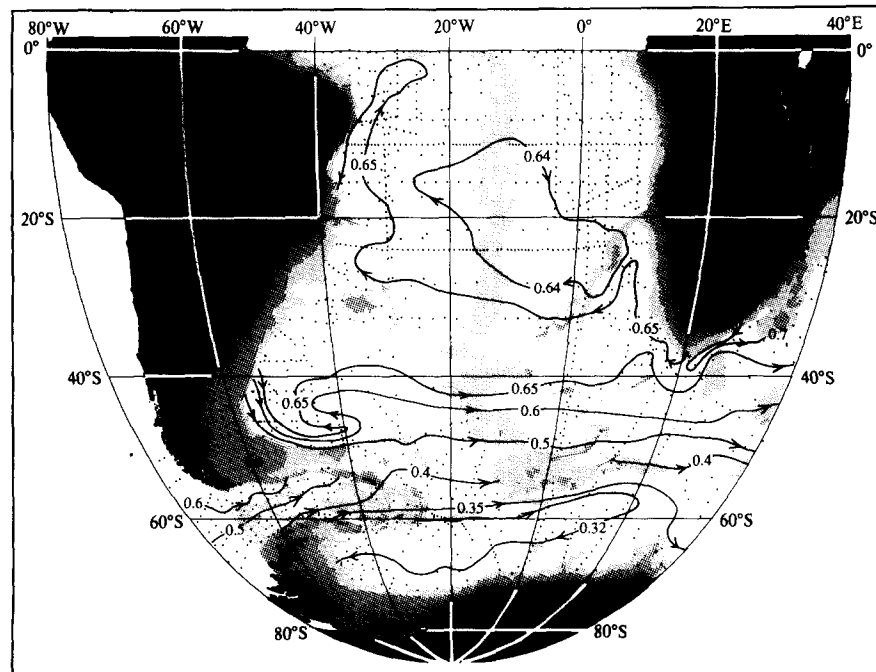


Fig. 25. Geopotential anomaly of the 2000 db surface with respect to the 3500 db surface ($10 \text{ m}^2 \text{ s}^{-2}$ or 10 J kg^{-1}). Depths less than 3500 m are shaded.

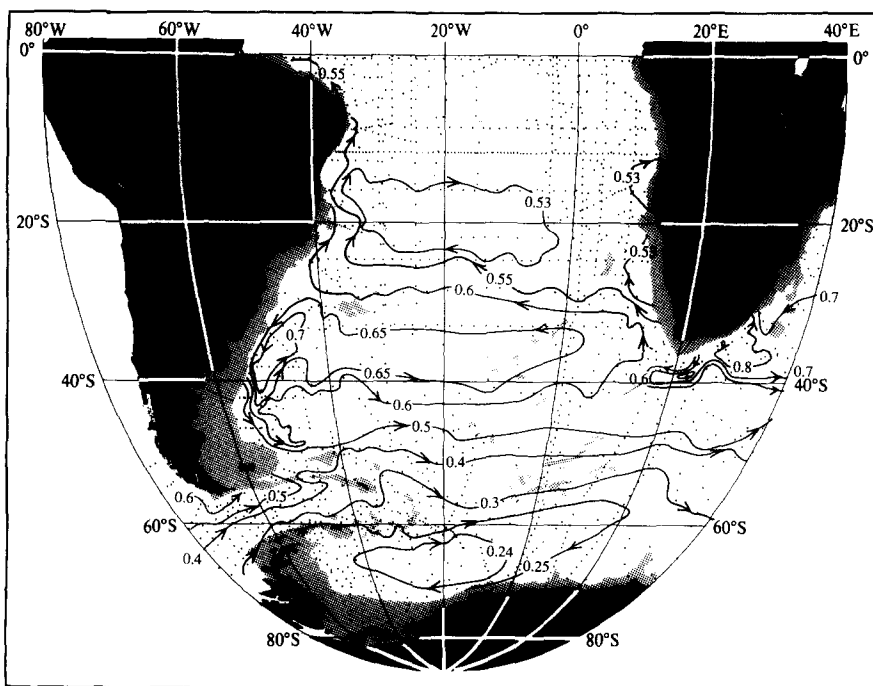


Fig. 26. Geopotential anomaly of the 1000 db surface with respect to the 2000 db surface ($10 \text{ m}^2 \text{ s}^{-2}$ or 10 J kg^{-1}). Depths less than 2000 m are shaded.

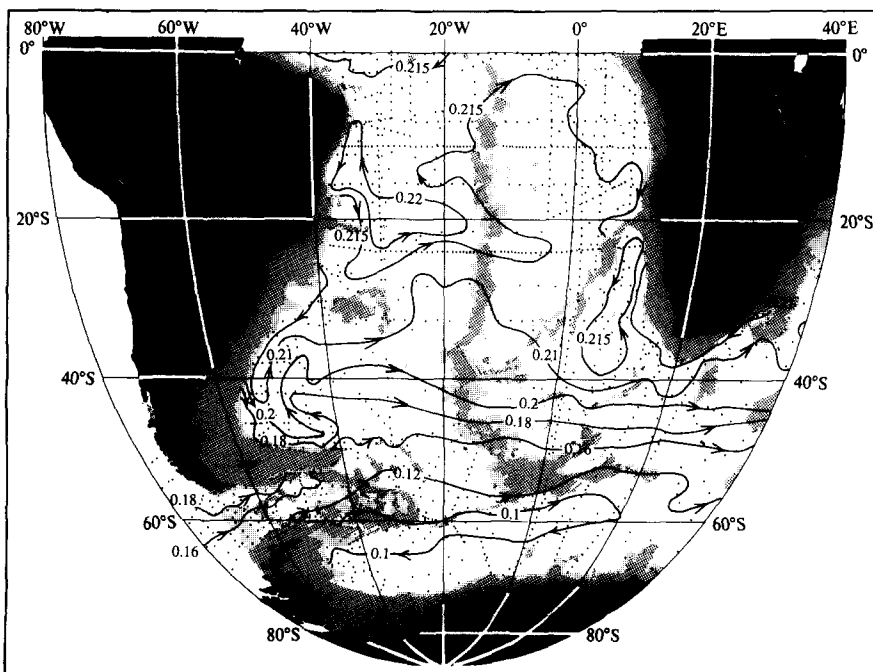


Fig. 27. Geopotential anomaly of the 3000 db surface with respect to the 3500 db surface ($10 \text{ m}^2 \text{ s}^{-2}$ or 10 J kg^{-1}). Depths less than 3500 m are shaded.

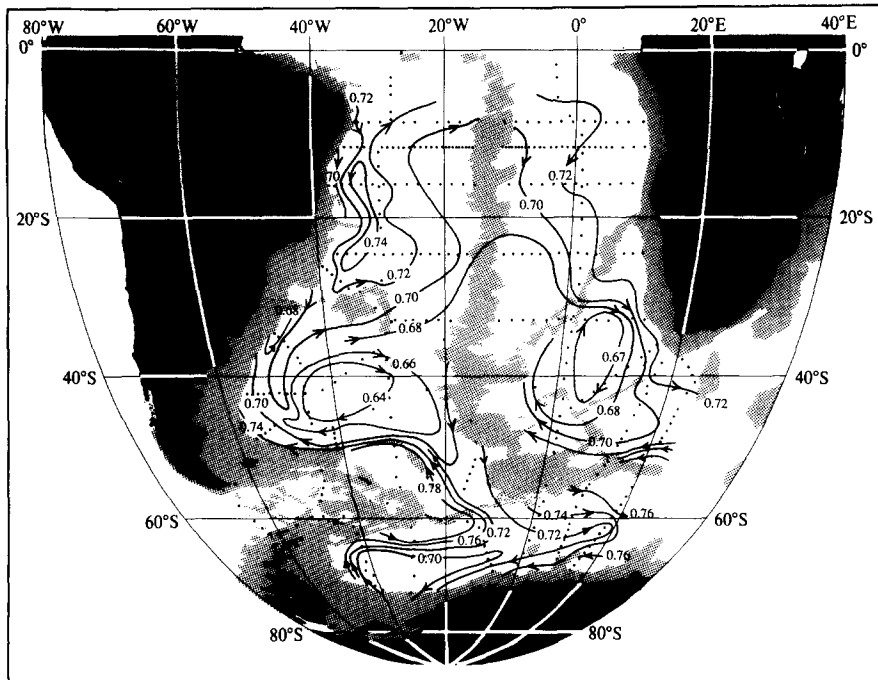


Fig. 28. Adjusted steric height ϕ_A at 3500 db ($10 \text{ m}^2 \text{ s}^{-2}$ or 10 J kg^{-1}). Depths less than 3500 m are shaded.

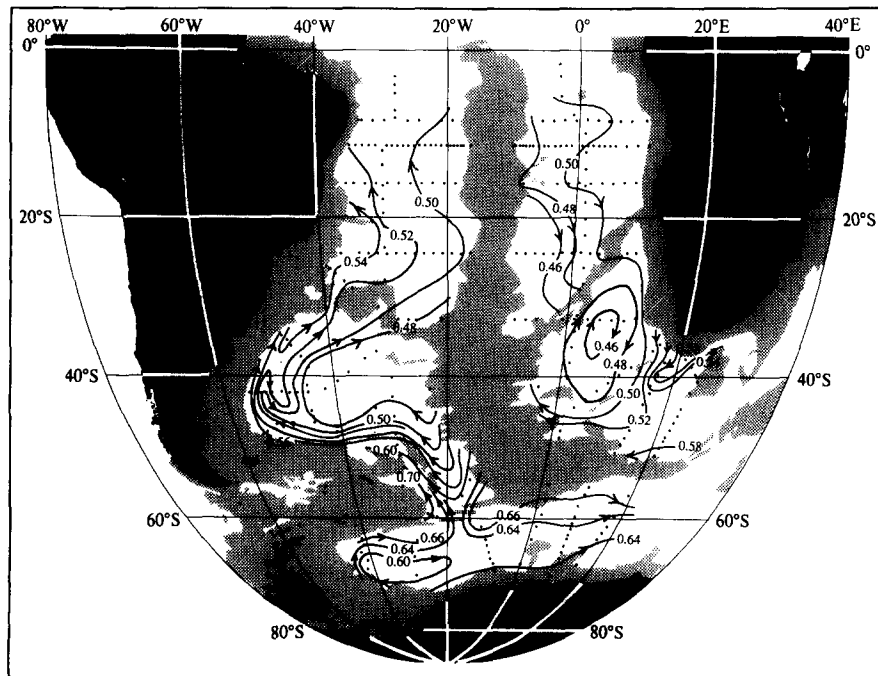


Fig. 29. Adjusted steric height ϕ_A at 4000 db ($10 \text{ m}^2 \text{ s}^{-2}$ or 10 J kg^{-1}). Depths less than 4000 m are shaded.

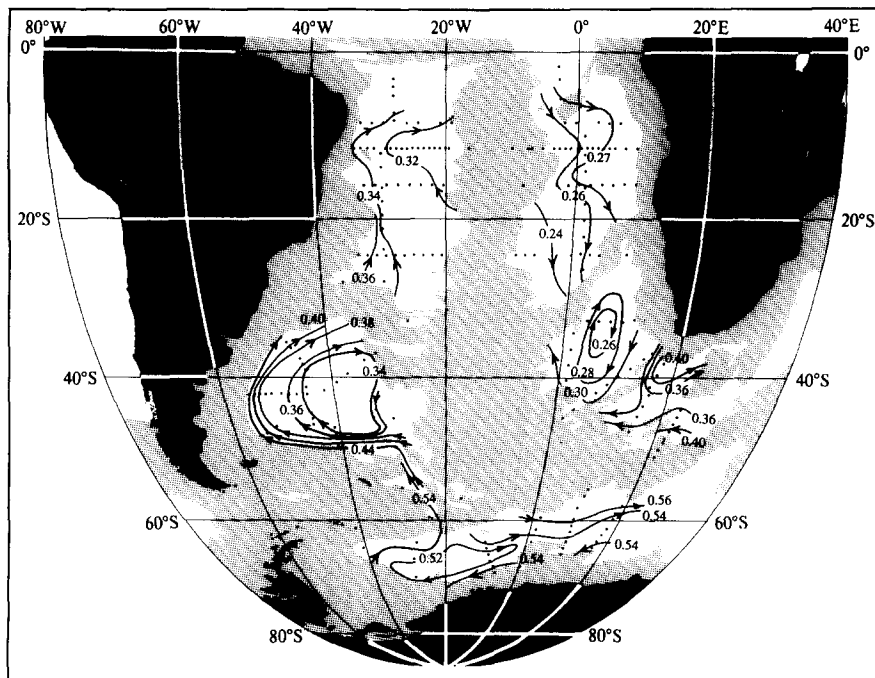


Fig. 30. Adjusted steric height ϕ_A at 4500 db ($10 \text{ m}^2 \text{ s}^{-2}$ or 10 J kg^{-1}). Depths less than 4500 m are shaded.

However, between 2000 and 3000 m these great extrema are penetrated laterally near 15°S – 20°S along 30°W by a layer with the characteristics of circumpolar water. As the circulation is different in this depth range, the patterns are different. The anticyclonic gyre has contracted to the west and below 2000 m is centered north of the Rio Grande Rise (Figs. 22–24), and lies west of the Mid-Atlantic Ridge. In this range of depth and density (Figs. 32 and 33) there is a northward flow of circumpolar water through the Argentine Basin. It mixes with the northern water of the western boundary current and flows around the anticyclonic gyre to pass westward across 30°W and then turn eastward again near 10°S near the equator (Figs. 22–24). This layer retains enough of its circumpolar characteristics to be recognized west of 30°W near 10°S – 15°S . The lower salinity and oxygen and higher nutrients are seen on the isopycnals (Figs. 32 and 33) and at 15°S – 20°S on the vertical section along 30°W (Fig. 12) as intrusions near 2000–3000 m where they have spread laterally into the great layer of high-salinity, high-oxygen, low-nutrient water from the North Atlantic.

These apparent breaches in the layer from the North Atlantic were shown in WUST's (1935) vertical sections. He noted the oxygen minimum near 2500 m north of 25°S , as separating his Middle and Lower North Atlantic Deep Water, but did not account for it. EDMOND and ANDERSON (1971) made the first measurements in the Brazil Basin that had closely-spaced bottles. Their data showed the break very clearly. At about 2800 m they found a vertical minimum in oxygen, maxima in phosphate and silica, and even a slight but real minimum in salinity. They identified this as the layer between Wust's Middle and Lower North Atlantic Deep Water (both characterized by oxygen maxima). They were able to trace the extent of the oxygen minimum in other data from about 26°N to 15°S .

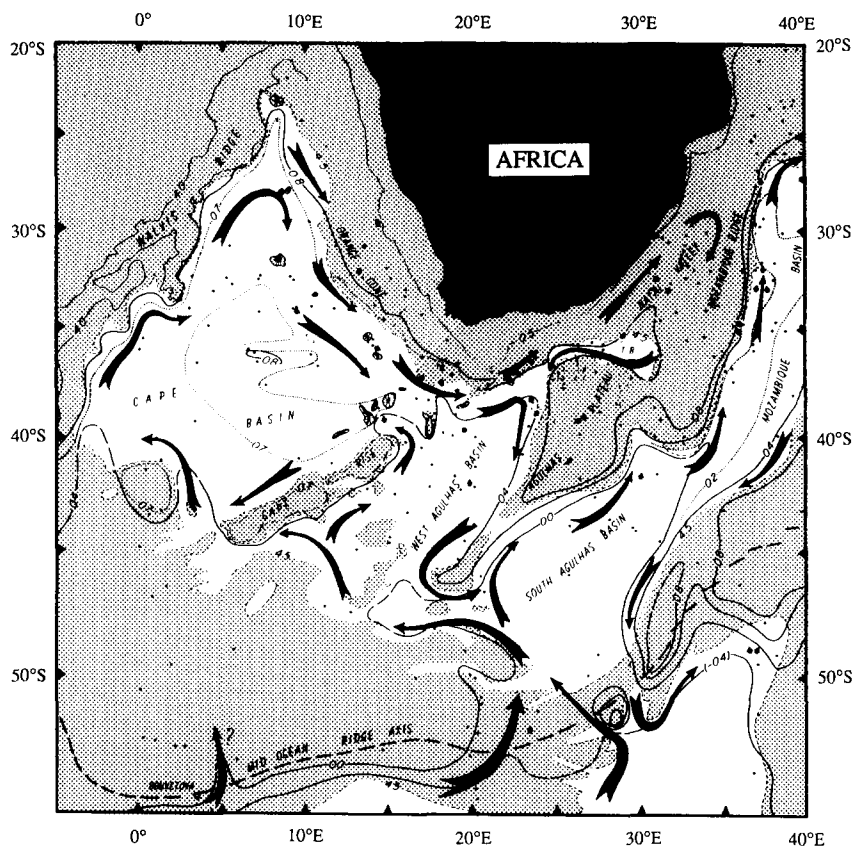


Fig. 31. Bottom circulation determined from sediment patterns. Adapted from TUCHOLKE and EMBLEY (1984).

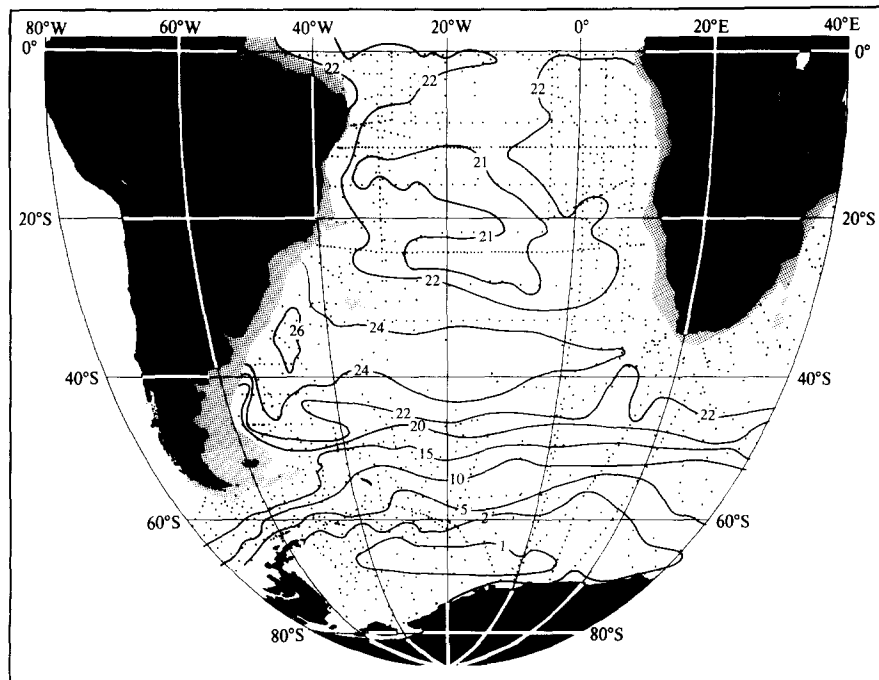


Fig. 32a. Depth (hm) of the isopycnal defined by $36.98 \text{ in } \sigma_2$ below 1500 m.

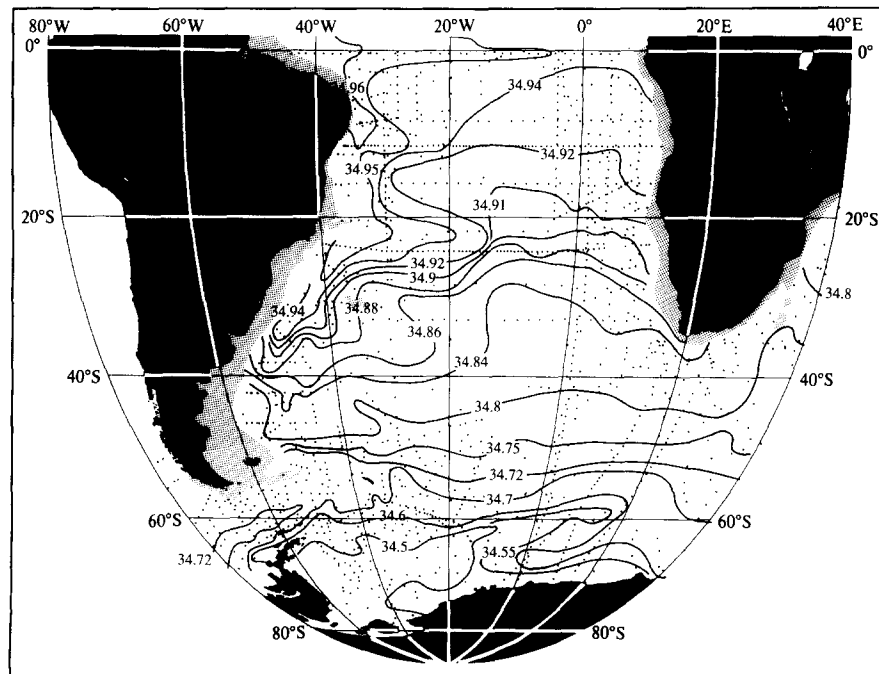


Fig. 32b. Salinity on the isopycnal defined by $36.98 \text{ in } \sigma_2$ below 1500 m.

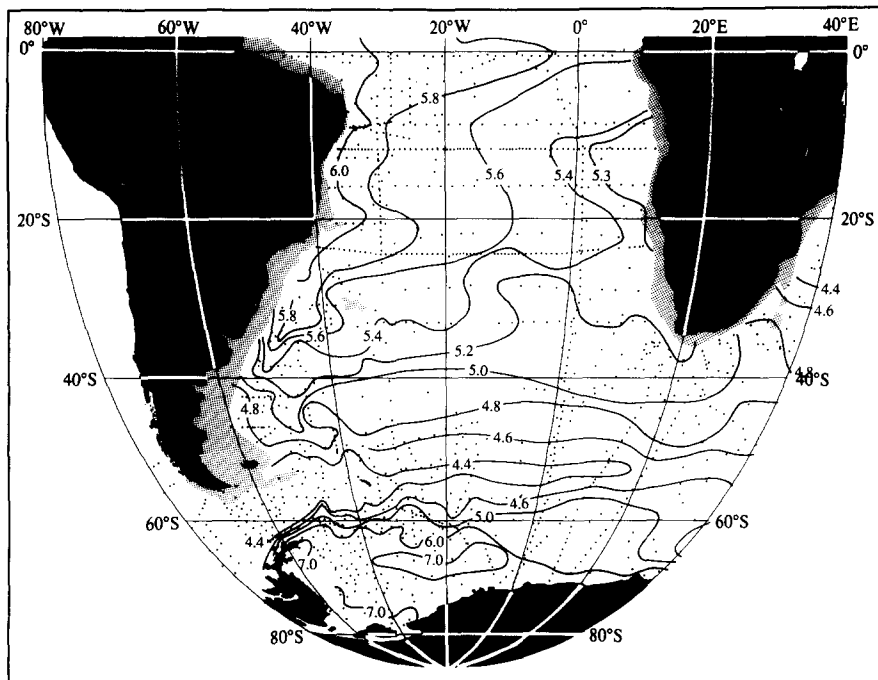


Fig. 32c. Oxygen ($\times 10^3$) on the isopycnal defined by 36.98 in σ_2 below 1500 m.

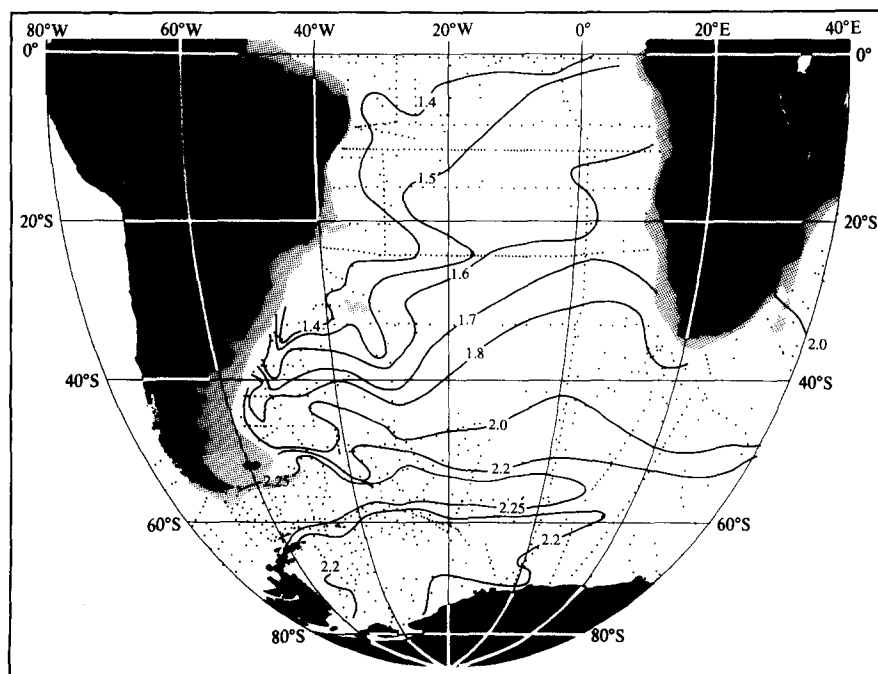


Fig. 32d. Phosphate (m mol m^{-3}) on the isopycnal defined by 36.98 in σ_2 below 1500 m.

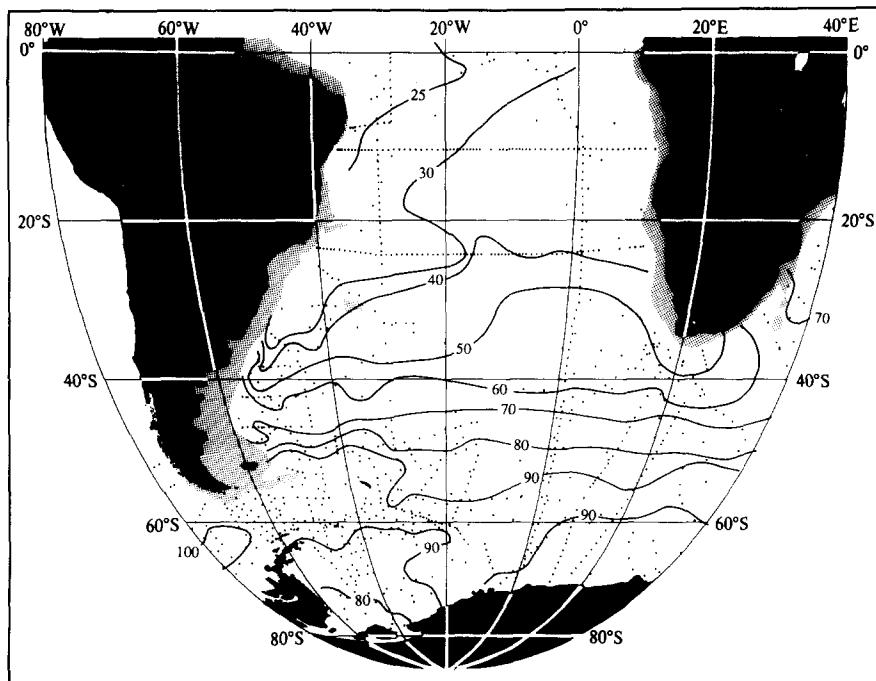


Fig. 32e. Silica (m mol m^{-3}) on the isopycnal defined by 36.98 in σ_2 below 1500 m.

The Geosecs section in the western Atlantic (BAINBRIDGE, 1980) lies close to the section herein (Fig. 12) north of 25°S . In addition to the breach in characteristics shown on that section, JENKINS and CLARKE (1976) have shown $\delta(^3\text{He})$ and STUIVER and OSTLUND (1980) have shown $\Delta^{14}\text{C}$ on the Geosecs section.

For both $\delta(^3\text{He})$ and $\Delta^{14}\text{C}$ (Figs. 34 and 35) the extrema from the south — the circumpolar water — are split north of about 45°S by the waters from the North Atlantic, which are lower in $\delta(^3\text{He})$ and higher in $\Delta^{14}\text{C}$, just as the other tracers are as seen on the section along 30°W (Fig. 12). The presence of circumpolar water characteristics near $15^\circ\text{--}20^\circ\text{S}$ at about 2000–3000 m seen along 30°W is also indicated by the high $\delta(^3\text{He})$ and the low $\Delta^{14}\text{C}$ seen here (Figs. 34 and 35). Furthermore, the $\Delta^{14}\text{C}$ section extends through the North Atlantic and near 3000 m between 10°N and 30°N shows a minimum that corresponds to the circumpolar water feature at $15^\circ\text{--}20^\circ\text{S}$. It corresponds roughly to the oxygen, phosphate and nitrate extrema shown there on the Geosecs western section by BAINBRIDGE (1980), and indicates that the layer of circumpolar water extends north of the equator.

An eastward flow of northern water near the equator in the depth-range about 1500–2000 m is suggested by the patterns of oxygen and salinity on the 30°W section (Fig. 12), by the salinity and silica on the 0°W section (Fig. 13), and by the patterns on isopycnals from 36.84 in σ_2 (about 1500 m) down to 41.48 in σ_3 (3000 m), about the crest of the Mid-Atlantic Ridge (Figs. 21, 32, 33). The deepest recognizable extremum of the North Atlantic water is the underlying oxygen maximum near 3500 m north of 30°S at about 37.04 in σ_2 , 41.50 in σ_3 , 45.84 in σ_4 . This is just at the knee of the θ/S curve that marks the shift to circumpolar water. The high values below the maximum extend eastward near the equator as deep as 3600 m (Fig. 36c). This flow was seen in

WUST's (1935) maps of the North Atlantic Deep Water. It appeared to be offset a little to the south of the equator (2° – 3° S). WATTENBERG's (1939) atlas of the oxygen also shows the eastward flow along the equator, particularly on the maps of oxygen saturation at 1250 m to 3000 m.

The saline layer from the North Atlantic extends not only through the South Atlantic, but with the Antarctic Circumpolar Current all around Antarctica. It spreads northward to the equator in the Indian and Pacific oceans, and during its long path its oxygen is decreased and its nutrients increased, but it is still a recognizable layer of maximum salinity as it returns to the Atlantic through the Drake Passage (REID and LYNN, 1971; REID, 1981).

The Falkland and Brazil currents bring these waters together near the Falkland Plateau and they flow together and mix in the South Atlantic. The flow at 2000–3500 m turns back north and west near 50° S, 40° W, carrying water from both sources northward and then eastward across or around the Mid-Atlantic Ridge (Figs. 33 and 36), and then southward in the eastern basin and eastward south of Africa.

The downstream extension through the Indian Ocean can be seen on the maps and vertical sections in WYRTKI's (1971) atlas. The maximum salinity has been mapped in the Southern Ocean by GORDON and MOLINELLI (1982), with the potential temperature and silica at the salinity maximum.

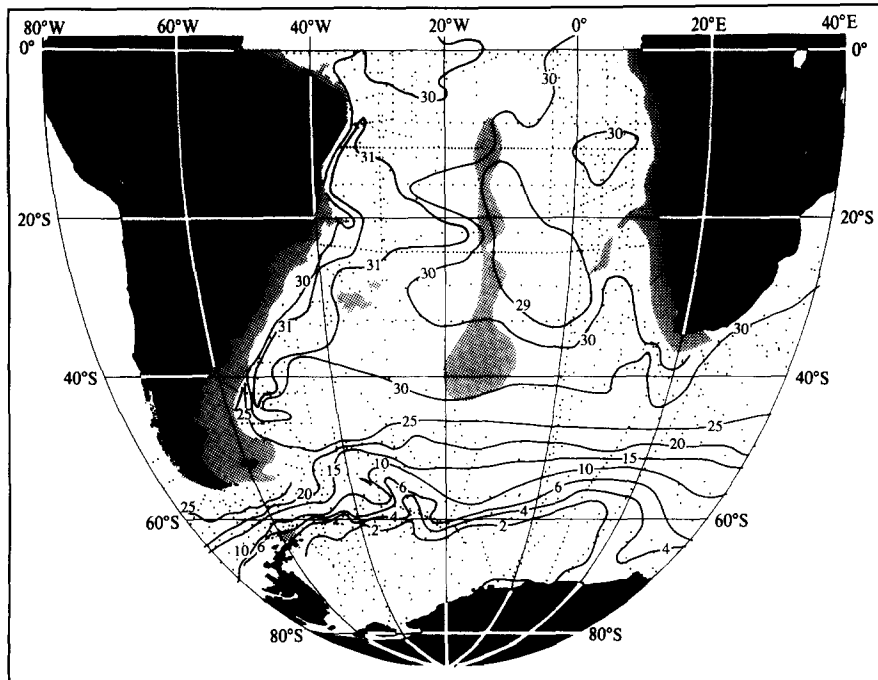


Fig. 33a. Depth (hm) of the isopycnal defined by 41.48 in σ_3 below 2500 m.

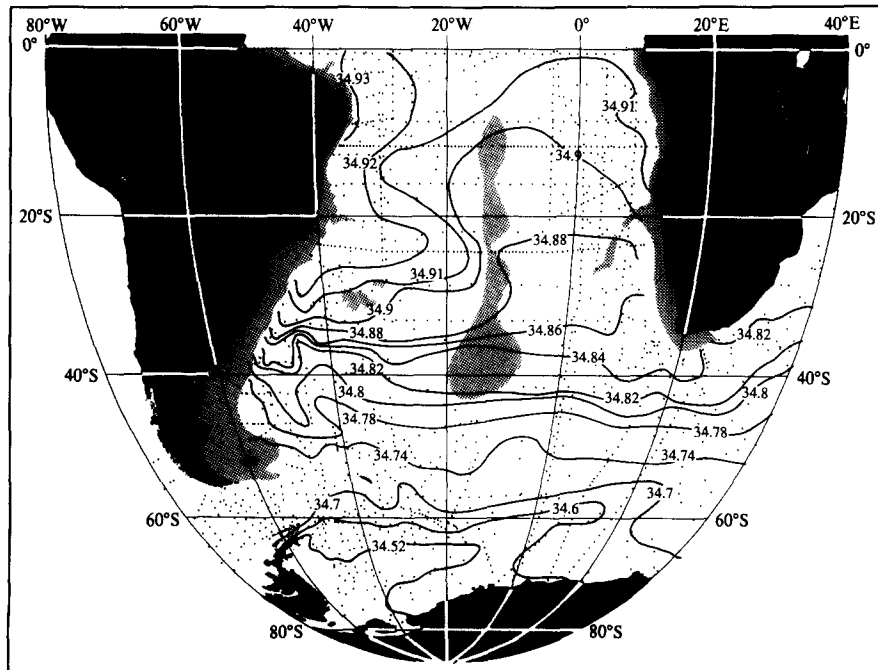


Fig. 33b. Salinity on the isopycnal defined by 41.48 in σ_3 below 2500 m.

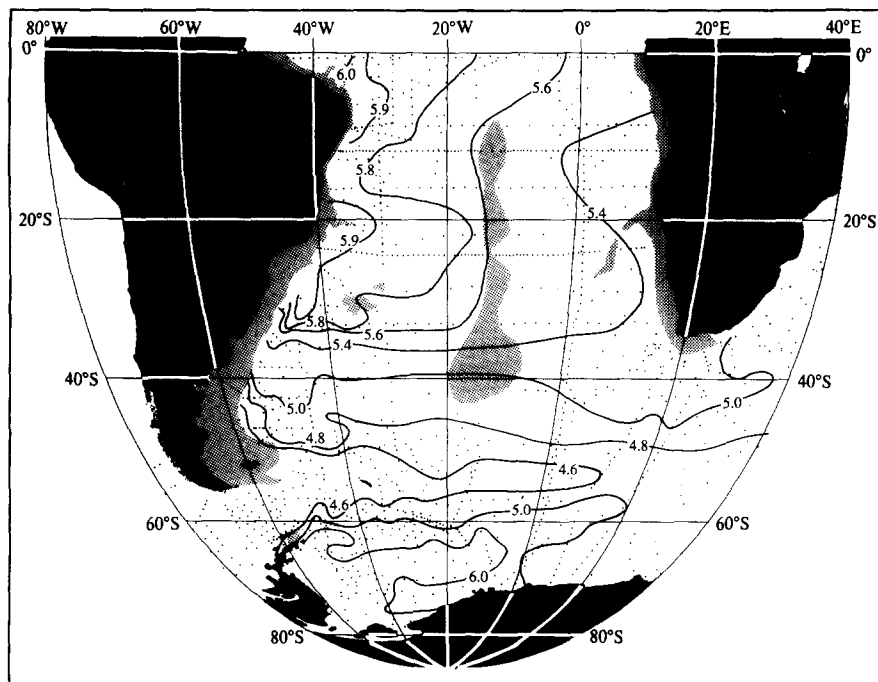


Fig. 33c. Oxygen ($\times 10^3$) on the isopycnal defined by 41.48 in σ_3 below 2500 m.

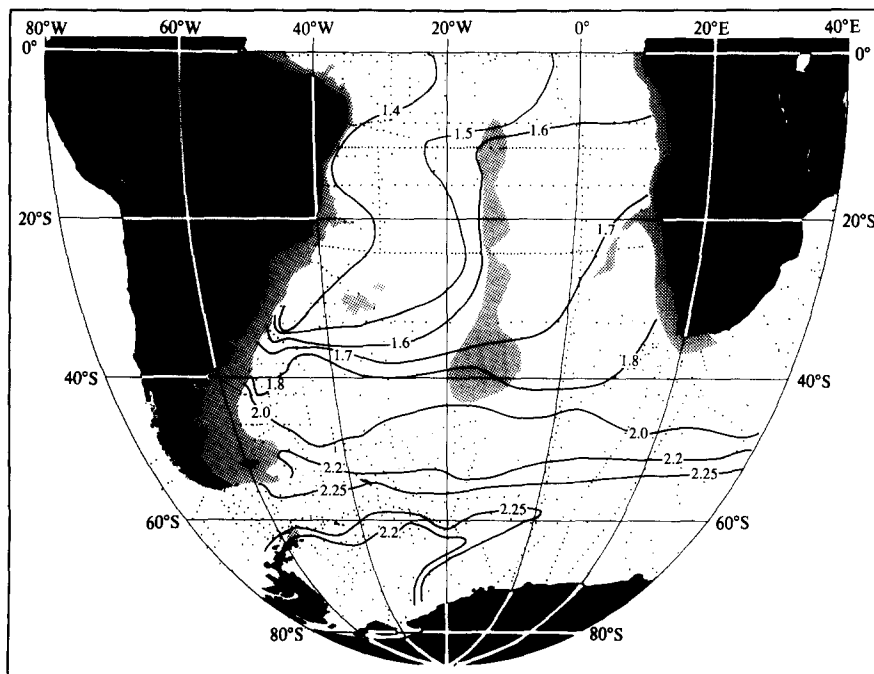


Fig. 33d. Phosphate (m mol m^{-3}) on the isopycnal defined by 41.48 in σ_3 below 2500 m.

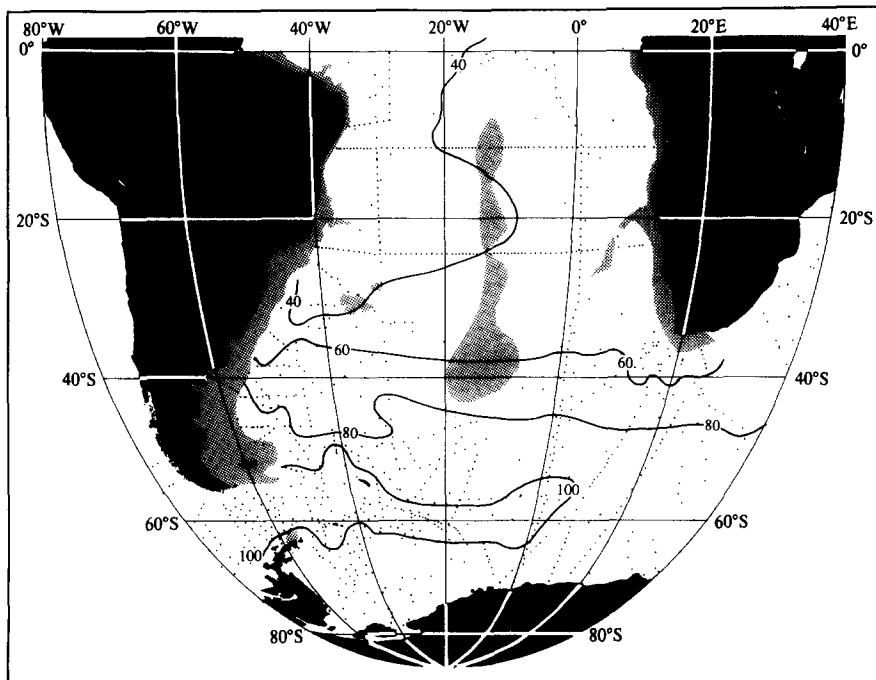


Fig. 33e. Silica (m mol m^{-3}) on the isopycnal defined by 41.48 in σ_3 below 2500 m.

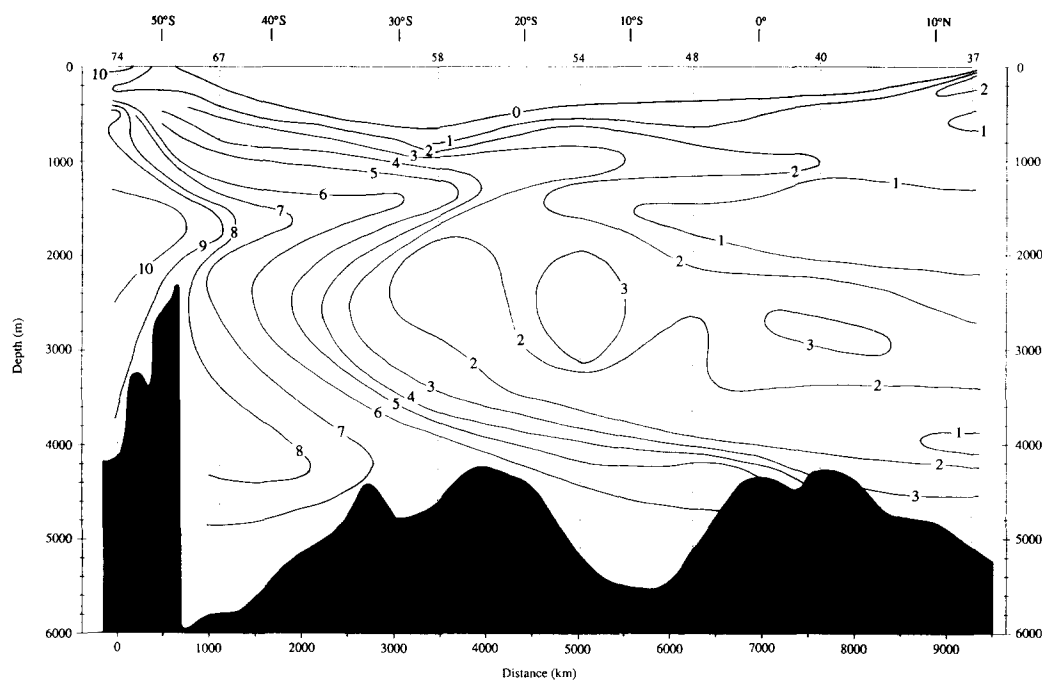


Fig. 34. The meridional distribution of $\delta^{3}\text{He}$ (%) in the South Atlantic. Adapted from JENKINS and CLARKE (1976).

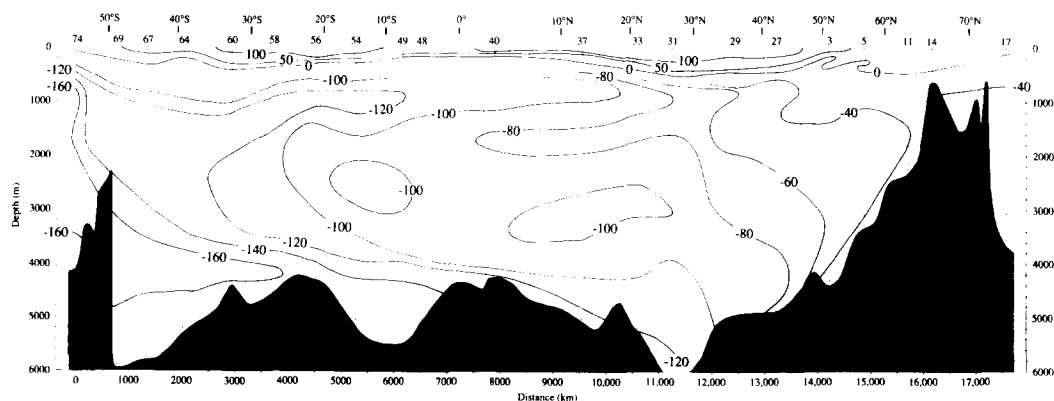


Fig. 35. The meridional distribution of $\Delta^{14}\text{C}$ (‰) along the western Atlantic Geosecs section. Adapted from STUIVER and OSTLUND (1980).

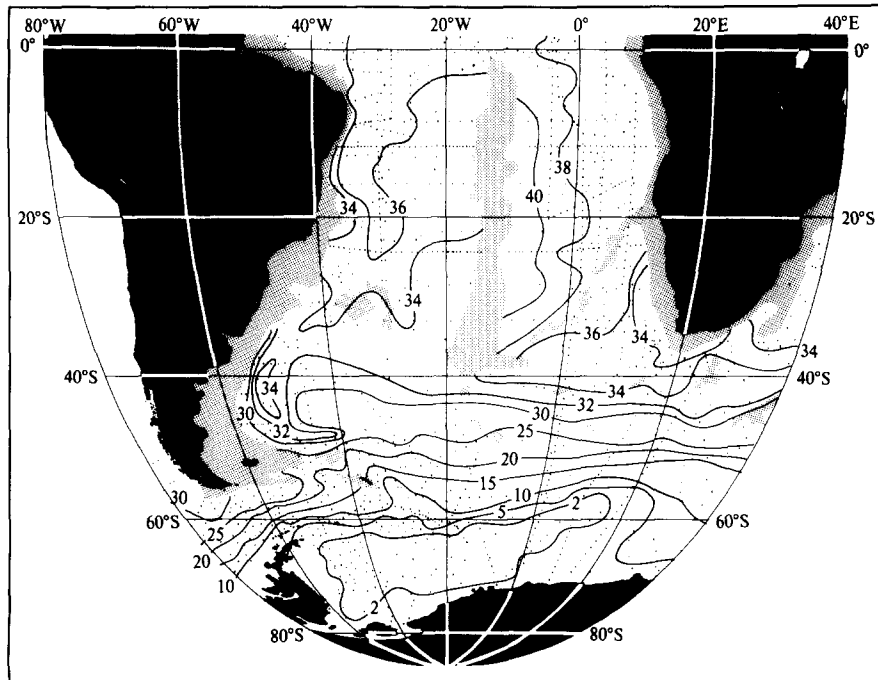


Fig. 36a. Depth (hm) of the isopycnal defined by 45.86 in σ_4 below 3500 m.

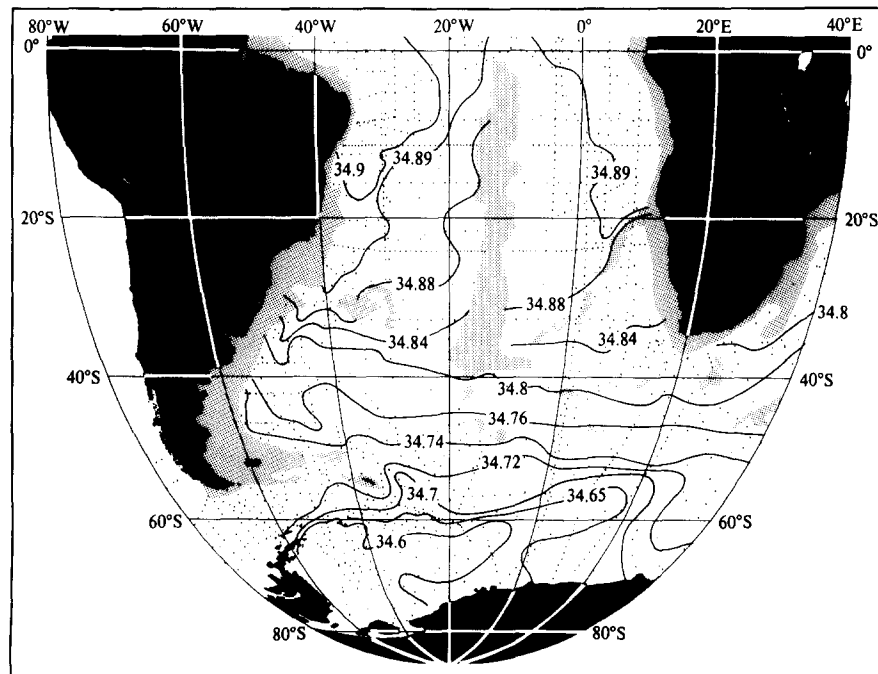


Fig. 36b. Salinity on the isopycnal defined by 45.86 in σ_4 below 3500 m.

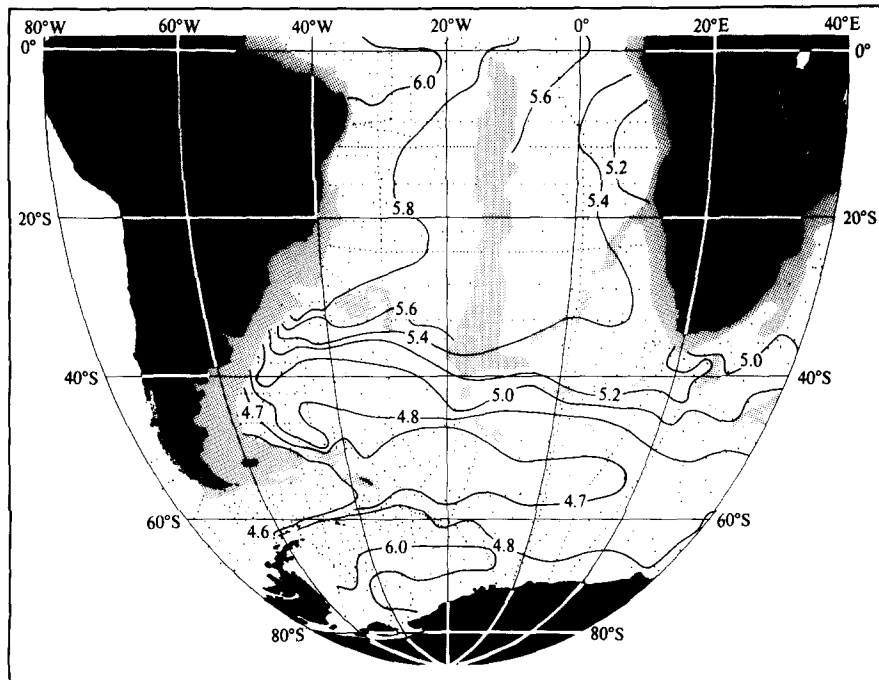


Fig. 36c. Oxygen ($\times 10^3$) on the isopycnal defined by 45.86 in σ_4 below 3500 m.

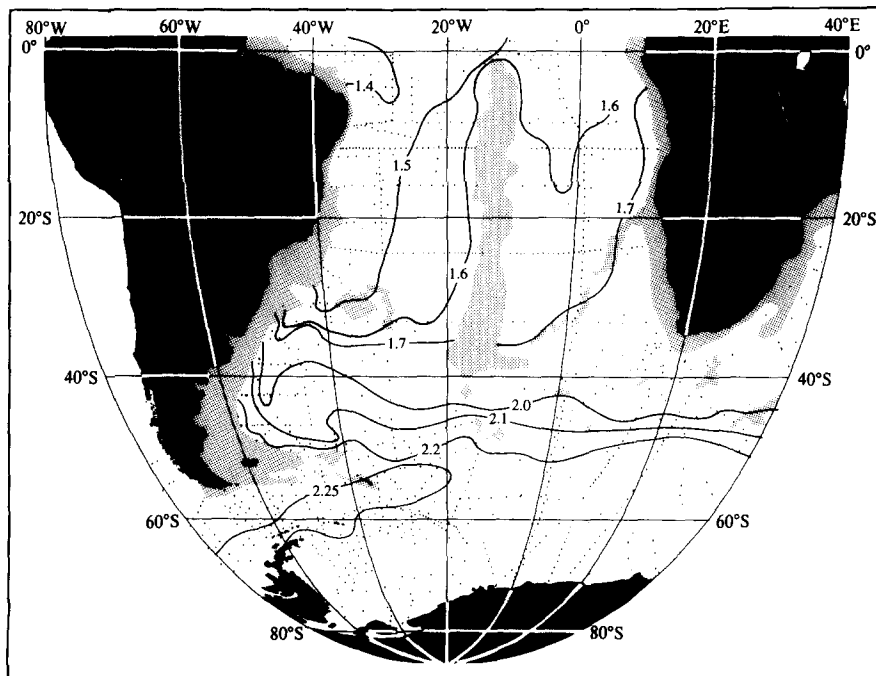


Fig. 36d. Phosphate ($m\text{ mol m}^{-3}$) on the isopycnal defined by 45.86 in σ_4 below 3500 m.

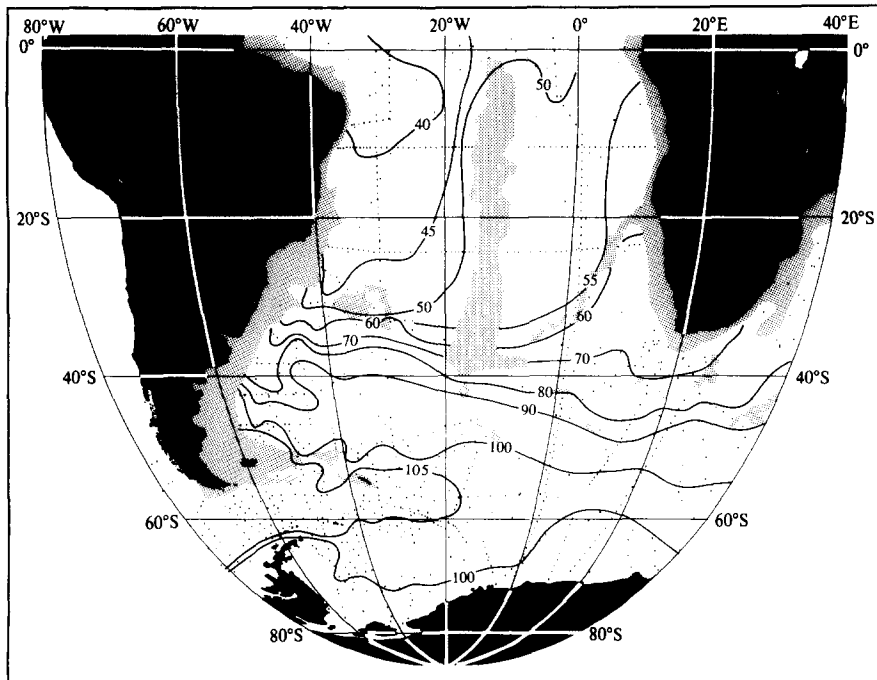


Fig. 36e. Silica (m mol m^{-3}) on the isopycnal defined by 45.86 in σ_4 below 3500 m.

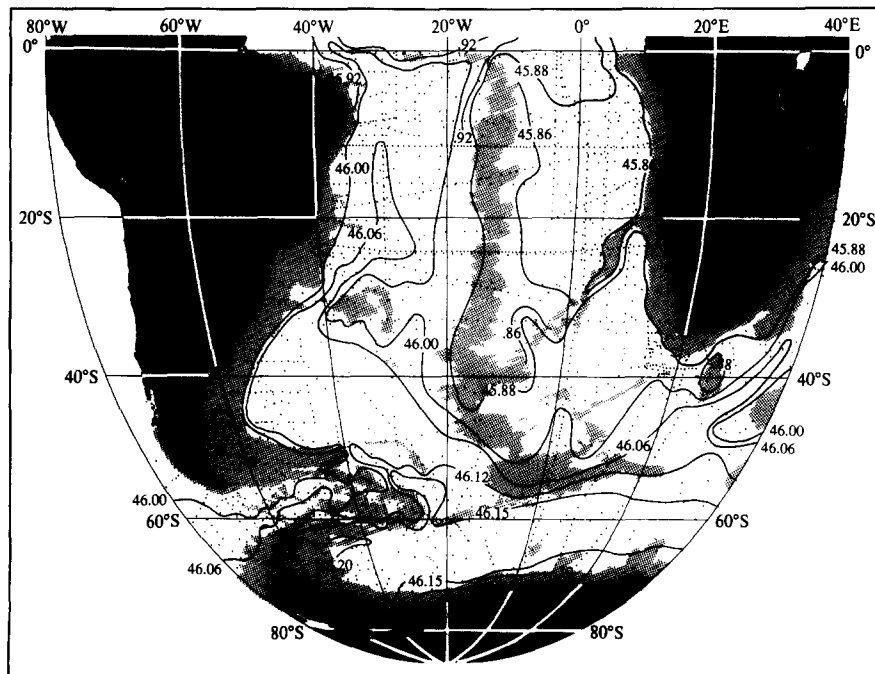


Fig. 37. Potential density (σ_4) at deepest sample. Values at depths less than 3500 m (shaded) are not contoured.

11. THE LOWER LAYER OF CIRCUMPOLAR WATER

North of about 45°S to 55°S the lower part of the circumpolar water is separated from the upper part by the layer from the North Atlantic, which extends down to about 45.85 in σ_4 . As the maximum density of the circumpolar water is about 46.06–46.07 in σ_4 , the lower part of the circumpolar water lies between 45.85 and 46.07 in σ_4 . Water denser than 46.07 has entered from the Weddell Sea and is found northward only to about 9°S, where the 46.07 isopycnal intersects the bottom. The deep and abyssal waters crossing the equator northward do not derive directly from the Weddell Sea but from the lower circumpolar layer: although they have undergone some mixing with Weddell Sea water along their northward flow, they are still recognized by their lower oxygen.

The layer of lower circumpolar water between 45.85 and 46.07 in σ_4 lies within the maximum in Vaisala frequency, just below the deep break in the θ/S curve. It has only one extremum, the deeper extension of the circumpolar oxygen minimum.

The oxygen minimum within the Drake Passage slopes down to 2000 m with a value of about 3.9×10^3 and at a density of about 36.80 in σ_2 . On the section at 30°W (Fig. 12) its minimum value near 48°S has been increased almost to 4.4×10^3 by exchange with the overlying Intermediate Water and the underlying northern water, but still lies near 36.80 in σ_2 .

After the split the deeper minimum lies near 37.05 in σ_2 (41.515 in σ_3) at 40°S as far as the Rio Grande Rise. This layer extends past the Rio Grande as a thin layer near 5000 m. Its concentration has been increased by mixing as it crosses the Rise and the density at the minimum depressed to about 41.63 in σ_3 , 46.02 in σ_4 in the Brazil Basin. (The slightly-higher values at the bottom near 25°S suggest an input of Weddell Sea water, which is higher in oxygen, but they are defined by only slightly higher values on the deepest bottles on two stations.)

The patterns and flow of this lower layer of circumpolar water are shown in Fig. 36 and the maps of adjusted steric height. This is the densest surface (45.86 in σ_4) that is continuous throughout the Angola Basin. Values as high as 45.93 are found at the bottom in the Romanche Fracture Zone (18°W at the equator) and 45.88 within the Guinea Basin, but the values decrease to less than 45.87 in the southern part of the Angola Basin. The colder abyssal water found in the Angola Basin just north of the Walvis Ridge near 36°S (CONNARY and EWING, 1972) has a density a little greater than 45.88 in σ_4 , but this density does not extend very far into the Basin (Fig. 37).

The high salinities from the north extend southward along the western boundary (Figs. 36b and c) and along the eastern side of the Angola Basin. Less saline (colder) waters from the south flow northward just west of the Mid-Atlantic Ridge, eastward through the Romanche Fracture Zone, where they are joined by northern waters, and both flow southward along the eastern side of the Ridge (Figs. 28 and 29), with the higher salinity from the north in the eastern side of the Angola Basin. The depth of this isopycnal is about 400 m greater in the Angola Basin than in the west as there is limited access for denser water.

The oxygen concentration on this isopycnal (Fig. 36c) is lowest near 6°S in the Angola Basin. WUST (1935) showed an oxygen minimum on his eastern section at about 3500 m near 10°S, 12°E and WATTENBERG (1938) showed a separate oxygen minimum on the continental slope at about 4000 m depth on the Meteor section at 8°S. The IGY data along 8°S and 16°S (FUGLISTER, 1960) also showed the feature. VAN BENNEKOM and BERGER (1984), with later data, have shown corresponding maxima in phosphate, nitrate and silica, and accounted for them as the decomposition products of suspended material carried down from the Zaire River outflow through the deep submarine canyon and to abyssal depths.

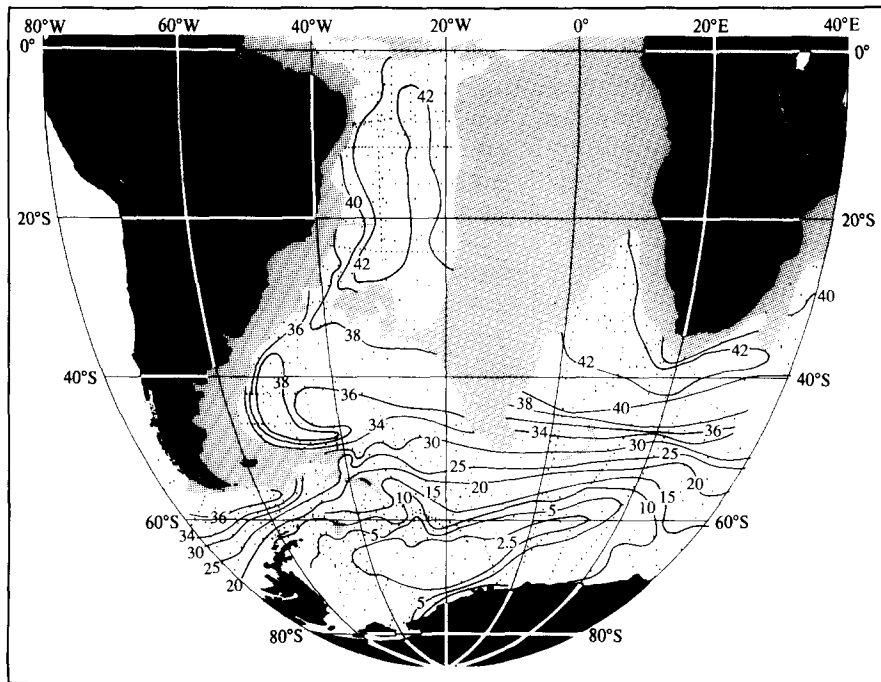


Fig. 38a. Depth (hm) of the isopycnal defined by 45.97 in σ_4 below 3500 m.

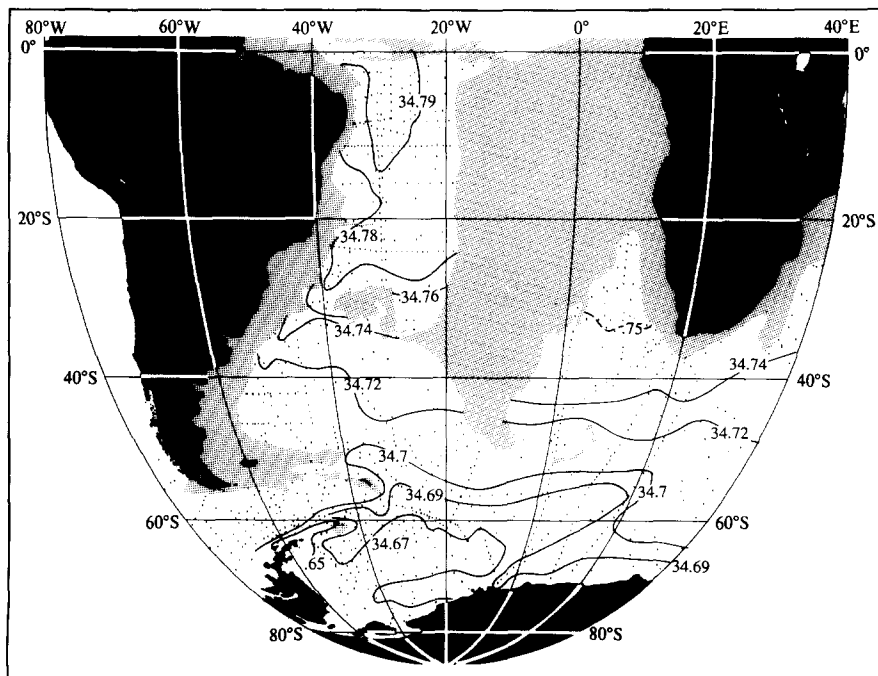


Fig. 38b. Salinity on the isopycnal defined by 45.97 in σ_4 below 3500 m.

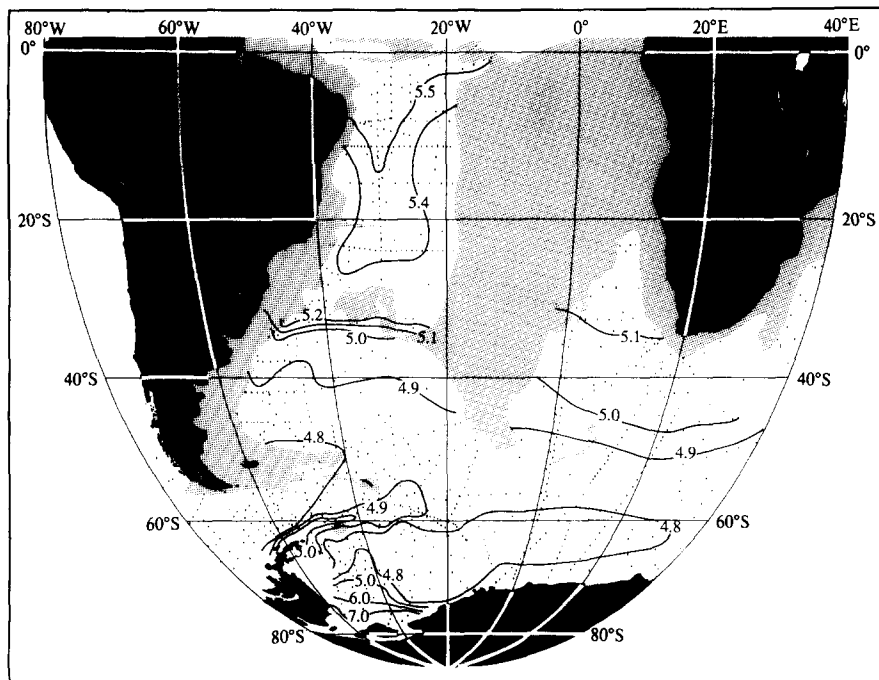


Fig. 38c. Oxygen ($\times 10^3$) on the isopycnal defined by 45.97 in σ_4 below 3500 m.

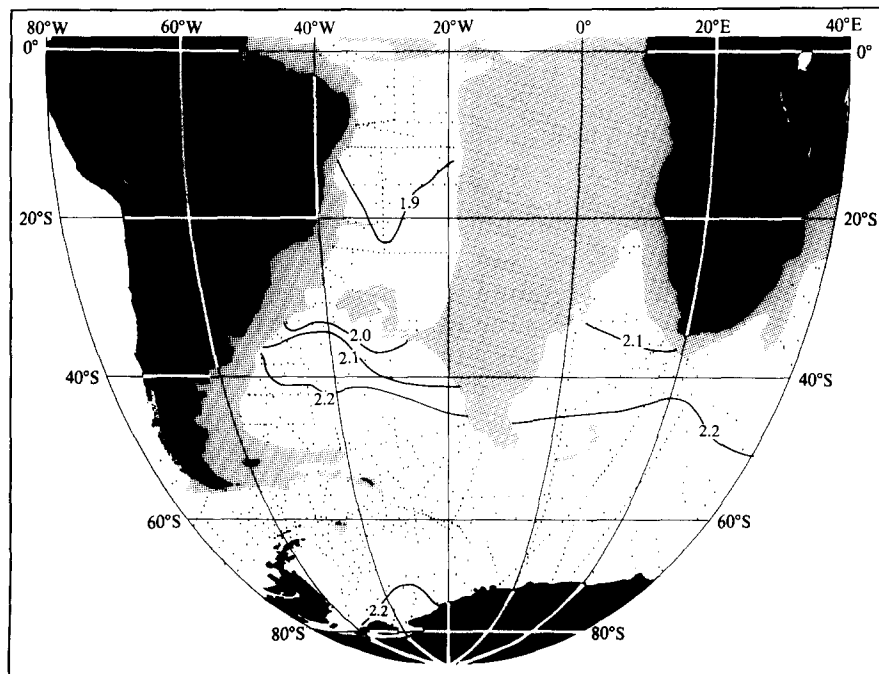


Fig. 38d. Phosphate ($m\text{ mol m}^{-3}$) on the isopycnal defined by 45.97 in σ_4 below 3500 m.

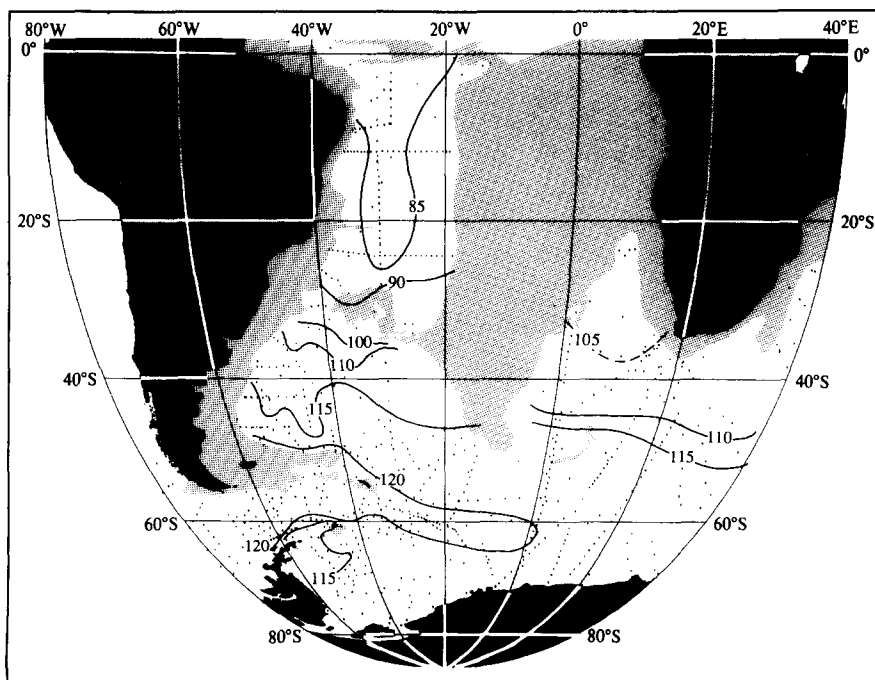


Fig. 38e. Silica (m mol m^{-3}) on the isopycnal defined by 45.97 in σ_4 below 3500 m.

SPEER (1985), with more recent data from a section taken along 11°S to the coast, has shown that these extrema extend westward to the Greenwich Meridian, where they are found near 3400 m at about 41.51 in σ_3 , 45.85 in σ_4 . He has modelled a deep western boundary current on the eastern side of the Mid-Atlantic Ridge to account for the tracer patterns.

The result of this source for nutrients and sink for oxygen shows on the maps of oxygen and nutrients (Figs. 36c, d, e) as an oxygen extremum and high nutrient values near 5°–10°S in the east, which might suggest an extension of circumpolar waters from the south. However, the salinity (and temperature) in this area (Fig. 36b) show that this water is principally northern in origin. The oxygen and nutrient extrema are from local processes.

A substantial part of the warm saline water from the North Atlantic does not reach the Antarctic Circumpolar Current along the western side of the South Atlantic. Instead it turns back northward along the western side of the Mid-Atlantic Ridge. Some of this, joined by waters from the south, extends back northward into the North Atlantic, and some of it turns eastward south of the equator and southward along the eastern boundary to reach the Antarctic Circumpolar Current south of Africa.

GEORGI (1981) has shown the increase in temperature and salinity of the circumpolar water that flows through the South Atlantic. He proposes that the greatest heat and salt exchange with the warm and saline northern water take place in the Argentine Basin. It appears that this exchange may take place also along the deep northward flow west of the Mid-Atlantic Ridge, some of which turns eastward and southward through the Angola and Cape basins (Figs. 24, 28, 29, 36 and 38).

12. THE WEDDELL SEA UPPER LAYERS

Within the Weddell Sea the waters less dense than about 46.06–46.07 in σ_4 have entered from the Drake Passage, and reflect those characteristics. These waters flow cyclonically around the Weddell Gyre and bring a layer of diminished but recognizable extrema from the Drake Passage to the southern limb of the gyre (WHITWORTH and NOWLIN, 1987). The shoaling of the isopycnals and the surface divergence along the axis of the gyre keep these extrema separate from those in the northern limb, which is flowing eastward, but in the westward flow south of the axis they are apparent (Figs. 12, 13 and 14).

These extrema, the maxima in temperature and salinity, and the minimum in oxygen, slope downward to the south from about 500 m at 65°S to about 1000 m at 75°S. Within the limits of the data (different ships, times, and methods) they appear to be fairly close in density (about 27.84 in σ_0 , 32.54 in σ_1). This may be simply because the layers are confined closely between the surface waters, of opposite extrema, and the underlying waters, which are not directly of circumpolar origin.

Along the westward path of the southern limb of the gyre the maxima in temperature and salinity decrease toward the west. It is not clear from the present data set that the oxygen and nutrients are changed during the westward flow.

In the southern limb of the Weddell Gyre there are no clearly-enclosed phosphate or silica maxima in the present data that appear to correspond to the other extrema. Instead the values remain high and nearly constant over a broad depth range, from about 200 m to the bottom near the Greenwich Meridian, from 500 m to about 3500 m along 30°W, from 500 m to the bottom along 41°W. The different concentrations may result from offsets in the different data sets as well as changes in concentration with longitude.

These waters, the denser parts of the circumpolar water, are illustrated on the $\sigma_4 = 45.97$ and 46.04 isopycnals (Figs. 38 and 39). They intersect the bottom in the western basins at about 5°N and 2°S, respectively (Fig. 37). The flow fields show the deep flow, extending farther north along the western boundary at greater depths (Figs. 24, 28, 29, 30), with lower salinity and oxygen.

The isopycnal 45.97 in σ_4 (Fig. 38) lies too deep to extend into the Angola Basin from either the north or the south. As it rises across the circumpolar flow it lies shallow enough to extend across the Mid-Atlantic Ridge south of about 50°S, and northward from there into the Cape Basin.

The salinity and oxygen in the Cape Basin just south of the Walvis Ridge are higher, and the nutrients lower, than in the waters farther south: they cannot have entered along this isopycnal (Fig. 38). Instead, the source of these lateral features is the overlying water (Fig. 36). The vertical exchange that takes place in the southward flow over the Walvis Ridge (Fig. 24) extends below the sill depth, and provides the higher temperature and salinity and lower nutrients seen on the 45.97 isopycnal and just south of the Walvis Ridge (30°S) on the vertical section along the Greenwich Meridian (Fig. 13).

Near the Rio Grande Rise at 3500 m (Fig. 36) the flow at the western boundary is southward (Fig. 28) and the patterns of tracers show the northern characteristics extending southward across the Rise. From 4000 m downward the flow is northward (Figs. 29 and 30) and the salinity and oxygen are lower and the nutrients higher along the western boundary than farther offshore. The western boundary current flows northward at and below the 45.97 isopycnal everywhere north of the Falkland Escarpment.

The maps of deep flow (Figs. 29 and 30) indicate a northward flow all across the Brazil Basin. The higher salinity and oxygen found offshore there, and the lower nutrients, may result from the vertical exchange with the overlying water extending southward.

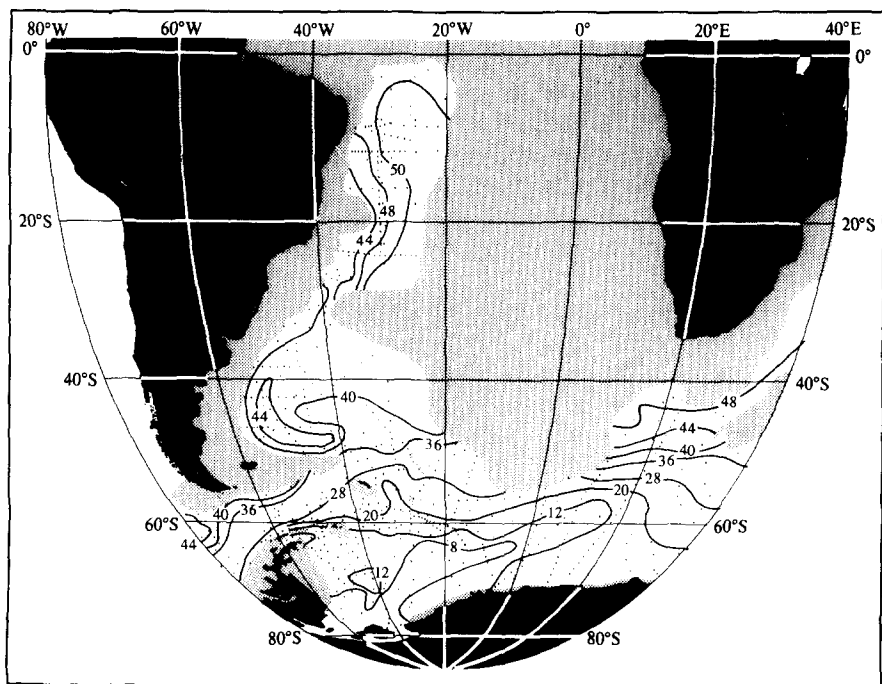


Fig. 39a. Depth (hm) of the isopycnal defined by 46.04 in σ_4 below 3500 m.

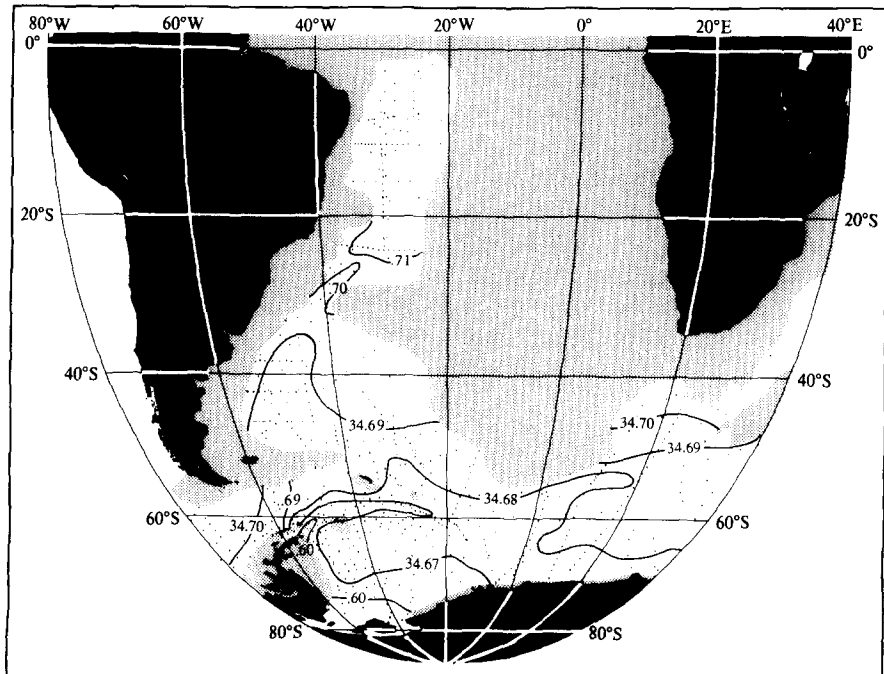


Fig. 39b. Salinity on the isopycnal defined by 46.04 in σ_4 below 3500 m.

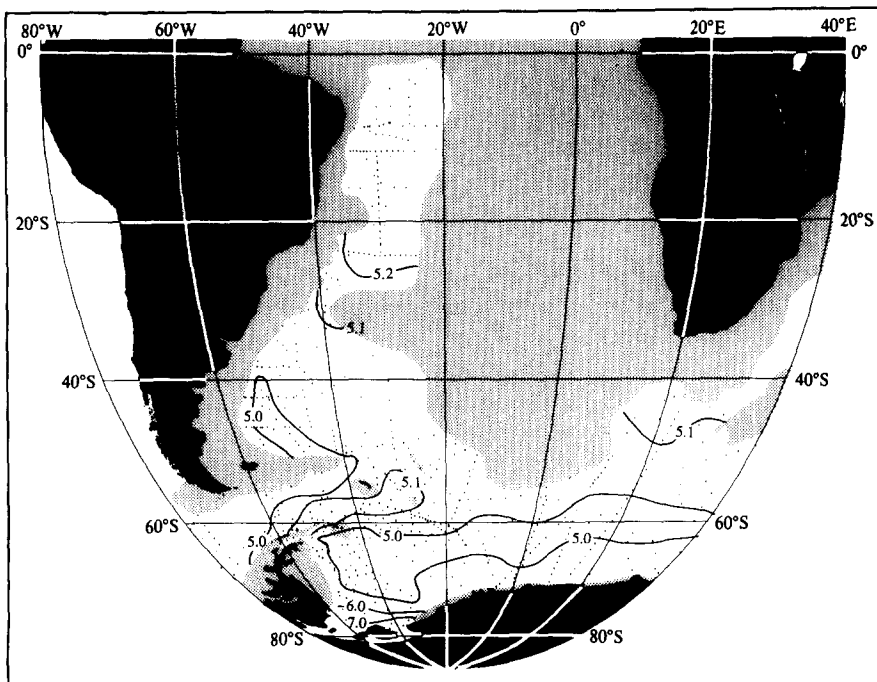


Fig. 39c. Oxygen ($\times 10^3$) on the isopycnal defined by 46.04 in σ_4 below 3500 m.

Just south of about 30°S there are very sharp lateral gradients in the west between the northern and southern characteristics along all of the isopycnals from 36.98 in σ_2 to the bottom. These are among the strongest lateral gradients of tracers found in deep water. In the upper waters they result from the confluence of waters from the north and south, both turning eastward between 25°S and 35°S . This occurs at and below 2000 m, where the anticyclonic gyre has shifted northwestward (Figs. 20 and 22). At depths from 3000 m the patterns of flow and the strong gradients in the tracers are related to the position of the Rio Grande Rise, which diminishes the flow and the north-south exchange of characteristics.

13. THE DEEPER WATERS OF THE WEDDELL SEA

The waters denser than 46.06 in σ_4 (which rises across the circumpolar current to about 32.555 in σ_1 and 27.845 in σ_0) are formed along the shelf of the Weddell Sea (GILL, 1973; CARMACK and FOSTER, 1975; FOSTER and CARMACK, 1976; DEACON, 1979; and FOSTER, FOLDVIK, and MIDDLETON, 1987). The extreme cooling, the source of salt from the circumpolar water, and the leaching of brine on the shelves produces waters dense enough to flow down the slopes into the deepest parts of the basin.

Exchange with the adjacent waters takes place as they flow downward along the slope. As they reach the bottom they have become warmer and less saline, somewhat lower in oxygen and higher in nutrients than those on the shelves and slopes where they are formed.

It is not only the densest waters of the Weddell Sea, as high at about 46.30 in σ_4 , that are produced by these shelf and slope exchanges, but the entire density range from 46.07 to 46.30 requires an input from the Weddell Sea processes, and beneath the gyre axis these extend from the bottom up to about 600 m. Against the coast of Antarctica, in the westward flow, they are found up to 2000 m.

Very high concentrations of silica are found in the southern part of the Drake Passage near 3000–3500 m at densities of about 46.02–46.04 in σ_4 . These are nearly the densest of the Drake Passage waters, and along the axis of the Weddell Sea gyre these isopycnals lie at about 500–600 m, falling to 1500 m near the coast and to 4000 m near 40°S. These isopycnals may be taken to represent the silica maximum in the Drake Passage, but in the Weddell Sea the maximum lies deeper and at higher densities. It has been eroded from the top by exchange with the water from the North Atlantic during its eastward path (CARMACK, 1973) and by exchange with the slope waters along its westward path. It has received substantial increments of silica by dissolution of the silica-rich sediments (WEISS, OSTLUND and CRAIG, 1979; and EDMOND, JACOBS, GORDON, MANTYLA and WEISS, 1979). The values within the deep Weddell Sea are high (mostly 120 to 130) but the variance is so wide between expeditions, and between stations on some lines, that no pattern can be determined. The data have not been contoured on isopycnals deeper than 45.97 in σ_4 .

Water with density greater than that entering through the Drake Passage is found only to about 9°S and only in the western basins (Fig. 37). It does not enter the Angola Basin from the north or cross the Cape Rise into the Cape Basin from the south.

The flow of these denser waters has about the same patterns in the Weddell Sea and southern Argentine Basin as the overlying waters. Near 3500 m (Fig. 28) a single cyclonic gyre extends through the Weddell and Argentine basins. At 4000 m depth (Fig. 29) the exchange is limited but the isopycnal 46.04 in σ_4 (Fig. 38) lies just shallow enough to extend into the Argentine Basin.

It is noteworthy that at depths below the crest of the Mid-Atlantic Ridge not only the Weddell Sea but the Argentine and Cape basins show cyclonic patterns (Figs. 28–30), though the western boundary current in the Argentine Basin continues a smaller anticyclonic flow in the west down to 4000 m.

The deepest isopycnal shown (Fig. 40) extends northward only to about 50°S where it intersects the bottom a little deeper than 4000 m. It shows the low salinity (cold) water from the western Weddell Sea extending eastward along about 60°S and slightly more saline (warmer) water entering from the east near 65°S–70°S.

The three deepest isopycnals (Figs. 38, 39 and 40) show the least saline (coldest) waters extending eastward just south of the South Scotia Ridge. The shallower two of these isopycnals lie between 500 and 1500 m in that area, and may contain a portion from the Bransfield Strait, where the waters are much colder, less saline, and higher in oxygen than the waters entering from the

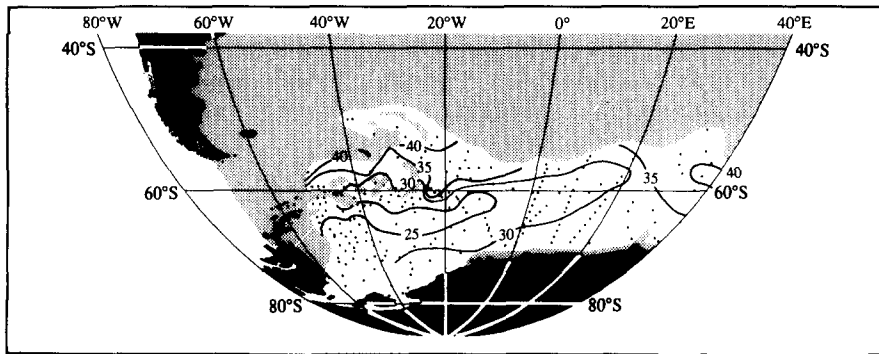


Fig. 40a. Depth (hm) of the isopycnal defined by 46.12 in σ_4 below 3500 m.

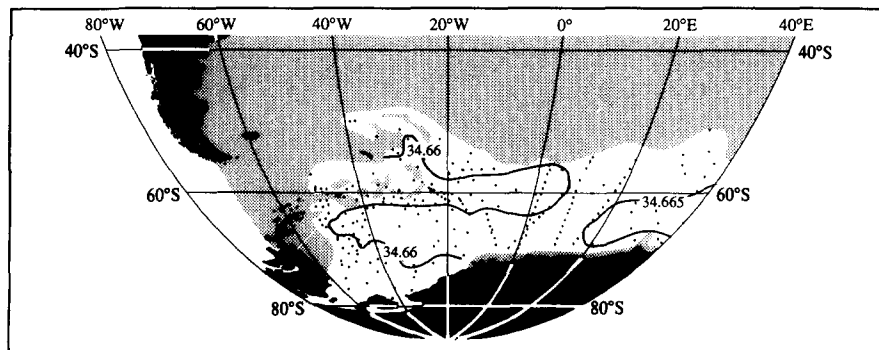


Fig. 40b. Salinity on the isopycnal defined by 46.12 in σ_4 below 3500 m.

west (CLOWES, 1934; GORDON and NOWLIN, 1978). The greater part of the waters in this tongue of lower salinity and higher oxygen is probably from the south, beneath the ice and the Larsen ice shelf of the western Weddell Sea, where we do not yet have data. Whether the Bransfield Strait contributes any part of the feature on these isopycnals is uncertain, but maps of the bottom characteristics (MANTYLA and REID, 1983) find no evidence of such an effect at greater depths, but indicate a source from the Weddell Sea.

As the deepest isopycnal shown (Fig. 40) rises above 2500 m within the Weddell Sea the characteristics are mapped also at 4000 m (Fig. 41). On these maps the coldest, least saline, lowest-phosphate, highest-oxygen and densest waters extend eastward from the northwestern Weddell Sea, along the axis of the cyclonic gyre.

The waters at 4000 m (Fig. 41) just south of the Walvis Ridge show the effect of the southward flow of the overlying water. They are warmer and more saline, higher in oxygen, and lower in nutrients than those to the west and the south.

The map of density (Fig. 41f) reflects the strong baroclinic fields still present at this depth within the Argentine and Cape basins. At 4000 meters depth (Fig. 29) the flow is northward in the Argentine and Brazil basins and southward in the Angola Basin. The same sense of flow is seen there at depths below the downstream sill depths (Fig. 30). Northward flow of the water of 46.04 in σ_4 from the Brazil Basin can take place only after mixing with the overlying less dense water. By this mixing the Weddell Sea can contribute to the less dense waters still farther north.

The flow along the bottom cannot be shown in maps along isobars. As the density along the bottom decreases northward from the Weddell Sea, and the isopycnals slope downward and intersect the bottom, isopycnal representations are not useful. Its features can be seen in the pattern of abyssal characteristics by MANTYLA and REID (1983) in more detail than in WUST's (1933) maps of abyssal temperature and salinity. The map of abyssal density (Fig. 37) is taken from work in progress by Arnold Mantyla, and includes additional, more recent data than the earlier version (MANTYLA and REID, 1983). It shows the northward limit of densities greater than the Drake Passage water, the northward path across the equator, the limitations at the entrances to the Argentine and Brazil basins, the northern entry to the Angola Basin, and at the southern entry to the Cape Basin.

LE PICHON, EITTREIM and LUDWIG (1971) had, from the bathymetry and sediment patterns, postulated a northward abyssal flow through a passage at about 48°S, 36°W through the Falkland Fracture Zone. Neither hydrographic nor bathymetric data to show this were available to WUST in his 1933 study of abyssal characteristics. LE PICHON, EWING, and TRUCHAN (1971) obtained bottom photographs and cores along the Vema Passage through the Rio Grande Rise that showed very little deposition, and indicated an acceleration of flow within the channel.

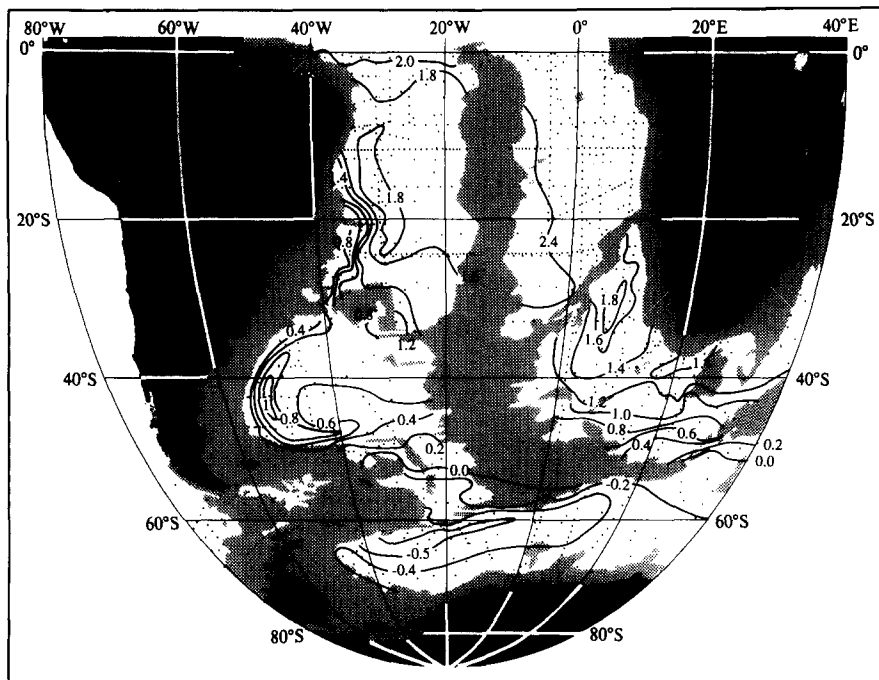
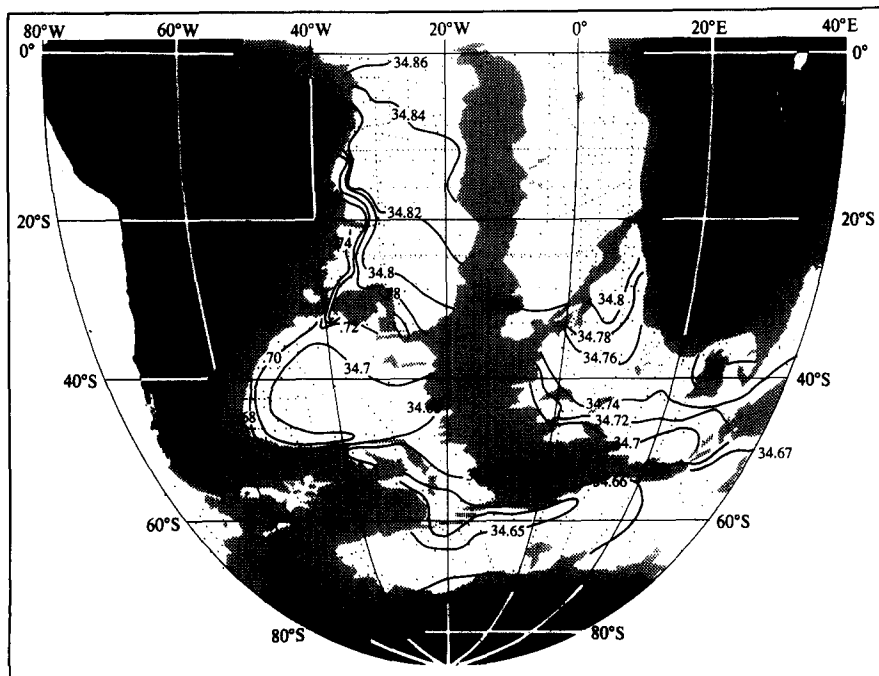
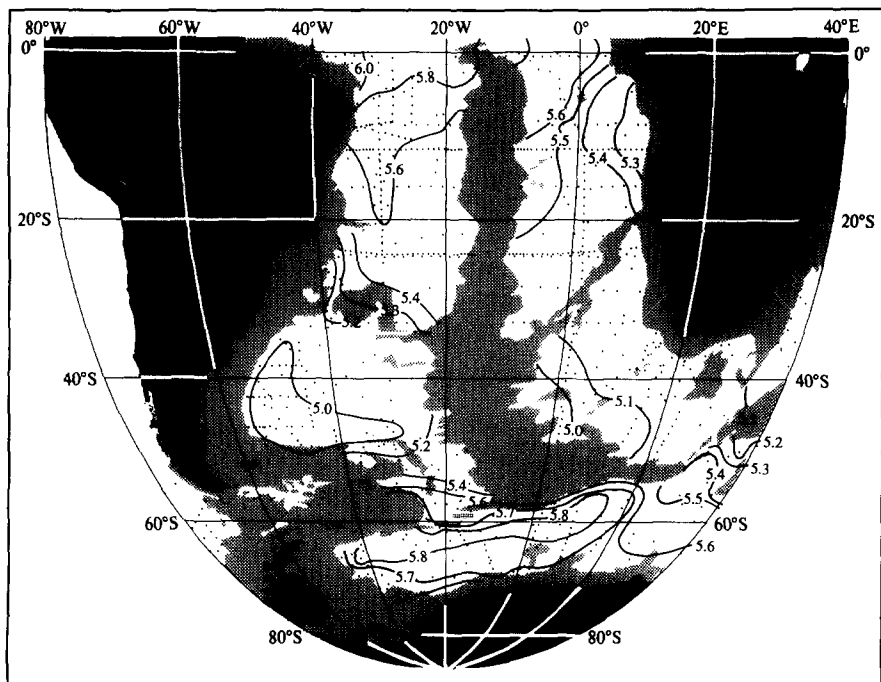
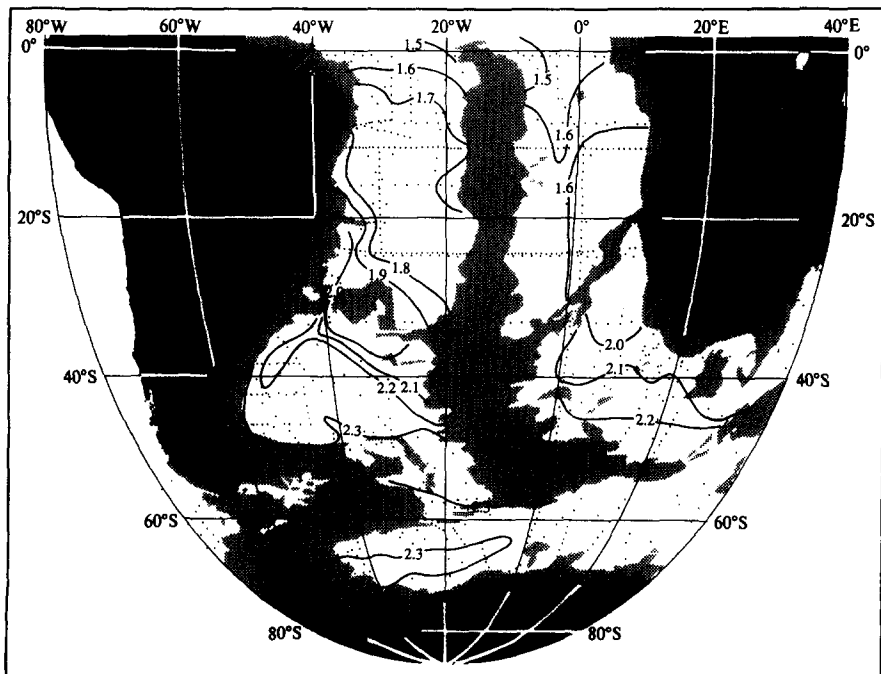
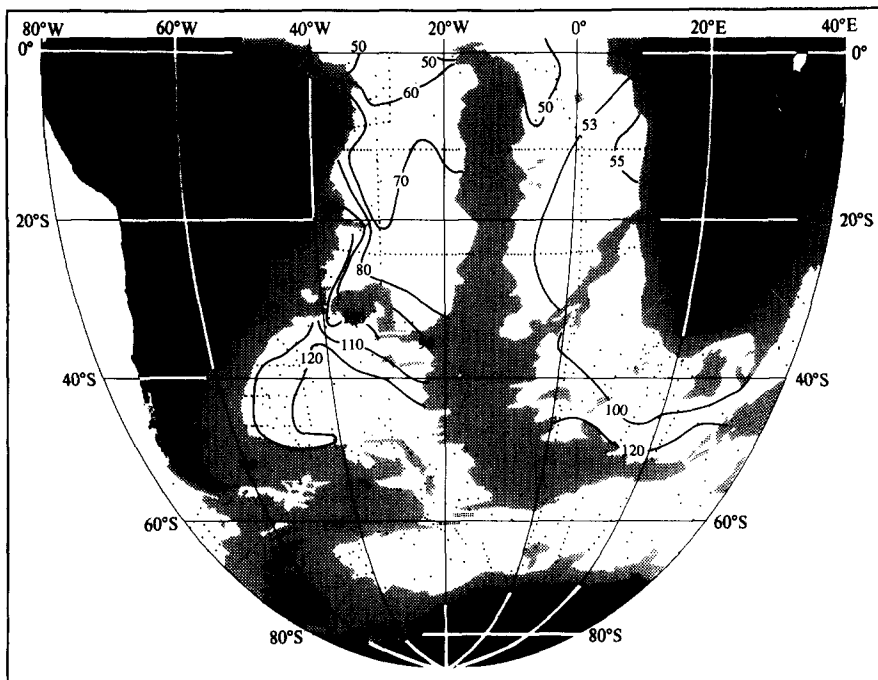
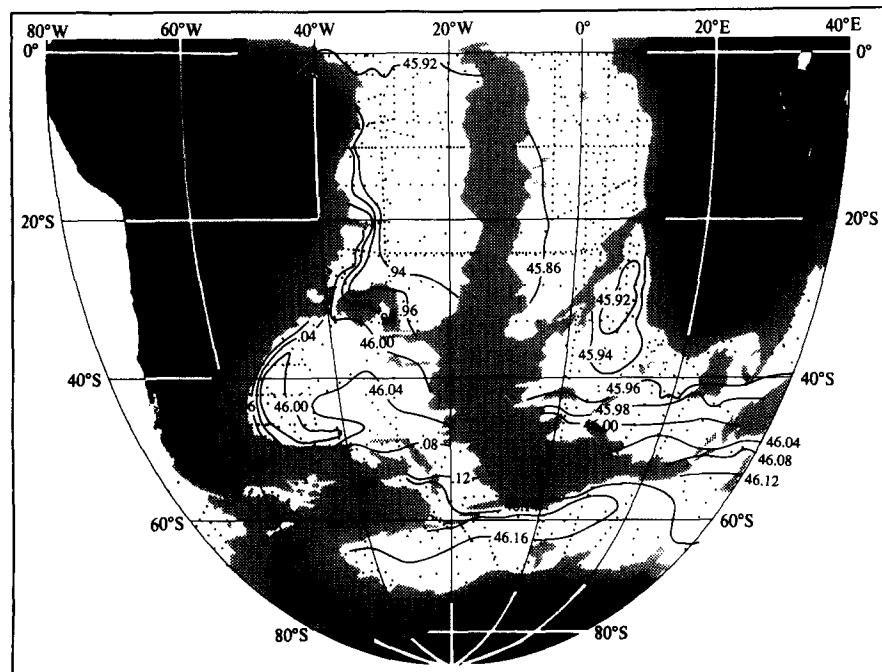
Fig. 41a. Potential temperature ($^{\circ}\text{C}$) at 4000 m.

Fig. 41b. Salinity at 4000 m.

Fig. 41c. Oxygen ($\times 10^3$) at 4000 m.Fig. 41d. Phosphate (m mol m^{-3}) at 4000 m.

Fig. 41e. Silica (m mol m^{-3}) at 4000 m.Fig. 41f. Potential density (σ_4) at 4000 m.

14. THE FALKLAND-BRAZIL CONFLUENCE AND INTERLEAVING

The section extending northward from the western Weddell Sea to the coast of Brazil near 40° - 45° W (Fig. 11) crosses both limbs of the Weddell Sea gyre, the Antarctic Circumpolar Current, the Falkland Current, the offshore extension of the anticyclonic gyre near 48° S, and the anticyclonic gyre again north of 40° S (Figs. 11, and 10, 19, 20, 22-24).

The Falkland and Brazil currents meet near 40° S at the western boundary, turn offshore together, and loop northwestward before turning eastward. Each of these currents is part of a large gyre. The anticyclonic gyre, which includes the Brazil Current, bends offshore south of 40° S. From the sea surface to about 3000 m, it penetrates the cyclonic gyre to about 48° S between the two limbs of cyclonic flow. At 3500 m it retreats northward to about 45° S, at 4000 m to 41° S, and at 4500 m and below it is not evident south of the Rio Grande Rise. At 4000 m the baroclinic signal of the anticyclonic gyre is still present in the west (Fig. 41f) but the cyclonic flow occupies most of the Argentine Basin (Fig. 29), connecting it with the Weddell Sea, and at greater depths the cyclonic flow obtains throughout the basin (Fig. 30).

As the anticyclonic gyre contains mostly the characteristics from the north, and the cyclonic gyre water from the south, their interleaving north of the Falkland Escarpment shows contrasting values in the tracers. This is illustrated by θ/S curves taken from the Antarctic-Brazil line between 46° S and 50° S along about $41^{\circ}20'$ W (Fig. 42). The northern station (13) shows the strong and relatively smooth salinity maximum characteristic of the waters from the north. The southern station (21) shows the weaker and even smoother maximum of the circumpolar water. The station in between (19), only about 33 km north of station 21, shows the interleaving that takes place in the strong lateral shear.

The section from Antarctica to Brazil (Fig. 11) shows separate salinity maxima. The highest values are in the layer from the north, that lies near 2500 m over most of the Argentine Basin but rises abruptly near the Escarpment. South of the Falkland Plateau the maximum represents the circumpolar water, part of which turns northward and downward to flow westward just north of the Plateau, beneath the northern maximum.

The oxygen shows the circumpolar minimum from Drake Passage south of 50° S, with a separate minimum farther south in the westward flow. As the oxygen minimum from the circumpolar current flows westward north of the Plateau into the Argentine Basin the incoming layer of high oxygen from the north splits it into an upper and a lower layer. This effect is seen in the silica pattern also (Fig. 11d) and in phosphate (BAINBRIDGE, 1980) on the Geosecs western section.

Near 33° S, where the section reaches Argentina, the deeper western boundary current carries the denser, colder, and less saline water northward beneath the warm and saline layer carried southward. The slope is so steep that the available data cannot show the narrow inshore northward flow that may extend as shallow as 3000 m between the last deeper station and the slope (Fig. 11f).

GEORGI (1981) used vertical sections and maps of potential temperature at 4000 m and the depth of the 0°C isotherm in the Argentine Basin and Scotia Sea to investigate the bottom circulation. The maps herein (Figs. 41a and 39a) are about the same as his. He noted the convolution of the temperature field by the confluence of the Falkland and Brazil currents on a section along about 43° S extending eastward from the coast of Argentina. He noted the difficulty in selecting a reference level for calculating geostrophic velocity in that area and pointed out that with a reference level at 2000 decibars the Falkland Current would split the Brazil Current into a shoreward and an offshore component. This sort of reference would show the sort of patterns seen in most of the shear fields (Figs. 25 and 27). With the barotropic component used herein, it is the Brazil Current that splits the Falkland Current into an onshore and offshore part down to 4000 decibars (Figs. 22, 24 and 29). Just north of the Falkland Plateau along 41° W these three flows with alternating westward and eastward senses are very narrow between 2000 and 3000 m (Figs. 22-24) and the

characteristics alternate accordingly between 46°S and 48°S along 41°W (Fig. 11). (Names are sometimes confusing. Perhaps the terms Falkland and Brazil Current are not satisfactory here.) GEORGI's (1981) schematic pattern of abyssal flow in the Argentine Basin and its connection with the Weddell Sea are very similar to those derived herein at 3500–4500 decibars, and include more detail in the western Georgia Basin than the lines I have used can define.

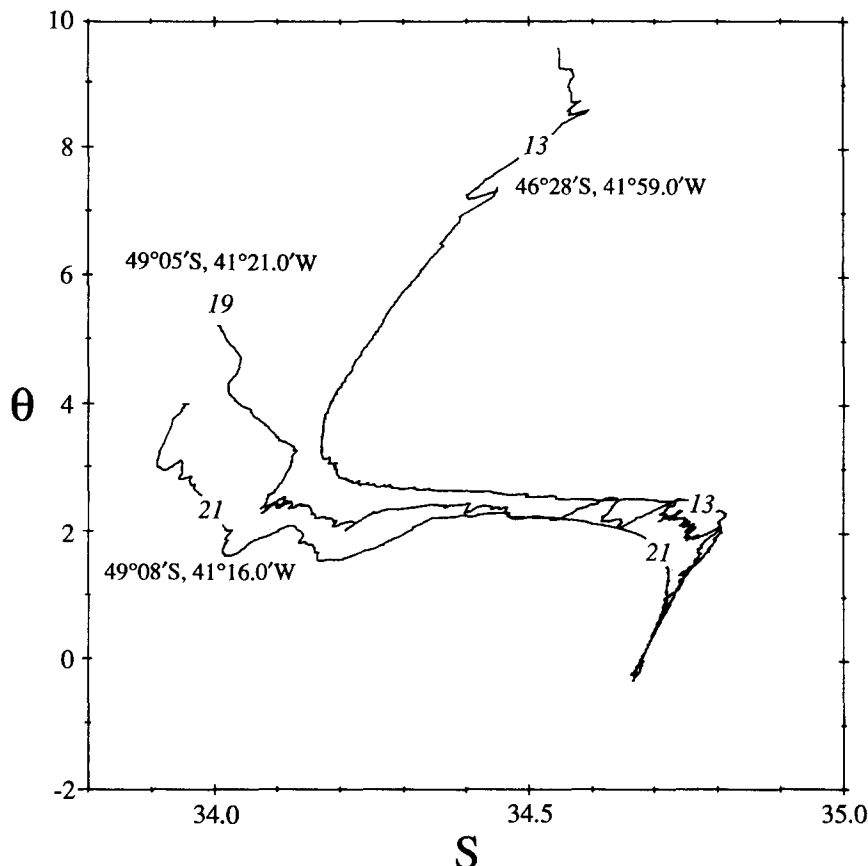


Fig. 42. Potential temperature/salinity curves for three stations just north of the Falkland Escarpment near 41°20'W, from the Indomed Expedition (SCRIPPS INSTITUTION OF OCEANOGRAPHY, 1979).

15. THE AGULHAS EXTENSION

The westward extension of the Agulhas Current south of Africa is apparent on all of the tracer fields from the surface down to at least 1800 m (Fig. 21) and perhaps to 2000 m. At greater depths the tracers indicate a source from the eastern basins of the South Atlantic, below 3400 m via the Cape Basin (Fig. 38). These Atlantic waters extend into the Indian Ocean northward through the Transkei Basin into the Natal Valley and also into the Mozambique Basin as well as extending eastward (CLOWES and DEACON, 1935; WYRTKI, 1971; JACOBS and GEORGI, 1977).

The westward flow at the southern tip of Africa is seen in the baroclinic field alone from the surface to the bottom (Figs. 4, 25–27) and in the total geostrophic flow down to 4000 db. The baroclinic transport of the Agulhas extension across the section near 20°E is about $125 \times 10^6 \text{ m}^3 \text{ s}^{-1}$ to the west. With barotropic component to the east added north of the Agulhas Plateau (Fig. 3) the total transport becomes $99 \times 10^6 \text{ m}^3 \text{ s}^{-1}$ (Fig. 43). The passage north of the Plateau is narrow and the tracer patterns near the bottom indicate that the waters of the Mozambique Basin have entered from the south of the Plateau (MANTYLA and REID, 1983) rather than through the passage. Therefore it does not seem possible to add a very strong eastward barotropic component beneath the westward flow north of the Agulhas Plateau.

The maxima in steric height just north of 40°S on the 10°E and 20°E lines have been treated here as if they represent a single Agulhas inflow and return to the south and east. There is of course reason to believe they are separate eddies, but this must be left to the more closely focused studies and data sets (OLSON and EVANS, 1986; GORDON, LUTJEHARMS, and GRUNDLINGH, 1987; BENNETT, 1988). It is interesting that the maps herein of surface flow south of Africa are very similar to those of KRUMMEL (1882).

Transport within the eddies has been calculated by GORDON, LUTJEHARMS, and GRUNDLINGH (1987) who find 35 and $40 \times 10^6 \text{ m}^3 \text{ s}^{-1}$ relative to 1500 decibars. BENNETT (1988) in her thesis has carried out a general review of the observations and an examination of the dynamics of the flow. She found on two transects 56 and $95 \times 10^6 \text{ m}^3 \text{ s}^{-1}$ in the westward extension of the Agulhas, and 54 and $65 \times 10^6 \text{ m}^3 \text{ s}^{-1}$ in the return flow, relative to 2400 m (beneath the oxygen minimum, and above the oxygen maximum of the Atlantic water).

16. CURRENT MEASUREMENTS

The section along 32°S crosses the Hunter Channel between about 20°W and 30°W, with a sill depth a little deeper than 4000 m, and turns northwestward at 30°W and passes across the Rio Grande Rise north of the Vema Channel, near 29°S, 39°W, with a sill depth about 4500 m.

The flow through the Vema Channel has been measured by several investigators (JOHNSON, McDOWELL, SULLIVAN and BISCAYE, 1976; REID, NOWLIN and PATZERT, 1977). Later, HOGG, BISCAYE, GARDNER and SCHMITZ (1982), with current meters and hydrographic measurements, carried out a study of the transport and modification of the waters flowing northward through the Vema Channel. They note the effect of the Channel on the flow and exchange of heat, and estimate a northward transport of the deeper water of $4 \times 10^6 \text{ m}^3 \text{ s}^{-1}$. The northward flow shown on the section here (Fig. 32°S flow), a little north of the Vema Channel, is about $3.1 \times 10^6 \text{ m}^3 \text{ s}^{-1}$, and through the Hunter Channel (between the Rio Grande Rise and the Mid-Atlantic Rise) is about $1.8 \times 10^6 \text{ m}^3 \text{ s}^{-1}$.

The INDOMED Expedition (SCRIPPS INSTITUTION OF OCEANOGRAPHY, 1979) had deployed five current meters that lie on the lines of stations used in calculating the velocity. Two of these were along 41°W, just north of the Falkland Escarpment. The deeper one proved to be in the short and narrow trough at the bottom of the slope mapped by LE PICHON, EITTREIM and LUDWIG (1971), and gave flow toward the northeast. The offshore meter gave a strong westward signal.

Of the three others, on the line extending northeastward from 48°22'S, 56°27'W, north of the Escarpment, the 1433-m and 5366-m records showed strong northwestward flows parallel to the slope. At the third, 220 km offshore of the 2000-m curve and at the greatest depth (5703 m), the flow simply looped and meandered.

17. THE TOTAL GEOSTROPHIC TRANSPORT

As the velocity field has been defined at all depths it can be integrated to produce a field of total geostrophic transport (Fig. 43). No assumptions about the nature of the total transport field were made initially other than those about the entering and departing quantities. The resulting field of transport, then, is simply the sum of the various velocities that were estimated by combining the baroclinic components with barotropic components derived from the tracer patterns along various isopycnals. There has been no attempt to match any earlier concept of the shape of the transport field, or of its magnitude in the interior.

The integration starts from Antarctica, and reaches $130 \times 10^6 \text{ m}^3 \text{ s}^{-1}$ everywhere along the coast of South America and $132 \times 10^6 \text{ m}^3 \text{ s}^{-1}$ along Africa: the net transport from the North Atlantic is $2 \times 10^6 \text{ m}^3 \text{ s}^{-1}$.

This field can be compared with that of the South Pacific prepared by the same method (REID, 1986). Setting aside the part of the Pacific west of New Zealand and the Tonga-Kermadec Ridge, which has no counterpart in the Atlantic, there is some correspondence in the features. Each has an anticyclonic gyre in mid-latitudes, mostly west of the major ridge; a cyclonic gyre in the north, centered near 10°S; southward transport along the eastern boundary (though weaker in the Atlantic), a cyclonic gyre south of 50°S; and an intense inflow from the Antarctic Circumpolar Current that turns northward along the western boundary, pinching into the central anticyclonic gyre just before they turn eastward together.

The wind-driven upper circulation in the two oceans is roughly similar, and intermediate and abyssal waters flow northward through both oceans and mid-depth waters return southward. The major differences in their patterns of flow result from the different ridge systems. The Mid-Atlantic Ridge is much closer to South America than the East Pacific Rise is to the Tonga-Kermadec Ridge. The deep Weddell Sea is more open to the Atlantic than the Ross Sea is to the Pacific.

The cyclonic flow near 10°S extends over a wider range of latitude in the Atlantic, but is of about the same magnitude (about $80 \times 10^6 \text{ m}^3 \text{ s}^{-1}$ from the anticyclonic high to the cyclonic low). With his inverse model FU (1981) found the cyclonic gyre to be narrower, but of about the same magnitude.

In this work I have not taken account of the Ekman transport. As the field of flow has been balanced without the Ekman flow, it is in error by that amount. Just how to apply the Ekman transport requires some thought. By what paths does the water leave that enters near the surface as Ekman transport? The part from the equator is of low density and can not submerge and depart at greater depths. It must leave near the surface. The Ekman transport from the westerlies is of denser water and can submerge and extend equatorward or return poleward at various depths, but in which part of the flow?

Because of this uncertainty I have chosen to set the Ekman transport aside and balance the geostrophic flow alone. However, the patterns of flow shown here might not be very different if the Ekman transport were added by assuming a uniform barotropic increment on each section. Adding 10 Sverdrups across 50° of longitude with an average depth of 4000 meters requires an average velocity increment of 0.046 cm/sec. At 5° latitude this requires a change in slope of 0.63 dynamic centimeters over 50° of longitude. Across 35° S the increment for 10 Sverdrups would be about 1.7 dynamic centimeters. This would not alter the patterns of flow very much in either case.

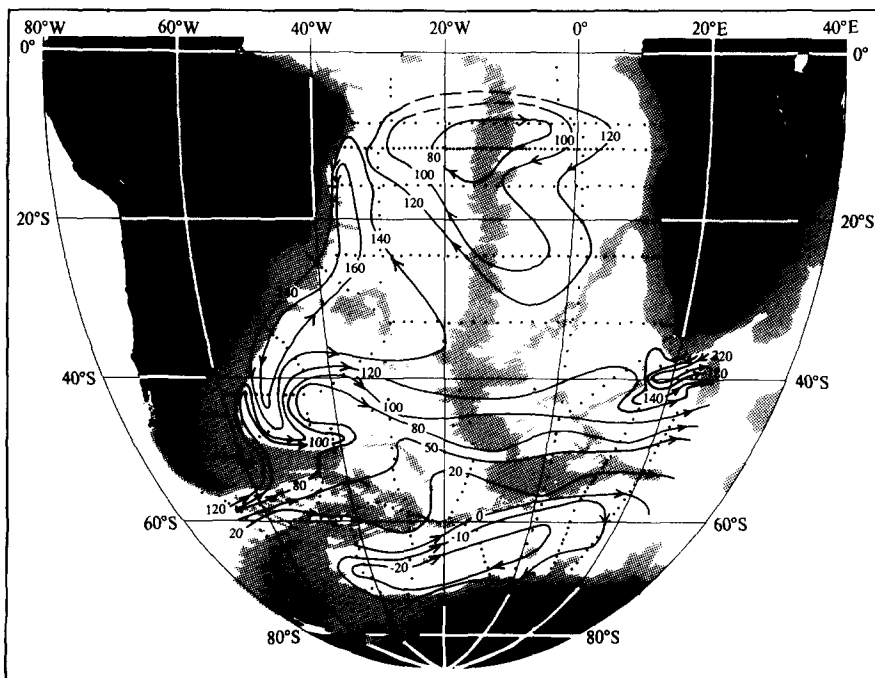


Fig. 43. Transport in units of $10^6 \text{ m}^3 \text{ s}^{-1}$. The shaded area represents depths less than 3500 m. Integration is from Antarctica northward, yielding 130 units along the coast of South America and 132 units along the coast of Africa, with 2 units crossing southward from the North Atlantic.

18. CONCLUSION

Waters from the North Atlantic, the Circumpolar Current, and the Weddell Sea enter the South Atlantic and are caught up in the circulation imposed by the winds and the thermohaline processes. They have different characteristics and vertical extrema. Their density ranges overlap, and as they meet within the South Atlantic Ocean they partly interleave, in order of density, and partly penetrate each other laterally as they circulate in different patterns. This results in more vertical extrema in the profiles of characteristics. The flow is more varied, both horizontally and vertically, than had been expected.

The wind-driven circulation provides near the surface the large anticyclonic gyre of mid-latitudes and the cyclonic gyre of high latitudes, and a cyclonic flow in the east near the equator. The thermohaline circulation appears to provide the deep meridional flow and the cyclonic abyssal flow. The Weddell Sea gyre extends to the bottom, and with little change in pattern down to about 3000 m. At greater depths it expands to include the cyclonic flow within the Argentine Basin.

The great anticyclonic gyre of mid-latitudes, which is roughly triangular at the surface and centered near 25°–30°S, narrows and retreats southward at greater depth, with its axis along about 35°S at 1000 and 1500 meters. Below 2000 m it is confined to the west of the Mid-Atlantic Ridge and contains two smaller cells north and south of the Rio Grande Rise.

North of about 15°S, and down to the crest of the Mid-Atlantic Ridge, the waters flow eastward, with part turning southward through the Angola and Cape basins, leaving the Atlantic with the circumpolar flow south of Africa.

In the Argentine Basin equatorward flow of circumpolar and Weddell Sea water takes place just offshore of the southward western boundary current. The densest parts of this water turn cyclonically back toward the Weddell Sea and eastward with the Circumpolar Current. The less-dense layers cross the Rio Grande Rise and flow northward in the eastern part of the Brazil Basin, at and below the sill depth of the Mid-Atlantic Ridge. Parts of them extend into the North Atlantic and parts cross the Mid-Atlantic Ridge near the equator through the Romanche Trench, and turn southward through the Angola Basin and along the eastern boundary of the Cape Basin. The Cape Basin also receives deep water from the south and east, which flows cyclonically within the Basin and leaves the Atlantic south of Africa.

There is an eastward flow at and below 2000 m just north of the Rio Grande Rise. This is the southern limb of the northern cell of the anticyclonic gyre, and the water is carried eastward to the Ridge and then northward with the gyre.

The southward flow along or near the western boundary extends down to about 4000 m or more and to about 50°S, though south of 40°S there is a northward-flowing current along the boundary inshore of the southward flow. Near 50°S the southward flow turns eastward and northward as a return flow and then eastward again south of the Rio Grande Rise. Above 1500 m it extends with the large anticyclonic gyre all across the South Atlantic and then northward. Below 2000 m it turns northward along the Mid-Atlantic Ridge.

Two different sources provide the waters of the depth and density range between the salinity minimum of the Intermediate Water and the deep layer of Weddell Sea water. The water from the North Atlantic is warmer, more saline, and having more recent contact with the upper layer is rich in oxygen and ^{14}C and poor in nutrients and ^3He . As it passes through the South Atlantic and flows with the Antarctic Circumpolar Current around the world, it has been described as warm, deep water. A major part of its flow is subsurface and on its circumpolar passage of more than 20,000 km it is mixed with waters that in the Indian and Pacific oceans are cooler and less saline, lower in oxygen, and higher in nutrients (CALLAHAN, 1972).

As the circumpolar water returns through the Drake Passage to the Atlantic its temperature and salinity extrema have been reduced and its extrema in oxygen, nutrients, $\delta^3\text{He}$ and $\Delta^{14}\text{C}$ are reversed and contrast sharply with those from the North Atlantic, but it has almost the same range of density. These two contrasting sources meet in the South Atlantic and are drawn into its sinuous, depth-varying, layered flow, with its western boundary currents and their eastward offshoots in the anticyclonic patterns near 25°S and 45°S.

The water from the north dominates the mid-depth range in the west, and divides the circumpolar waters into two layers, lying above and below the northern water. This division is less sharp in the eastern basins. As the mid-depth circumpolar water moves northward in mid-ocean some of it spreads laterally into the northern water. Along its westward loop near 15°–20°S at 2000–3000 m the lateral penetration of circumpolar characteristics splits the thick layer of salty, oxygen-rich and

nutrient-poor northern water into the two layers that WUST (1935) recognized as middle and lower parts of the northern water.

Near 3000 m the circumpolar characteristics extend northward across the equator in the east, and spread northward and westward. The oxygen minimum and phosphate and nitrate maxima found near 3000 m at 20°–30°N in the central North Atlantic are northward extensions of this circumpolar water. This extension also accounts for the low ^{14}C layer in the North Atlantic. Such an extension is also shown (REID, 1981) on a map of salinity along a slightly shallower isopycnal (36.95 in σ_2 , or 37.00 in the older equation). The phosphate shows a separate high north of the equator, and both oxygen and silica extrema may be of local origin, but the only possible origin for the water of low salinity there is the South Atlantic Ocean.

19. ACKNOWLEDGEMENTS

The work reported here represents one of the results of research supported by the National Science Foundation, the Office of Naval Research, and by the Marine Life Research Program of the Scripps Institution of Oceanography. I wish to acknowledge the assistance given by Mrs. Sarilee Anderson in data-management, programming, and especially her patience in handling the long sequence of adjustments made to the barotropic inputs. My thanks to Mizuki Tsuchiya and Arnold Mantyla for many discussions, and to Donald Olson and Thomas Whitworth for reading and commenting on the manuscript. I am grateful to Bruce Warren and Michael McCartney for providing the *Oceanus* data along the 11°S and 24°S transects.

REFERENCES

- ARNAULT, S. (1987) Tropical Atlantic geostrophic currents and ship drifts. *Journal of Geophysical Research*, **92**, 5076–5088.
- BAINBRIDGE, A. E. (1980) *GEOSECS Atlantic Expedition Volume 2, Sections and Profiles*. Sponsored by International Decade of Ocean Exploration, National Science Foundation, Washington, D. C., 198 pp.
- BANG, N. D. (1970) Dynamic interpretations of a detailed surface temperature chart of the Agulhas Current retroflexion and fragmentation area. *South African Geographical Journal*, **52**, 67–76.
- VAN BENNEKOM, A. J., and G. W. BERGER (1984) Hydrography and silica budget of the Angola Basin. *Netherlands Journal of Sea Research*, **17**, 149–200.
- BENNETT, S. L. (1988) Where three oceans meet: The Agulhas Retroflection region. Ph.D. Thesis, MIT/WHOI, WHOI-88-51, 365 pp.
- BROECKER, W. S., T. TAKAHASHI, and Y.-H. LI (1976) Hydrography of the central Atlantic—I. The two-degree discontinuity. *Deep-Sea Research*, **23**, 1083–1104.
- BROECKER, W. S., T. TAKAHASHI, and M. STUIVER (1980) Hydrography of the central Atlantic—II. Waters beneath the two-degree discontinuity. *Deep-Sea Research*, **27**, 397–419.
- BUBNOV, V. A., and V. D. YEGORIKHIN (1977) Investigation of the large-scale current structure in the tropical Atlantic Ocean along 23°30'W. *Oceanology*, **17**, 631–635.
- BURKOV, V. A. (1980) *General Circulation of the World Ocean* (in Russian). Leningrad, 256 pp.
- BUSCAGLIA, J. L. (1971) On the circulation of the Intermediate Water in the southwestern Atlantic Ocean. *Journal of Marine Research*, **29**, 245–255.
- CALLAHAN, J. E. (1972) The structure and circulation of Deep Water in the Antarctic. *Deep-Sea Research*, **19**, 563–575.

- CARMACK, E. C. (1973) Silicate and potential temperature in the deep and bottom waters of the western Weddell Sea. *Deep-Sea Research*, **20**, 927–932.
- CARMACK, E. C., and T. D. FOSTER (1975) On the flow of water out of the Weddell Sea. *Deep-Sea Research*, **22**, 711–724.
- CLOWES, A. J. (1933) Influence of the Pacific on the circulation in the south-west Atlantic Ocean. *Nature*, 189–191.
- CLOWES, A. J. (1934) Hydrology of the Bransfield Strait. *Discovery Report*, **9**, 1–64.
- CLOWES, A. J. (1938) Phosphate and silicate in the Southern Ocean. *Discovery Report*, **19**, 1–119.
- CLOWES, A. J. (1950) An introduction to the hydrology of South African waters. *Investigational Report, Division of Fisheries, Union of South Africa*, No. **12**, 42 pp., 20 charts.
- CLOWES, A. J., and G. E. R. DEACON (1935) The deep-water circulation of the Indian Ocean. *Nature*, (December 14), 936–938.
- COCHRANE, J. D., F. J. KELLY, JR., and C. R. OLLING (1979) Subthermocline countercurrents in the Western Equatorial Atlantic Ocean. *Journal of Physical Oceanography*, **9**, 724–738.
- CONNARY, S. D., and M. EWING (1972) The Nepheloid Layer and bottom circulation in the Guinea and Angola Basins. In: *Studies in Physical Oceanography, Volume 2*, Arnold L. Gordon, editor, Gordon and Breach, London, pp. 169–184.
- DEACON, G. E. R. (1979) The Weddell gyre. *Deep-Sea Research*, **26**, 981–995.
- DEFANT, A. (1941a) Die relative Topographie einzelner Druckflächen im Atlantischen Ozean. Quantitative Untersuchungen zur Statik und Dynamik des Atlantischen Ozeans. *Wissenschaftliche Ergebnisse der Deutschen Atlantischen Expedition auf dem Vermessungs- und Forschungsschiff "Meteor" 1925–1927*, **6**(2)(4), 183–190, Beilagen X–XVIII.
- DEFANT, A. (1941b) Die absolute Topographie des physikalischen Meeresniveaus und der Druckflächen sowie die Wasserbewegungen im Raum des Atlantischen Ozeans. Quantitative Untersuchungen zur Statik und Dynamik des Atlantischen Ozeans. *Wissenschaftliche Ergebnisse der Deutschen Atlantischen Expedition auf dem Vermessungs- und Forschungsschiff "Meteor" 1925–1927*, **6**(2)(5), 191–260, Beilagen XIX–XXIX.
- DIETRICH, G. (1935) Aufbau und Dynamik des Südlichen Agulhasstromgebietes. *Veröffentlichungen des Instituts für Meereskunde an der Universität Berlin, Neue Folge*, A., Heft. **27**, 1–79.
- EDMOND, J. M., and G. C. ANDERSON (1971) On the structure of the North Atlantic Deep Water. *Deep-Sea Research*, **18**, 127–133.
- EDMOND, J. M., S. S. JACOBS, A. L. GORDON, A. W. MANTYLA, and R. F. WEISS (1979) Water column anomalies in dissolved silica over opaline pelagic sediments and the origin of the deep silica maximum. *Journal of Geophysical Research*, **84**, 7809–7826.
- EMILSSON, I. (1961) The shelf and coastal waters off southern Brazil. *Institute of Oceanography, São Paulo, Boletim*, **11**, 101–112.
- ENIKEYEV, V. Kh., and M. N. KOSHLYAKOV (1973) Geostrophical currents of the tropical Atlantic. *Oceanology*, **13**, 781–793.
- EVANS, D. L., and S. S. SIGNORINI (1985) Vertical structure of the Brazil Current. *Nature*, **315**, 48–50.
- FOFONOFF, N. P. (1962) Dynamics of ocean currents. In: *The Sea: Ideas and Observations on Progress in the Study of the Seas, Volume 1*. M. N. Hill, editor, Interscience Publishers, New York, London, 323–395.

-
- FOFONOFF, N. P. (1985) Physical properties of seawater: A new salinity scale and equation of state for seawater. *Journal of Geophysical Research*, **90**, 3332–3342.
- FOSTER, T. D., and E. C. CARMACK (1976) Temperature and salinity structure in the Weddell Sea. *Journal of Physical Oceanography*, **6**, 36–44.
- FOSTER, T. D., A. FOLDVIK, and J. H. MIDDLETON (1987) Mixing and bottom water formation in the shelf break region of the southern Weddell Sea. *Deep-Sea Research*, **34**, 1771–1794.
- FU, L.-L. (1981) The general circulation and meridional heat transport of the subtropical South Atlantic determined by inverse methods. *Journal of Physical Oceanography*, **11**, 1171–1193.
- FUGLISTER, F. C. (1960) Atlantic Ocean atlas of temperature and salinity profiles and data from the International Geophysical Year of 1957–1958. *Woods Hole Oceanographic Institution Atlas Series*, **1**, 209 pp.
- GEORGI, D. T. (1981) Circulation of bottom waters in the southwestern South Atlantic. *Deep-Sea Research*, **28**, 959–979.
- GILL, A. E. (1973) Circulation and bottom water production in the Weddell Sea. *Deep-Sea Research*, **20**, 111–140.
- GORDON, A. L., and K. T. BOSLEY Cyclonic gyre in the tropical South Atlantic. *Deep-Sea Research*, in press.
- GORDON, A. L., and C. L. GREENGROVE (1986) Geostrophic circulation of the Brazil–Falkland confluence. *Deep-Sea Research*, **33**, 573–585.
- GORDON, A. L., J. R. E. LUTJEHARMS, and M. L. GRUNDLINGH (1987) Stratification and circulation at the Agulhas Retroflection. *Deep-Sea Research*, **34**, 565–599.
- GORDON, A. L., and E. J. MOLINELLI (1982) *Southern Ocean Atlas*. Columbia University Press, New York.
- GORDON, A. L., and W. D. NOWLIN, JR. (1978) The basin waters of the Bransfield Strait. *Journal of Physical Oceanography*, **8**, 258–264.
- HART, T. J., and R. I. CURRIE (1960) The Benguela Current. *Discovery Reports*, **31**, 123–298.
- HELLERMAN, S., and M. ROSENSTEIN (1983) Normal monthly wind stress over the World Ocean with error estimates. *Journal of Physical Oceanography*, **13**, 1093–1104.
- HENTSCHEL, E., and H. WATTENBERG (1930) Plankton und phosphat in der Oberflächenschicht des Sudatlan-tischen Ozeans. *Annalen der Hydrographie und Maritimen Meteorologie*, **58**, 273–277.
- HOGG, N., P. BISCAYE, W. GARDNER, and W. J. SCHMITZ, JR. (1982) On the transport and modification of Antarctic Bottom Water in the Vema Channel. *Journal of Marine Research*, **40**(Supplement), 231–263.
- JACOBS, S. S., and D. T. GEORGI (1977) Observations on the southwest Indian/Antarctic Ocean. In: *A Voyage of Discovery* (George Deacon 70th Anniversary Volume). Martin Angel, editor, Pergamon Press, Oxford, New York, Toronto, Sydney, Paris, Frankfurt, 696 pp.
- JENKINS, W. J., and W. B. CLARKE (1976) The distribution of ^3He in the western Atlantic Ocean. *Deep-Sea Research*, **23**, 481–494.
- JOHNSON, D. A., S. E. McDOWELL, L. G. SULLIVAN, and P. E. BISCAYE (1976) Abyssal hydrography, nephelometry, currents, and benthic boundary layer structure in the Vema Channel. *Journal of Geophysical Research*, **81**, 5771–5786.
- KATZ, E. J. (1981) Dynamic topography of the sea surface in the equatorial Atlantic. *Journal of Marine Research*, **39**, 53–63.

- KIRWAN, A. D. (1963) Circulation of Antarctic Intermediate Water deduced through isentropic analysis. *Texas A&M University Reference* **63-34 F**, 34 pp., 47 figs.
- KOLESNIKOV, A. G. (editor) (1973a) *Equalant I & Equalant II — Oceanographic Atlas, Volume I, Physical Oceanography*. UNESCO, Paris, 289 pp.
- KOLESNIKOV, A. G. (editor) (1973b) *Equalant I & Equalant II — Oceanographic Atlas, Volume II, Chemical and Biological Oceanography*. UNESCO, Paris, 358 pp.
- KRUMMEL, O. (1882) Bemerkungen über die Meeresstromungen und Temperaturen in der Falklandsee. *Aus dem Archiv der Deutschen Seewarte*, V, Hamburg, Nr. 2, 25 pp.
- LE PICHON, X., S. L. EITTREIM, and W. J. LUDWIG (1971) Sediment transport and distributions in the Argentine Basin. 1. Antarctic Bottom Current Passage through the Falkland Fracture Zone. In: *Physics and Chemistry of the Earth, Volume 8*. L. H. Ahrens, F. Press, S. K. Runcorn, and H. C. Urey, editors, Pergamon Press, Oxford, pp. 1-27.
- LE PICHON, X., M. EWING, and M. TRUCHAN (1971) Sediment transport and distributions in the Argentine Basin. 2. Antarctic Bottom Current Passage into the Brazil Basin. In: *Physics and Chemistry of the Earth, Volume 8*. L. H. Ahrens, F. Press, S. K. Runcorn, and H. C. Urey, editors, Pergamon Press, Oxford, pp. 29-48.
- LUSQUINOS, A. J., and A. G. SCHROTT (1983) Corrientes en el mar epicontinental argentino en invierno. *Report Subsecretaría de Ciencia y Tecnología, República Argentina*, Buenos Aires, 74 pp.
- LUTJEHARMS, J. R. E., and R. C. VAN BALLEGOOYEN (1988) The retroflection of the Agulhas Current. *Journal of Physical Oceanography*, **18**, 1570-1583.
- LYNN, R. J., and J. L. REID (1968) Characteristics and circulation of deep and abyssal waters. *Deep-Sea Research*, **15**, 577-598.
- MANN, C. R., A. R. COOTE, and D. M. GARNER (1973) The meridional distribution of silicate in the western Atlantic Ocean. *Deep-Sea Research*, **20**, 791-801.
- MANTYLA, A. W., and J. L. REID (1983) Abyssal characteristics of the world ocean waters. *Deep-Sea Research*, **30**, 805-833.
- MASCARENHAS, A. S., JR., L. B. MIRANDA, and N. J. ROCK (1971) A study of the oceanographic conditions in the region of Cabo Frio. In: *Fertility of the Sea, Volume 1*, symposium held in São Paulo, Brazil, December 1-6, 1969, sponsored by Latin American universities. J. D. Costlow, Jr., editor, Gordon and Breach, New York, pp. 285-308.
- MERLE, J. (1978) Atlas hydrologique saisonnier de l'Océan Atlantique Intertropical. *Travaux et Documents de l'O.R.S.T.O.M.*, Office de la Recherche Scientifique et Technique Outre-Mer, Paris.
- MERLE, J., and S. ARNAULT (1985) Seasonal variability of the surface dynamic topography in the tropical Atlantic Ocean. *Journal of Marine Research*, **43**, 267-288.
- MIRANDA, L. B. de (1985) T-S correlation in water masses of the coastal and oceanic regions between Cabo de São Tomé (RJ) and São Sebastião Island (SP), Brazil. *Bolm Inst. Oceanogr., São Paulo*, **33**, 105-119.
- MOROSHKIN, K. V., V. A. BUBNOV, and R. P. BULATOV (1970) Water circulation in the eastern South Atlantic Ocean. *Oceanology*, **10**, 27-34.
- OLSON, D. B., and R. H. EVANS (1986) Rings of the Agulhas Current. *Deep-Sea Research*, **33**, 27-42.
- OLSON, D. B., G. P. PODESTA, R. H. EVANS, and O. B. BROWN (1988) Temporal variations in the separation of Brazil and Malvinas Currents. *Deep-Sea Research*, **35**, 1971-1990.

-
- REID, J. L. (1973) The shallow salinity minima of the Pacific Ocean. *Deep-Sea Research*, **20**, 51–68.
- REID, J. L. (1981) On the mid-depth circulation of the World Ocean. In: *Evolution of Physical Oceanography*, B. A. Warren and C. Wunsch, editors, The MIT Press, Cambridge, MA, and London, England, pp. 70–111.
- REID, J. L. (1986) On the total geostrophic circulation of the South Pacific Ocean: Flow patterns, tracers and transports. *Progress in Oceanography*, **16**, 1–61.
- REID, J. L. (1987) On the field of baroclinic flow in the South Atlantic Ocean. *Programme and Abstracts Volume, XIX General Assembly of the International Union of Geodesy and Geophysics* (Vancouver, Canada, August 9–22, 1987), p. 1018.
- REID, J. L., and R. J. LYNN (1971) On the influence of the Norwegian–Greenland and Weddell seas upon the bottom waters of the Indian and Pacific oceans. *Deep-Sea Research*, **18**, 1063–1088.
- REID, J. L., W. D. NOWLIN, JR., and W. C. PATZERT (1977) On the characteristics and circulation of the Southwestern Atlantic Ocean. *Journal of Physical Oceanography*, **7**, 62–91.
- RICHARDSON, P. L., and G. REVERDIN (1987) Seasonal cycle of velocity in the Atlantic North Equatorial Countercurrent as measured by surface drifters, current meters, and ship drifts. *Journal of Geophysical Research*, **92**, 3691–3708.
- RINTOUL, S. R. (1988) Mass, heat and nutrient fluxes in the Atlantic Ocean determined by inverse methods. Ph.D. thesis, Massachusetts Institute of Technology, and Woods Hole Oceanographic Institution, 287 pp.
- RODEN, G. I. (1989) The vertical thermohaline structure in the Argentine Basin. *Journal of Geophysical Research*, **94**, 877–896.
- SCHUBERT, O. VON (1935) Die Stabilitätsverhältnisse im Atlantischen Ozean. *Wissenschaftliche Ergebnisse der Deutschen Atlantischen Expedition auf dem Vermessungs- und Forschungsschiff "Meteor" 1925–1927*, **6**(2)(1), 54 pp.
- SCRIPPS INSTITUTION OF OCEANOGRAPHY (1979) Physical and chemical data, INDOMED Expedition, Leg XIII, 9 November – 22 December 1978. University of California, Scripps Institution of Oceanography, *SIO Reference 79–15*, 112 pp.
- SHANNON, L. V. (1985) The Benguela ecosystem Part I: Evolution of the Benguela, physical features and processes. *Oceanography and Marine Biology Annual Review*, **23**, 105–182.
- SHANNON, L. V., and D. HUNTER (1988) Notes on Antarctic Intermediate Water around southern Africa. *South African Journal of Marine Science*, **6**, 107–117.
- SIEVERS, H. A., and W. D. NOWLIN, JR. (1984) The stratification and water masses at Drake Passage. *Journal of Geophysical Research*, **89**, 10,489–10,514.
- SIGNORINI, S. R. (1978) On the circulation and the volume transport of the Brazil Current between the Cape of São Tome and Guanabara Bay. *Deep-Sea Research*, **25**, 481–490.
- SPEER, K. G. (1985) Property distributions and circulation in the Angola Basin. M.S. dissertation, Massachusetts Institute of Technology, 130 pp.
- STUIVER, M., and H. G. OSTLUND (1980) GEOSECS Atlantic Radiocarbon. *Radiocarbon*, **22**, 1–24.
- TAFT, B. A. (1963) Distribution of salinity and dissolved oxygen on surfaces of uniform potential specific volume in the South Atlantic, South Pacific, and Indian oceans. *Journal of Marine Research*, **21**, 129–146.
- TSUCHIYA, M. (1985) Evidence of a double-cell subtropical gyre in the South Atlantic Ocean. *Journal of Marine Research*, **43**, 57–65.

- TSUCHIYA, M. (1986) Thermostads and circulation in the upper layer of the Atlantic Ocean. *Progress in Oceanography*, **16**, 235–267.
- TSUCHIYA, M. (1989) Circulation of the Antarctic Intermediate Water in the North Atlantic Ocean. *Journal of Marine Research*, **47**, in press.
- TUCHOLKE, B. E., and R. W. EMBLEY (1984) Cenozoic regional erosion of the abyssal sea floor off South Africa. In: *Interregional Unconformities and Hydrocarbon Accumulation*, John S. Schlee, editor, American Association of Petroleum Geologists Memoir 36, pp. 145–164.
- VISSEER, G. A. (1969) Analysis of Atlantic waters off the west coast of southern Africa. *Investigational Report, Division of Sea Fisheries, Union of South Africa*, **75**, 1–26.
- WARREN, B. A. (1981) Deep circulation of the world ocean. In: *Evolution of Physical Oceanography*, B. A. Warren and C. Wunsch, editors, The MIT Press, Cambridge, MA, and London, England, pp. 6–41.
- WATTENBERG, H. (1938) Die Verteilung des Sauerstoffs im Atlantischen Ozean. *Wissenschaftliche Ergebnisse der Deutschen Atlantischen Expedition auf dem Vermessungs—und Forschungsschiff "Meteor" 1925–1927*, **9**(2)(1), 132 pp.
- WATTENBERG, H. (1939) Atlas zu: Die Verteilung des Sauerstoffs im Atlantischen Ozean. *Wissenschaftliche Ergebnisse der Deutschen Atlantischen Expedition auf dem Vermessungs—und Forschungsschiff "Meteor" 1925–1927*, **9**(Atlas), 72 Beilagen.
- WATTENBERG, H. (1957) Die Verteilung des Phosphats im Atlantischen Ozean. *Wissenschaftliche Ergebnisse der Deutschen Atlantischen Expedition auf dem Vermessungs—und Forschungsschiff "Meteor" 1925–1927*, **9**(2)(2), 133–180.
- WEISS, R. F., J. L. BULLISTER, R. H. GAMMON, and M. J. WARNER (1985) Atmospheric chlorofluoromethanes in the deep equatorial Atlantic. *Nature*, **314**, 608–610.
- WEISS, R. F., H. G. OSTLUND, and H. CRAIG (1979) Geochemical studies of the Weddell Sea. *Deep-Sea Research*, **26**, 1093–1120.
- WHITWORTH, T., III, and W. D. NOWLIN, JR. (1987) Water masses and currents of the Southern Ocean at the Greenwich Meridian. *Journal of Geophysical Research*, **92**, 6462–6476.
- WHITWORTH, T., III, W. D. NOWLIN, JR., and S. J. WORLEY (1982) The net transport of the Antarctic Circumpolar Current through Drake Passage. *Journal of Physical Oceanography*, **12**, 960–971.
- WRIGHT, W. R. (1970) Northward transport of Antarctic Bottom Water in the Western Atlantic Ocean. *Deep-Sea Research*, **17**, 367–371.
- WUST, G. (1933) Das Bodenwasser und die Gliederung der Atlantischen Tiefsee. *Wissenschaftliche Ergebnisse der Deutschen Atlantischen Expedition auf dem Vermessungs—und Forschungsschiff "Meteor" 1925–1927*, **6**(1)(1), 1–107.
- WUST, G. (1935) Die Stratosphäre. *Wissenschaftliche Ergebnisse der Deutschen Atlantischen Expedition auf dem Vermessungs—und Forschungsschiff "Meteor" 1925–1927*, **6**(1)(2), 109–288.
- WUST, G., and A. DEFANT (1936) Atlas zur Schichtung und Zirkulation des Atlantischen Ozeans. Schnitte und Karten von Temperatur, Salzgehalt und Dichte. *Wissenschaftliche Ergebnisse der Deutschen Atlantischen Expedition auf dem Vermessungs—und Forschungsschiff "Meteor" 1925–1927*, **6**(Atlas), Beilagen I–CIII.

WYRTKI, K. (1971) *Oceanographic Atlas of the International Indian Ocean Expedition*. National Science Foundation, Washington, DC, 531 pp.

ZYRYANOV, V. N., and D. N. SEVEROV (1979) Water circulation in the Falkland-Patagonia region and its seasonal variations. *Oceanology*, **19**, 518-522.